REFER TO:	Action	Info	Int
Mat'ls & Resh Engr.			
Mat'ls Engr.			Clt
Ass't Mat'ls Engr.		✓	
Research Engr.		✓	Ow
Assoc Resh Engr.			
Soils Engr.		✓	Wil
Geologist			
Testing Engr.		✓	C
Office Mgr.			
Quality Control			
Project Devlp.			
E. I. T.			

NATIONAL COOPERATIVE HIGHWAY RESEARCH PROGRAM
REPORT 77

DEVELOPMENT OF DESIGN CRITERIA FOR SAFER LUMINAIRE SUPPORTS

HIGHWAY RESEARCH BOARD
NATIONAL RESEARCH COUNCIL
NATIONAL ACADEMY OF SCIENCES—NATIONAL ACADEMY OF ENGINEERING

NATIONAL COOPERATIVE HIGHWAY RESEARCH PROGRAM
REPORT 77

DEVELOPMENT OF DESIGN CRITERIA FOR SAFER LUMINAIRE SUPPORTS

THOMAS C. EDWARDS, J. E. MARTINEZ,
WILLIAM F. McFARLAND, AND HAYES E. ROSS, JR.
TEXAS A & M UNIVERSITY
COLLEGE STATION, TEXAS

RESEARCH SPONSORED BY THE AMERICAN ASSOCIATION
OF STATE HIGHWAY OFFICIALS IN COOPERATION
WITH THE BUREAU OF PUBLIC ROADS

SUBJECT CLASSIFICATION:
HIGHWAY DESIGN
HIGHWAY SAFETY

HIGHWAY RESEARCH BOARD
DIVISION OF ENGINEERING NATIONAL RESEARCH COUNCIL
NATIONAL ACADEMY OF SCIENCES—NATIONAL ACADEMY OF ENGINEERING 1969

NATIONAL COOPERATIVE HIGHWAY RESEARCH PROGRAM

Systematic, well-designed research provides the most effective approach to the solution of many problems facing highway administrators and engineers. Often, highway problems are of local interest and can best be studied by highway departments individually or in cooperation with their state universities and others. However, the accelerating growth of highway transportation develops increasingly complex problems of wide interest to highway authorities. These problems are best studied through a coordinated program of cooperative research.

In recognition of these needs, the highway administrators of the American Association of State Highway Officials initiated in 1962 an objective national highway research program employing modern scientific techniques. This program is supported on a continuing basis by funds from participating member states of the Association and it receives the full cooperation and support of the Bureau of Public Roads, United States Department of Transportation.

The Highway Research Board of the National Academy of Sciences-National Research Council was requested by the Association to administer the research program because of the Board's recognized objectivity and understanding of modern research practices. The Board is uniquely suited for this purpose as: it maintains an extensive committee structure from which authorities on any highway transportation subject may be drawn; it possesses avenues of communications and cooperation with federal, state, and local governmental agencies, universities, and industry; its relationship to its parent organization, the National Academy of Sciences, a private, nonprofit institution, is an insurance of objectivity; it maintains a full-time research correlation staff of specialists in highway transportation matters to bring the findings of research directly to those who are in a position to use them.

The program is developed on the basis of research needs identified by chief administrators of the highway departments and by committees of AASHO. Each year, specific areas of research needs to be included in the program are proposed to the Academy and the Board by the American Association of State Highway Officials. Research projects to fulfill these needs are defined by the Board, and qualified research agencies are selected from those that have submitted proposals. Administration and surveillance of research contracts are responsibilities of the Academy and its Highway Research Board.

The needs for highway research are many, and the National Cooperative Highway Research Program can make significant contributions to the solution of highway transportation problems of mutual concern to many responsible groups. The program, however, is intended to complement rather than to substitute for or duplicate other highway research programs.

This report is one of a series of reports issued from a continuing research program conducted under a three-way agreement entered into in June 1962 by and among the National Academy of Sciences-National Research Council, the American Association of State Highway Officials, and the U. S. Bureau of Public Roads. Individual fiscal agreements are executed annually by the Academy-Research Council, the Bureau of Public Roads, and participating state highway departments, members of the American Association of State Highway Officials.

This report was prepared by the contracting research agency. It has been reviewed by the appropriate Advisory Panel for clarity, documentation, and fulfillment of the contract. It has been accepted by the Highway Research Board and published in the interest of an effectual dissemination of findings and their application in the formulation of policies, procedures, and practice on the subject problem area.

NCHRP Project 15-6 FY '68
NAS-NRC Publication 309-01773-4
Library of Congress Catalog Card Number: 74-603417

FOREWORD

By Staff

Highway Research Board

This report is recommended to highway engineers and others concerned with highway safety. It contains an evaluation of "safe" luminaire supports, design recommendations, design charts, and suggested cost-effectiveness methodology for selecting the most efficient system for any given installation. It is believed that this report represents a large advancement in the rational design and selection of safe luminaire support systems.

An argument to justify an improved method of design for roadway hardware is unnecessary. Certainly, there is agreement that the chance of serious injury to occupants should be limited to some acceptable value when luminaire supports are struck by out-of-control vehicles. The state-of-the-art up to the time of NCHRP Project 15-6, "Development of Design Criteria for Safer Luminaire Supports," indicated that most of the work in this subject area dealt with relative effectiveness; i.e., one device appeared to be better than another, but it could not be stated in absolute terms that either device was safe.

Texas Transportation Institute, as a result of this one-year NCHRP project and other experience, offers a valuable, rational method that appears to relate to the absolute question: Is it safe enough? TTI used a varied approach that included a mathematical model for prediction of the results of a vehicle-luminaire support collision, verified the model by full-scale crash testing while simultaneously evaluating the relative performance of various systems, correlated the full-scale tests with comparatively simple and inexpensive laboratory tests, related vehicle damage to potential injury to occupants, and arrived at design recommendations—with real numbers—that should assure safer luminaire support designs.

Beyond these accomplishments, the verified mathematical model was used to prepare a series of design charts that describe the dynamic response of a luminaire support after being struck by a vehicle. Using these charts, the designer can predict whether the support will fall on the vehicle, whether it will fall on the traveled roadway, and the potential severity of injury to the occupants.

The designer is also offered a cost-effectiveness methodology which, when used with appropriate input, should be useful in selecting an efficient luminaire support system. The absence of reliable input numbers may be a problem in applying this technique at the present time. However, at such time as the necessary data can be generated it appears likely that this analysis will provide a valuable tool for decision makers.

An 18-min documentary film, entitled "Lights Out," shows some of the crash tests and summarizes the research findings. The film is available on loan by writing to the Community Services Department of the Texas Transportation Institute, Texas A&M University, College Station, Texas 77843, or to the Program Director, National Cooperative Highway Research Program, 2101 Constitution Avenue, Washington, D.C. 20418.

CONTENTS

ACKNOWLEDGMENTS

The research reported herein was performed under NCHRP Project 15-6 and was conducted at Texas A&M University by personnel of the Texas Transportation Institute. Thomas C. Edwards, Assistant Research Engineer, represented the Institute as principal investigator. The development of the mathematical model and studies related to it were under the supervision of J. E. Martinez, Assistant Research Engineer. The cost-effectiveness study was conducted by William F. McFarland, Assistant Research Economist, and Hayes E. Ross, Jr., Assistant Research Engineer.

The authors wish to acknowledge the assistance and cooperation of the following individuals: R. A. Hartmann, HAPCO Company, Division of Kearney-National, Inc.; Paul Millerbernd and Joe Reardon, Millerbernd Manufacturing Co.; A. R. Dayson, Kerigan Iron Works Co.; V. E. Gensemer, University Pole and Structures Division, A. B. Chance and Co.; T. R. Koessler, Kaiser Aluminum Co., R. J. Rice, International Nickel Co.; John S. Lengel, Aluminum Company of America; E. M. Carl, H. D. Jones, C. E. Moore, A. W. Ratliff, E. M. Smith, and S. S. Williams, all of the Texas Highway Department; Eric T. Nordlin, California Division of Highways; and J. G. Allen, J. L. Anderson, and H. M. Reilly of the Texas Turnpike Authority.

DEVELOPMENT OF DESIGN CRITERIA FOR SAFER LUMINAIRE SUPPORTS

SUMMARY

A review of published literature revealed that preliminary research that was conducted to develop safer luminaire supports has established guidelines that subsequent research has followed. It was established that, to insure low impact resistance, it is necessary to incorporate a base which will break away in a collision but which possesses sufficient strength to resist static and wind-induced loads. Concepts that have been developed and accepted by at least one state in the U.S. can be broadly classified as: (1) frangible insert bases, (2) progressive-shear bases, (3) aluminum shoe bases, and (4) slip joints.

Full-scale tests were conducted in such a manner that a comparative evaluation could be made of the four basic concepts. Several variations of the basic concepts were also tested and evaluated (stainless steel progressive-shear base coupled with stainless steel davit and mast arm type supports, and a cast aluminum shoe base with an integral riser). In addition, one test was conducted on a prestressed concrete support. The collisions were performed with nominal 3,500-lb vehicles moving generally at about 40 mph.

The tests were compared by using test data to calculate severity ratios and a Severity Index (see Chapter Three). The values were used to rank the four concepts tested from the most severe to the least severe, as follows: (1) aluminum shoe base with aluminum shaft, (2) progressive-shear base, (3) frangible insert (aluminum transformer base), and (4) the triangular slip joint.

Based on the response of dummies in the vehicles, all collisions tested were judged to be safe, with only the most severe likely to produce minor occupant injury.

A mathematical model was developed that was used to study the variables that influenced the collision. The results of this study, coupled with the full-scale test data, were used to develop design criteria. The criteria are formulated such that proposed designs can be evaluated for safe performance.

In general, the conclusions drawn from the research are as follows:

1. All of the luminaire supports tested (except the prestressed concrete) can be considered safe for collisions similar to those of the test conditions. It is likely that only minor injuries would have occurred in the most severe case. Prestressed concrete supports should be considered as being rigid barriers.

2. Existing frangible insert (transformer bases) and progressive-shear bases should be of such height as to allow the vehicle bumper to contact them, rather than the luminaire support shaft (new designs may invalidate this conclusion).

3. The base fracture energy (energy absorbed at fracture or breakaway) determined from laboratory impact tests can be used as a measure of energy absorbed by the base in a full-scale collision. This allows a relatively simple

laboratory test to substitute for full-scale vehicle crash tests in the evaluation of new concepts or design.

4. Any type of base for which the base fracture energy depends on its orientation should be oriented so that the most probable collision angle coincides with the direction of least resistance.

5. When luminaire supports must be located in places where the probability of low-velocity collisions is high, support bases should have the lowest possible fracture energy and the support pole should be constructed of lightweight materials. (The most severe collisions—those more likely to result in personal injury—occur with lightweight vehicles moving at velocities below 15 mph.)

6. Under most conditions the luminaire support, after a collision, will assume a longitudinal position roughly paralleling the vehicle path, with the top of the pole displaced laterally toward the roadway. The danger of encroachment of the shaft into the traveled lanes is highest for low-velocity collisions (15 mph). At collision velocities above 30 mph, the lateral displacement decreases, and, under normal circumstances, no encroachment should occur. With supports now in use, the danger of the support falling into the traveled lanes is small if it is located at a distance from the pavement edge equal to or greater than the mast-arm length.

7. In collisions between vehicles moving at velocities of 40 mph or greater and supports (40-ft mounting height or less) with bases which exhibit fracture energies of approximately 9,000 ft-lb or less, the luminaire support will clear the vehicle (not fall on the vehicle).

8. A collision speed of about 35 mph appears to be the lower limit at which a conventional support (30- to 40-ft mounting height) can be expected to clear the vehicle or hit behind the passenger compartment.

9. Large supports (50-ft mounting height or greater), with base fracture energies in excess of 9,000 ft-lb, should be considered with caution, because low-velocity collisions may be severe (more likely to result in personal injury).

10. Breakaway-type bases result in considerably lower average accident costs than do the more rigid-type bases.

CHAPTER ONE

INTRODUCTION

DESCRIPTION OF THE PROBLEM

Conventional luminaire support poles, under present design practices, are mounted close to the traveled roadway. In this location, they constitute a severe roadside hazard and are frequently struck by vehicles that are out of control, with attendant severe vehicle damage and injury or death to the occupants.

Statistics for single-vehicle accidents on completed sections of the Interstate System for the period July to December, 1966, show that of 933 fatal accidents, 566 (57%) involved the vehicle running off the road. Of these 566 fatal accidents, 433 (78%) were caused by collisions with roadside obstacles. Of the 433, 16 (4%) were with luminaire supports. This represents 1.61% of all fatal accidents. This may seem insignificant unless one considers that of the 55,000 deaths which occur each year on highways in the United States, at least 885 can be attributed to collisions with luminaire supports (*1*, p. 12). Property damage and personal injury figures are just as staggering.

Several alternative solutions to the problem exist: (1) move the supports farther away from the roadway surface; (2) use high-level area lighting; (3) limit the impact se-

verity by including some type of breakaway base. Although the first two alternatives have been adopted to some extent in many states in the U.S., they cannot always be done practically due to limitations in right-of-way and terrain. The inclusion of breakaway bases has gained acceptance because it allows the use of present illumination and design criteria, hardware, and, in many instances, modification of existing installations.

Another important consideration in the design of safe luminaire supports is that of the relative economics of the various concepts. Although one concept may prove to offer the highest safety, it must be evaluated with other concepts to weigh its cost against its effectiveness.

This research is directed toward the study and evaluation of breakaway base concepts and the development of design criteria which can be applied to minimize the safety hazards associated with luminaire support collisions.

RESEARCH APPROACH

A search of the present literature was performed to establish the state-of-the-art in safer luminaire support construction. This information was used to classify the various concepts which are used to limit collision severity. A survey of U.S. state highway departments established the acceptability and application of the various concepts. Full-scale collision tests were conducted under controlled conditions. The data from these tests provided information which could be used to make a comparative evaluation. Inasmuch as the design concepts tested include those that are presently in use, each state will have the basis for making its own evaluation.

A mathematical simulation of the luminaire support collision was developed and verified by full-scale tests. The model was used to conduct a study of the effects of the various vehicle and support parameters. This study was used to aid in the formulation of design criteria.

Laboratory and analytical investigations were conducted to establish the basic structural characteristics of the various breakaway concepts. These data were used in the development of design criteria and in checking the validity of a standard testing procedure to establish the acceptability of a particular breakaway base design.

In the cost-effectiveness part of this study (Appendix C), a model was developed which could be used to calculate the present value of total highway lighting cost for a project with stated characteristics. Included in the model is a method for predicting the number of vehicles that might be expected to hit lighting poles in different circumstances. The model was used in example calculations, using costs given by manufacturers, crash tests, and accident records.

Because it was realized that costs vary in different areas of the country, the answers given in the cost calculations are only examples of the use of the model.

CONCEPTS FOR SAFE LUMINAIRE SUPPORTS

U.S. Federal agencies, U.S. state highway departments, government agencies of other countries, and private industry have initiated projects to develop safer luminaire supports. The initial research in this area was conducted by the Road Research Laboratory, of the Ministry of Transport in England, beginning in the late 50's. Their work defined the problem and established the guidelines which subsequent research and development have followed.

The preliminary research established that to insure a low impact resistance it is necessary to incorporate some type of device at the base of the support shaft, near ground level, which will enable the support to break away in a collision but possess sufficient strength to resist static and wind-induced loads. Since the establishment of the guideline, the efforts in both England and the United States have been directed toward the development of suitable breakaway base devices. The concepts that have been developed, and have proved satisfactory, can be broadly classified into the following groups: (1) slip joints; (2) cast aluminum transformer base (base of sufficient height so that the vehicle contacts the casting); (3) cast aluminum inserts used in conjunction with steel transformer bases; (4) cast aluminum inserts placed directly under the mounting flange of the support shaft [this type is differentiated from (3) in that the casting is not contacted by the vehicle]; (5) notched bolt inserts; (6) progressive-shear bases (sheet steel transformer base with button welded connections); and (7) cast aluminum flanged bases used with aluminum shafts.

The following sections summarize the details of these concepts, developed prior to this report.

Slip Joints

Initial Research

In the initial stages of the research conducted at the Road Research Laboratory, low-speed (approximately 25 mph) controlled collisions were conducted on a number of supports. The types of supports included concrete (reinforced and prestressed), tubular steel, thin sheet steel (sectional), aluminum, timber, and fiberglas. These tests showed that the concrete and tubular steel columns stopped the vehicles with resulting decelerations that were high enough to possibly cause severe injury to an unbelted occupant. High decelerations occurred also in the test of the wood support. The shaft broke on impact, but the stub left protruding from the ground proved to act like a rigid obstacle. Some types of aluminum supports produced high decelerations while others behaved satisfactorily. The fiberglas supports broke away with acceptable decelerations. Although some of the aluminum and fiberglas supports were acceptable from a safety standpoint, they were rejected because of large deflections under wind and static loads (*2*, p. 3).

The preliminary tests showed the lowest decelerations were produced by a thin sheet steel support. The shaft was embedded in tamped earth and had two concrete collars below ground level: one at the base, and one below the electrical cable entry slot (see Fig. 1). The support was struck centrally at a velocity of 22 mph by a 1,750-lb vehicle. Upon impact, the shaft bent and tore off 1 ft below ground level (at the top of the concrete collar, which coincided with the top of the cable entry slot). The total change in velocity of the vehicle was 8 mph, and the maximum

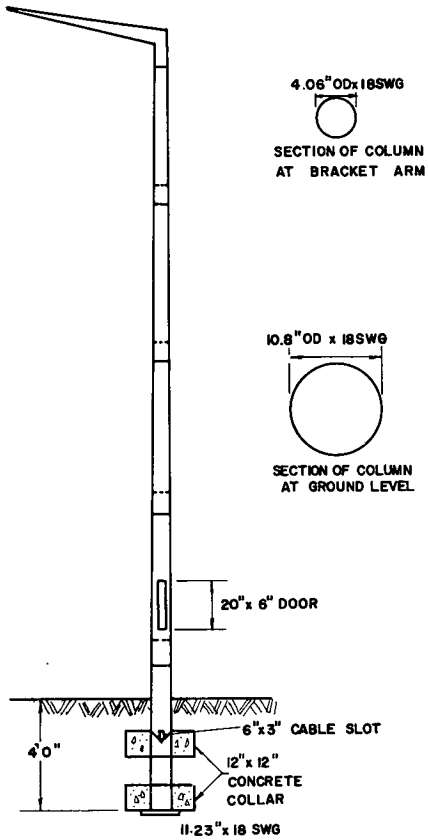

Figure 1. Thin sheet steel support.

deceleration was 8 g. The damage to the vehicle was minor —a collapsed bumper and a crushed radiator (*3*).

It was concluded from these preliminary tests that, to insure a low impact resistance, it would be necessary to incorporate some type of shear joint near ground level which would enable the support to break away in a collision but possess sufficient strength to resist static and wind-induced loads. Tests were conducted on a number of shear joints; the most effective was the Cambridge joint (*2*).

Cambridge Slip Base

The Cambridge slip base (Fig. 2) was developed from a design by Mr. P. W. Turner of Cambridge University, who acted as consultant to the Road Research Laboratory. The shaft of the support is attached to the foundation stub by clamping bolts placed in four V-slots. The bolts are held in position by a thin sheet steel retaining ring and tab washers on the flanges. The clamping force is applied by tightening the bolts to a torque which depends on the height of the support. In a collision, the shaft of the support is forced to slip across the fixed flange, tearing the restraining ring and forcing the bolts out of the V-slots. A device to disconnect the electrical cable is used.

Supports up to 40 ft in height have been subjected to collision tests at vehicle speeds up to 60 mph. Figure 3 shows the results of one such test, in which a 2,400-lb vehicle impacted a 40-ft support at 62 mph. The maximum deceleration experienced by the vehicle was 4.8 g, and the vehicle change in velocity was 2 mph. The front end of the vehicle was deformed 9 in.; damage to the vehicle was estimated at $140. The tests clearly show that a support with this type of base can be impacted with very little damage to the vehicle and probably no serious injury to the occupants. One significant conclusion can be drawn from the post-collision position of the support in Figure 3(b). At the speeds used in these tests, the shaft fell to the ground roughly along the path of the colliding vehicle, the top of the support falling vertically, striking the ground near the

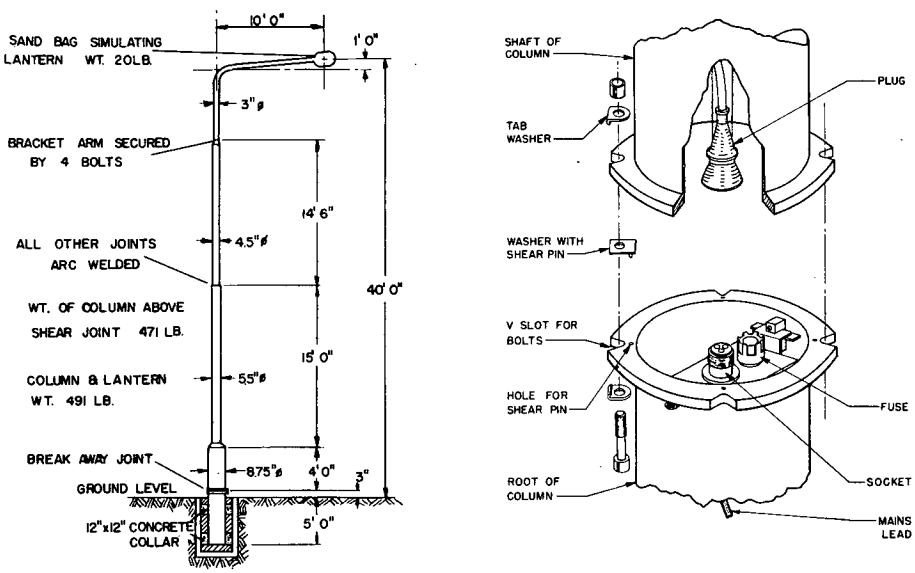

Figure 2. Cambridge slip base (*4, pp. 67.1, 67.2*).

base. This suggests that the danger of the support falling in the roadway is minimized if the supports are set back from the main roadway edge at least 5 ft (*4*, p. 24).

General Motors Slip Base

The basic concept developed in the Cambridge joint has been applied by the General Motors Proving Grounds. Figure 4(a) shows the General Motors design. The basic difference in this design is in the washers, the elimination of the retaining ring, and the use of a bolt-on bottom flange for modification of existing supports. Full-scale collision tests have been conducted to demonstrate the safe behavior of both steel and aluminum supports mounted on this slip base. Figure 4(b) shows the damage to the vehicle in a full-scale collision test on a steel support. The vehicle velocity at impact was approximately 40 mph.

Triangular Slip Base

The Texas Transportation Institute (TTI) and the Texas Highway Department, in cooperation with the Bureau of Public Roads, have developed a slip base (Fig. 5) which uses the same principle as the Cambridge base but employs a different arrangement of V-slots (*5*, p. 12).

Two full-scale collision tests were conducted to validate the safe performance of supports equipped with this type of base. The support, a 45-ft mounting height steel shaft, shown in Figure 5(b), was used for both tests. One test was conducted at a 0° vehicle collision angle of approach (normal to the plane of the mast arm), and the other at 30° (60° to the mast arm). The base bolts were torqued to 2,000-lb initial tension. In both tests and collision vehicle was a standard 4-door sedan (3,400 lb) with a nominal impact speed of 40 mph. Figure 6 shows the test results. In both tests the support cleared the vehicle after release. Damage to the vehicles was minor. Although dummies were not used, the decelerations and velocity change of the vehicles indicate a mild vehicle collision response.

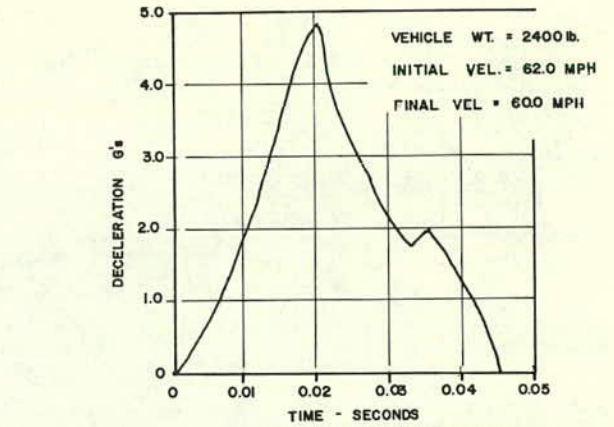

(a) VEHICLE DECELERATION RECORD

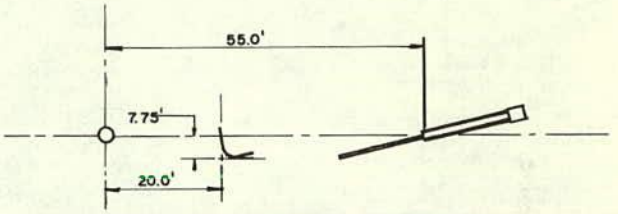

(b) FINAL POSITION OF SUPPORT

Figure 3. Results of test on Cambridge base (4, *pp. 67.3, 67.5*

In the 0° test the vehicle was slowed from 38.3 mph at impact to 35.9 mph at loss of contact. The position of the support after the test is shown in Figure 6(a). For the 30° test the initial vehicle velocity was 35.7 mph; the vehicle was slowed to 34.0 mph. Note the position of the support after the test, in Figure 6(b). Despite the difference in collision angle, the support shaft aligned itself with the vehicle path (*5*, p. 23).

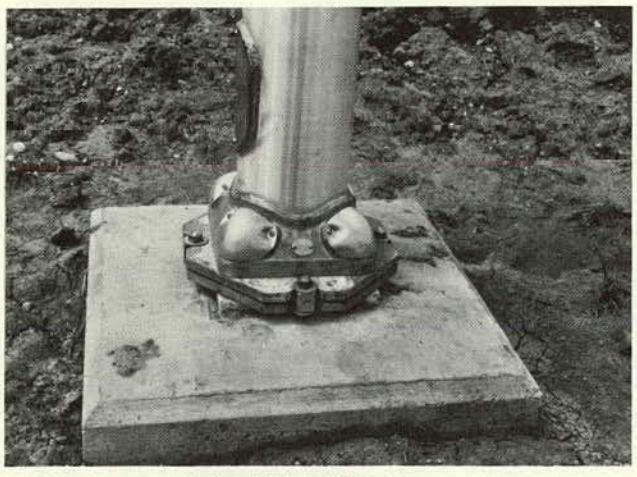

(a) BASE DETAILS

(b) VEHICLE DAMAGE

Figure 4. General Motors slip base. (*Photos courtesy General Motors Proving Grounds.*)

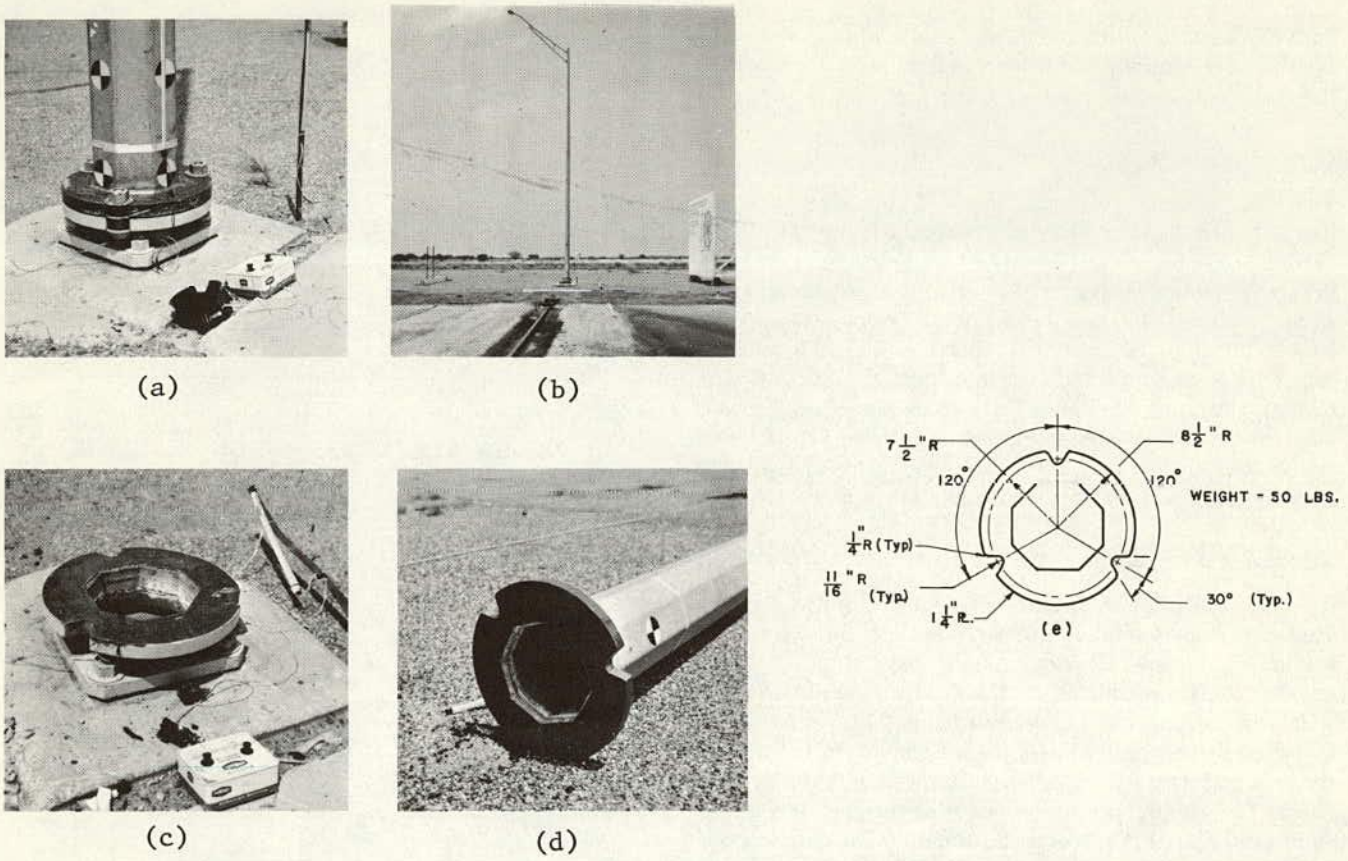

Figure 5. Details, triangular slip base (5, *p. 13*).

Cast Aluminum Transformer Base

Although the transformer base is no longer used to house the luminaire transformer, its use has been continued in many states because of favorable accident experience.

The TTI and the Texas Highway Department in cooperation with the Bureau of Public Roads conducted five tests to establish the severity of collisions with supports mounted on aluminum transformer bases (*6*). Table 1 gives the pertinent data and results on each test. Figure 7 shows a typical installation of an aluminum transformer base, as well as the failure which occurs by breaking out the front lower portion held by the two anchor bolts on the impact side of the base. In the 40 mph test, the support completely cleared the vehicle in its trajectory; in the

TABLE 1

SUMMARY OF TEXAS TESTS [a]

COMBINATION	VEH. YR. & MAKE	VEHICLE WEIGHT (LB)	SPEED (MPH) BEFORE IMPACT	SPEED (MPH) AFTER IMPACT	SPEED (MPH) CHANGE	DEFORMATION OF VEH. (IN.)
Steel pole, aluminum transformer base	1959 Ford	3460	22.2	18.1	4.1	12.7
	1959 Ford	3700	44.8	41.5	3.3	15.5
	1960 Simca	2140	45.7	38.0	7.7	12.3
Aluminum pole, aluminum transformer base	1959 Ford	3680	21.3	17.0	4.3	10.9
	1957 Ford	3600	43.2	38.0	5.2	10.2
Steel pole, steel transformer base, aluminum insert	1955 Ford	3460	32.2	27.3	4.9	14.4
	1955 Ford	3580	53.2	47.0	6.2	15.8
Flange-mounted aluminum pole	1957 Ford	3500	44.0	37.2	6.8	23.1

[a] From Rowan and Kanak (*6*, p. 7).

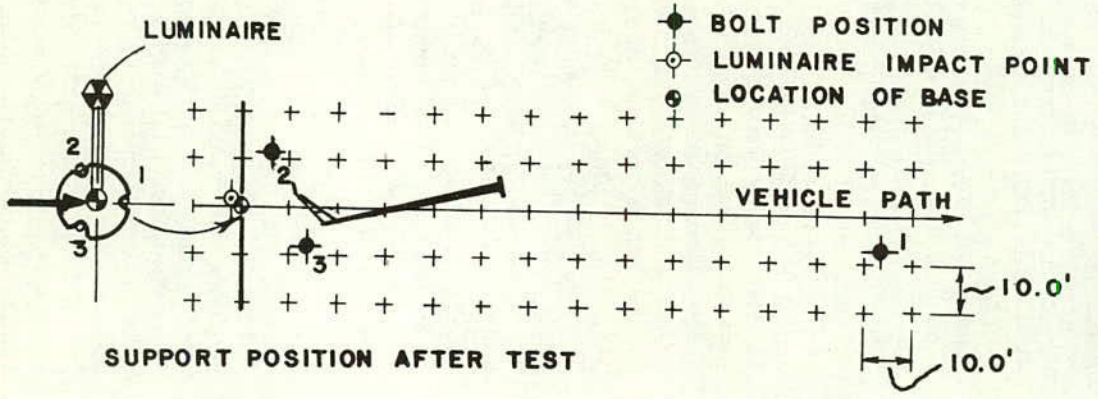

(a) 0° ANGLE OF APPROACH

DAMAGE

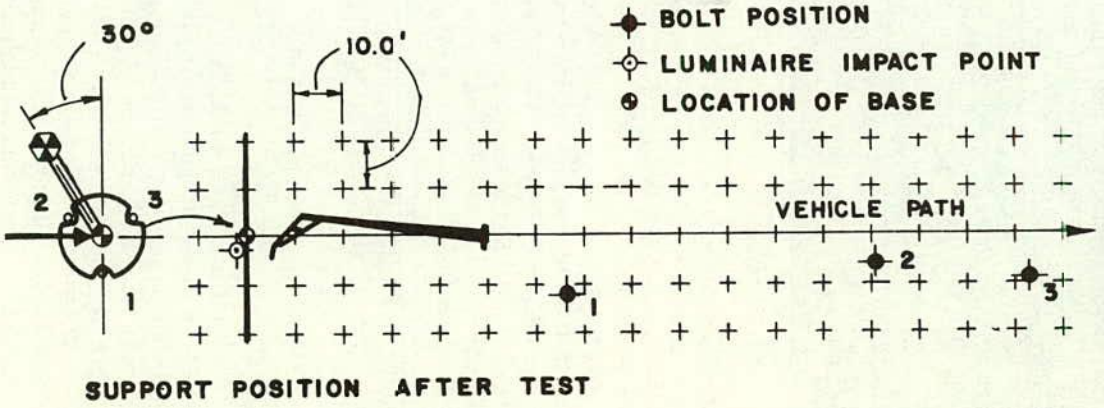

(b) 30° ANGLE OF APPROACH

DAMAGE

Figure 6. Test of triangular slip base (5).

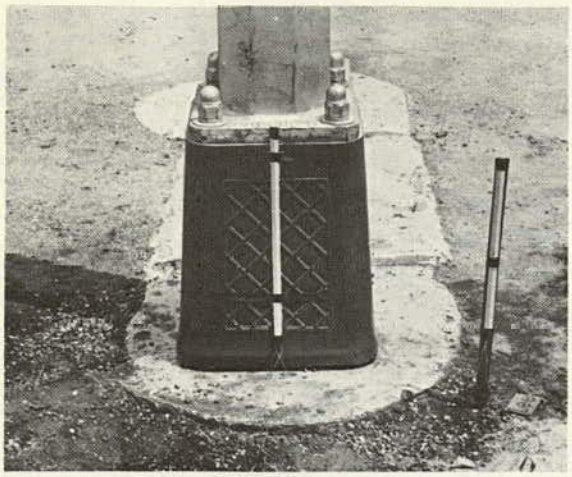

(a) BEFORE

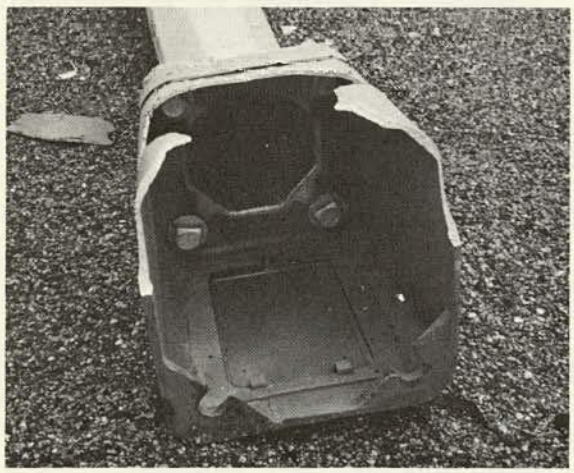

(b) AFTER

Figure 7. Aluminum transformer base (6).

20-mph test the pole fell across the hood and top and struck severely across the rear of the top of the automobiles. The base failure was essentially the same in all five tests. It was concluded from these tests that the cast aluminum transformer base appears to be a satisfactory device to reduce the impact severity of vehicle collisions. However, this conclusion is based only on head-on collisions, no work having been done on skidding or side impacts (*6*, p. 26).

Cast Aluminum Inserts, With and Without Steel Transformer Bases

Two tests were conducted to evaluate the cast aluminum insert (Fig. 8) which was designed as a remedial measure to be used in conjunction with steel transformer bases already in service. Test results are given in Table 1. In both tests the failure was initiated by a tensile crack forming in the top surface of the insert. As the collision progressed, the crack propagated diagonally toward the anchor bolts and the rear portion of the insert broke away, freeing the shaft and attached steel transformer base. In the 53 mph test, the support cleared the vehicle; in the slow-speed test the shaft fell on the vehicle. It was concluded from these tests that a cast aluminum insert placed between the foundation and a steel transformer base appeared to be a satisfactory remedial design; however, it did not appear to be feasible for new designs (*6*, p. 26).

The Materials and Research Department of the California Division of Highways has investigated the safety that can be achieved when a cast aluminum insert is used as a breakaway device. In this concept, the insert is placed between the foundation and the support shaft. Three tests were conducted. One test was conducted using the insert shown in Figure 9(a). Two additional tests were run using modifications of the insert shown in Figure 9(b). The object of the modifications was to introduce stress risers in the vertical wall of the insert to reduce the shear capacity. All three tests were conducted using California type XV steel light standards with 400-watt luminaires. The test vehicle was a 1965 Dodge sedan traveling at ±43 mph at impact. The vehicle bumper contacted the support shaft and did not contact the insert directly. In the first test (standard base) the base failed in a combination of shear and tension. Before the base failed, the shaft buckled and bent (almost 90°) at the bumper impact point. When the base fractured, the lower end of the shaft was accelerated forward and the shaft fell back onto the vehicle. The vehicle was deformed approximately 16 in. The dummy simulating the driver (unrestrained) showed slight decelerations. The first modification (drilled holes) proved to have little effect on the fracture of the base. The weakening afforded by the holes did have some effect, however, because the shaft was bent only 60° (compared to 90° in the first test) and the shaft cleared the vehicle in its travel through the impact zone. Moderate damage was done to the vehicle. The dummy showed mild decelerations.

The second modification (drilled holes and milled slots) proved to significantly alter the fracture strength of the base. On impact, the insert failed in a combination of shear and tension, the fracture occurring through the milled slots. The shaft was bent only 3°, indicating a greatly reduced fracture force. The support completely cleared the vehicle. The vehicle sustained moderate damage, with the dummy experiencing mild decelerations.

In all three tests, the support impacted the ground and settled into a position with no portion of the support on the traveled lanes (base of support offset 18 ft from the edge of the traveled lane) (*7*).

Notched Bolt Insert

The notched bolt insert (Fig. 10) was developed by the Weld Rite Manufacturing Company and was tested by the Materials and Research Department of the California Division of Highways. It consisted of four 1-in.-diameter Armco 17-4PH stainless steel bolts notched down to 7/16-in. diameter. The bolts were heat-treated to an H1050 condition. The support used in the test was a California type XV with a 400-watt luminaire. The collision vehicle was a 1965 Dodge sedan traveling at ±43 mph. On contact, the bolts sheared in the necked-down area, releasing the shaft, which

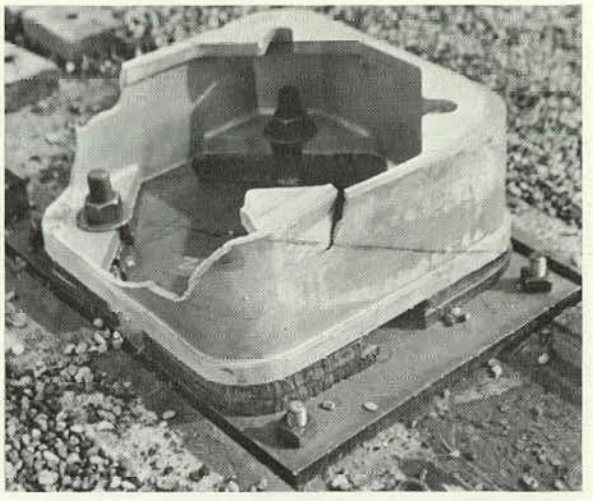

Figure 8. Cast aluminum insert with steel T*-base.*

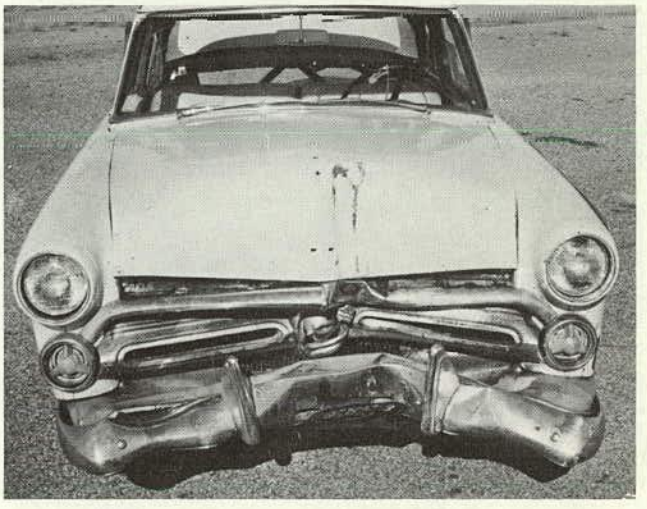

cleared the vehicle in its subsequent trajectory. The shaft was dented slightly in the bumper contact area. The crash vehicle sustained moderate damage to the front end. No discernible decelerations were recorded on the unrestrained dummy which simulated the driver. The post-collision position of the support was within the 18-ft zone between the foundation and the edge of the traveled lane (*7*).

Progressive-Shear Bases

In late 1965, the Minnesota Highway Department, concerned about the alarming increase in personal injury due to fixed-object collisions, initiated a study into the subject of luminaire supports as hazards to safety. In early 1966, criteria were established for the development of breakaway

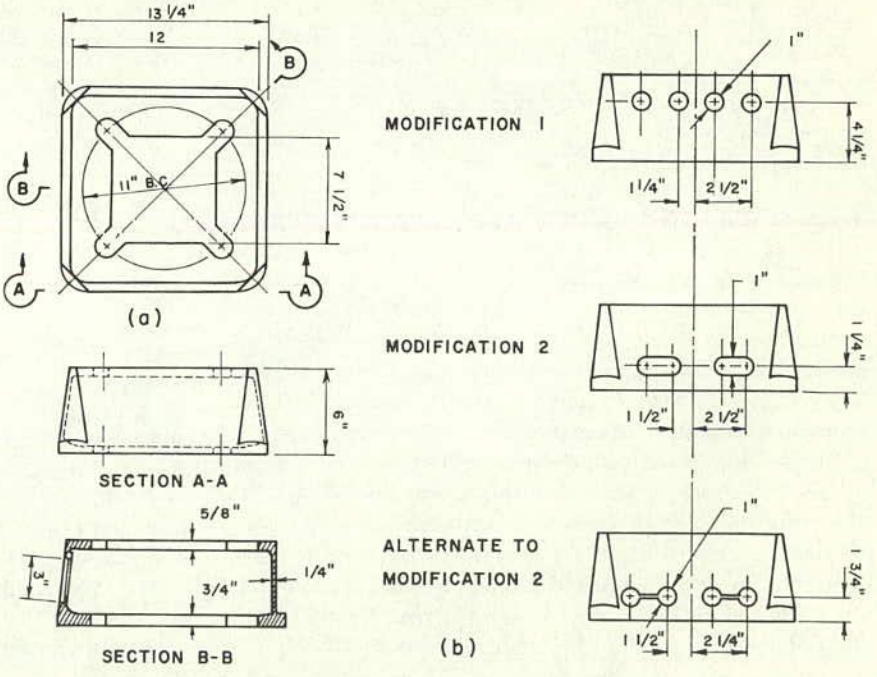

Figure 9. Cast aluminum insert.

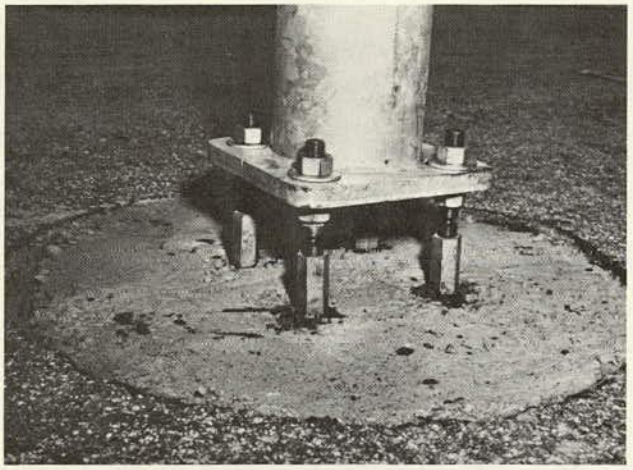

(a) BEFORE TEST

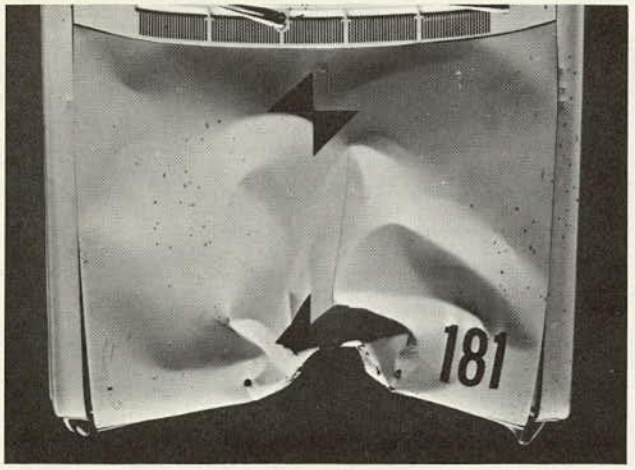

(b) VEHICLE DAMAGE

Figure 10. Notched steel bolt insert. (Photo courtesy California Division of Highways.)

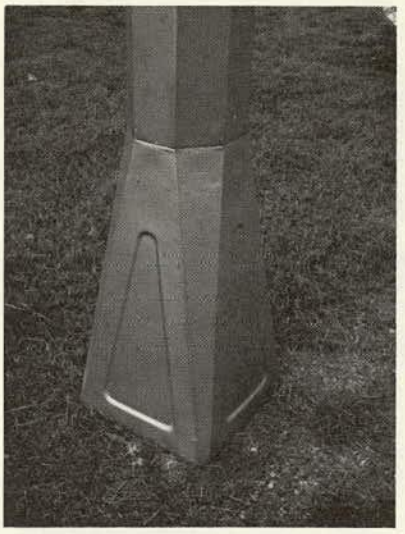

(a) BASE

(b) TEST

Figure 11. Stainless steel progressive-shear base. (Photos courtesy Millerbernd Manufacturing Company.)

luminaire supports. The progressive-shear base, developed by the Millerbernd Manufacturing Company, is a direct response to Minnesota's requirements.

Figure 11 shows this base in the first configuration subjected to full-scale tests. The base has since undergone several design modifications. The complete assembly, base and shaft, was fabricated from stainless steel (a 30-ft-high version weighs only 165 lb). The transformer base is riveted to a base plate with stainless steel rivets. The rivets act as shear pins which allow the shearing strength of the base to be controlled. In later designs, the rivets have been replaced with button welds.

Full-scale collision tests on this support were conducted by the Millerbernd Manufacturing Company (*8*, p. *5*). The tests consisted of having an automobile, traveling at 20 mph, collide with a 30-ft mounting height, 15-ft davit arm pole. A 50-lb simulated luminaire was used. As the vehicle struck the pole, the transformer base sheared from the base plate, releasing the shaft. The shaft fell on the vehicle roof, doing negligible damage (slight indentation). There was no damage to the bumper or hood. A new transformer base was attached to the undamaged shaft, and the assembly was erected for a second test. The driver of the test vehicle reported that he thought the impact was minor and similar to that felt when driving through a puddle of water.

A design for a carbon steel transformer base using the progressive-shear principle has been developed by Millerbernd (Fig. 12). The sheet metal base is attached to a steel base plate by 32 button welds at the lower corners. A test similar to that previously described (the same vehicle was used) was conducted using a 30-ft mounting height steel shaft. The resulting damage to the base is shown in Figure 12(b). Minor damage was done to the vehicle. The driver of the test vehicle reported no physical discomfort

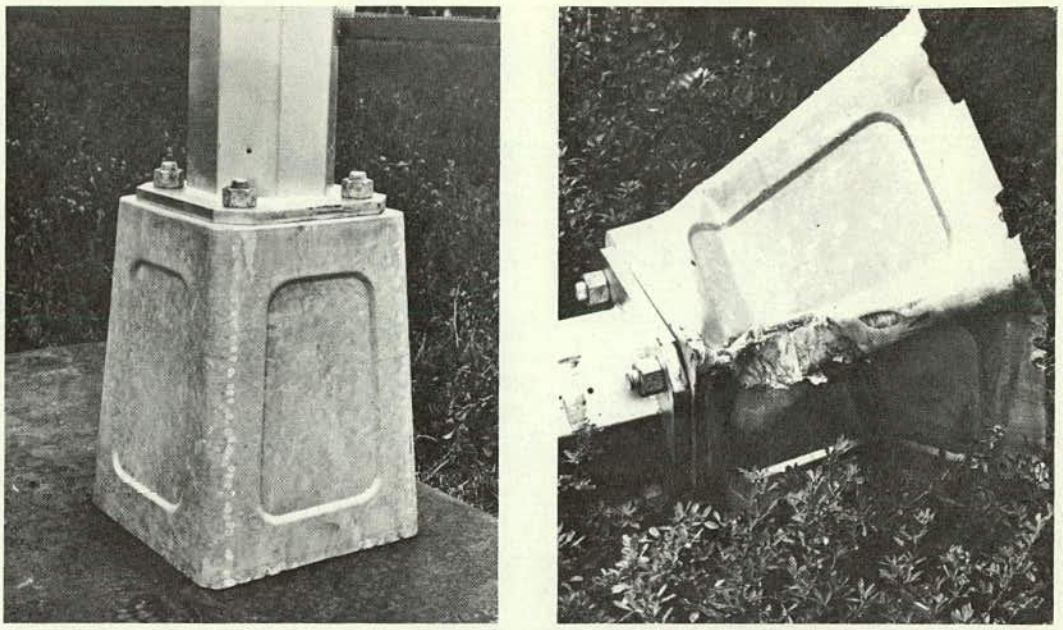

(a) BEFORE (b) AFTER

Figure 12. Carbon steel progressive-shear T-base. (Photos courtesy Millerbernd Manufacturing Company.)

due to the collision force. No quantitative data concerning change in velocity or deceleration were recorded in the Millerbernd test (*9*).

Cast Aluminum Shoe Base

Accident experience with aluminum shafts on cast aluminum shoe bases has indicated that these supports produce safe collisions. To obtain a quantitative measure of the severity of collisions with this type of support, several tests were conducted by the research agency and the Texas Highway Department in cooperation with the Bureau of Public Roads (*6*, p. 26). Tests have also been conducted by the General Motors Proving Grounds and the aluminum industry. The Texas tests are significant inasmuch as they were conducted on 40-ft mounting height supports, whereas the others were on 30-ft supports.

Table 1 gives the results of the Texas tests on one support. Failure occurred by the crushing of the shaft on the impact side at the vehicle bumper height and subsequent fracture of the cast aluminum flange (Fig. 13). When the shaft crushed, a hook was formed which caught on the front bumper, which gave the support a forward and a downward motion so that it struck the vehicle top. The pole stayed in contact with the vehicle for approximately 45 ft beyond the point of initial contact (*6*, p. 26). It appears from this one test that although a survivable accident occurred, the severity was the highest of all the accidents occurring with the "safe" supports tested in the TTI series.

Selection of Concepts for Evaluation

All seven broad classifications of concepts for safe luminaire supports are based on the guidelines established by the Road Research Laboratory; i.e., that some type of breakaway device be incorporated at the base of the support near ground level.

Study of the concepts showed that bases which are not integral with the shaft or are not frangible (transformer bases, inserts, and slip bases) have certain advantages over those that are integral with the shaft (shoe bases and thin sheet steel). If only the base is destroyed in performing its intended function, the shaft in many collision incidents is not destroyed and may be re-erected with minor repairs made in the field. The supports with integral bases are usually damaged to the extent that they cannot be reused without major shop repairs.

Of the seven basic concepts discussed, four require further attention by virtue of their performance or their acceptability. These are: (1) frangible (cast aluminum) transformer base, (2) progressive-shear base (stainless steel or carbon steel transformer base), (3) cast aluminum shoe bases, and (4) slip bases.

Acceptability by States

Table 2 is a summary of a survey of the state highway departments, conducted to ascertain the acceptability of the various concepts. The survey revealed that 30 states use or contemplate the use of a frangible transformer base in conjection with steel or aluminum shafts; one specifies the use of the progressive-shear principle in either stainless steel

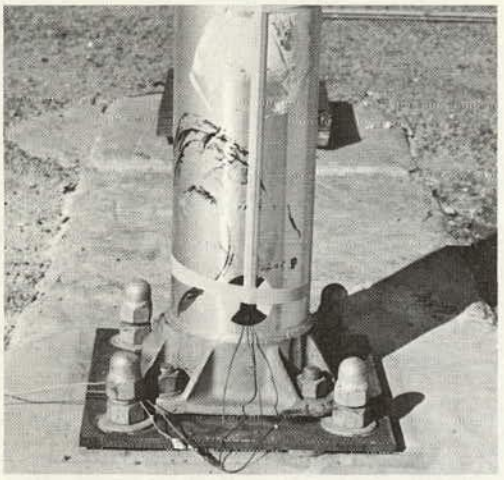

Figure 13. Aluminum shoe base (6).

davit-type supports or carbon steel transformer bases used with steel shafts; 12 use or prefer aluminum shoe base integral with an aluminum shaft; and 6 have shown interest in slip bases (either the General Motors or Texas Transportation Institute designs).

Because frangible transformer base and aluminum shoe base supported poles are in widespread use, their behavior in actual highway collisions is well documented. Because of the acceptability these supports have received, they are used as the basis for evaluating the other concepts.

Full-Scale Collision Tests

The controlled full-scale collision tests were conducted in such a manner that the concepts could be evaluated directly from the test results. Figure 14(a) shows the two cast aluminum insert bases tested (the construction of the bases differs). Figure 14(b) shows the triangular slip base. The base has 30° slot angles and was constructed with a 20° lifting cone to give the shaft a vertical velocity component at release. This was done to investigate a means of improving the low-velocity response of this type of base.

Figure 15 shows two types of progressive-shear bases. Figure 15(a) is a stainless steel base which was tested using the two stainless steel shafts shown. The transformer base, in Figure 15(b), supported a conventional steel shaft. These tests were conducted to evaluate this type of base for the three types of supports on which it can be used.

Figure 16 shows the two types of cast aluminum shoe bases that were tested. Four tests were conducted; two used conventional shoe bases. Figure 16(b) shows the details of a noticeably different type of shoe base. This base is cast with a riser which extends into the shaft. A structural connection is made with epoxy adhesive. This base was tested because it was apparent that its response would be different from the more conventional shoe base. A discussion of the bases tested appears in Appendix A and Appendix B.

All tests, except that with the triangular slip base, were conducted at a nominal vehicle velocity of 40 mph. Electronic and photographic instrumentation provided data from which vehicle velocity and deceleration could be obtained. Anthropomorphic dummies simulated a driver and front-seat passenger. All vehicles were of the same model year and had nominal weights of 3,600 lb.

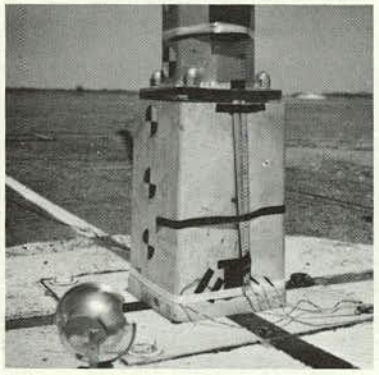

BASE B

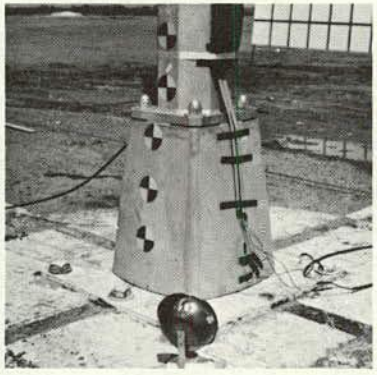

BASE A

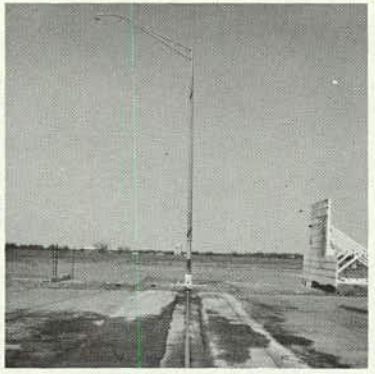

40' M.H.

(a) CAST ALUMINUM TRANSFORMER BASE

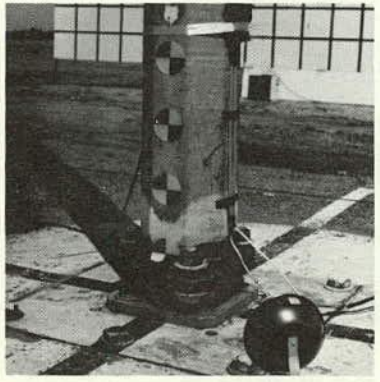

20° CONE

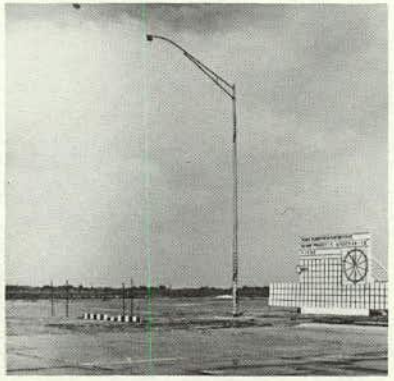

40' M.H.

(b) TRIANGULAR SLIP BASE

Figure 14. Aluminum T-base and triangular slip base.

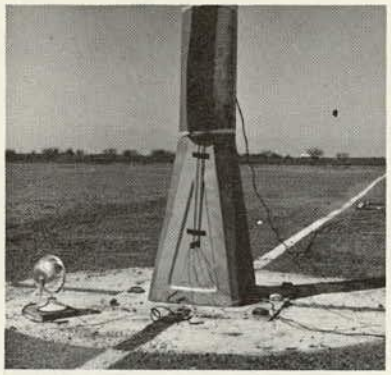

PROGRESSIVE SHEAR BASE

40 ft. M.H. DAVIT

40 ft. M.H.

(a) STAINLESS STEEL SUPPORTS

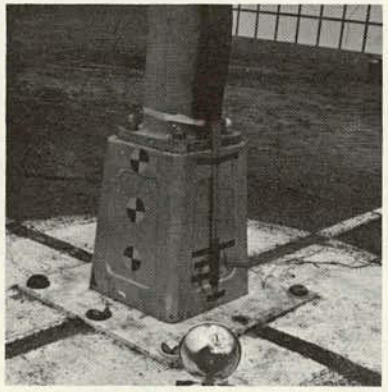

40 ft. M.H.

(b) CARBON STEEL PROGRESSIVE SHEAR BASE

Figure 15. Progressive-shear bases.

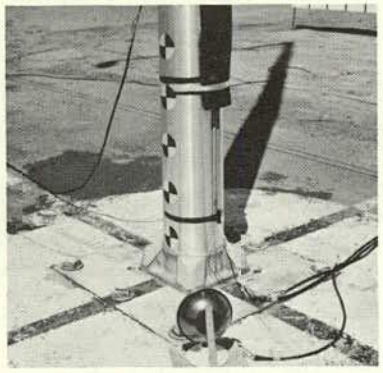

ALUM. SHOE BASE

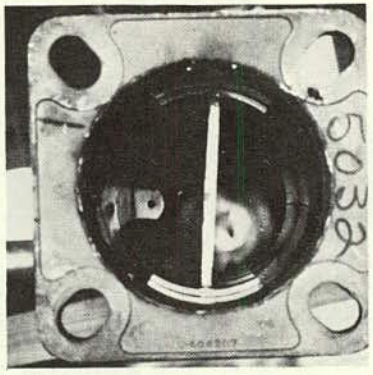

MODIFIED SHOE BASE

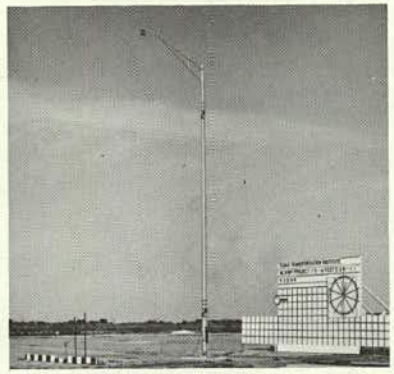

40' ft. M.H.

(a) CAST ALUMINUM SHOE BASE

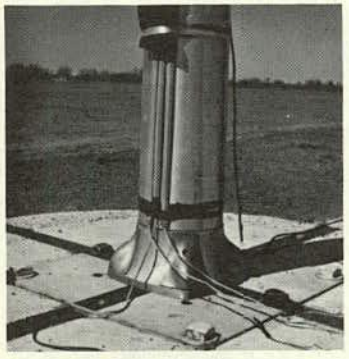

EXTERIOR

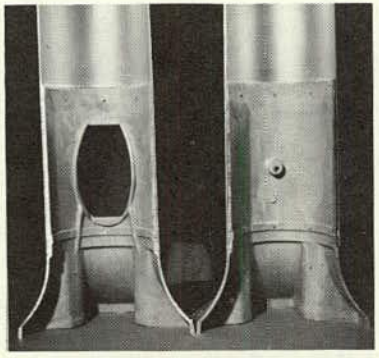

INTERIOR

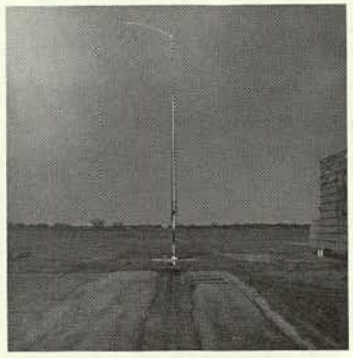

30 ft. M.H.

(b) CAST ALUMINUM SHOE BASE WITH INTEGRAL RISER

Figure 16. Aluminum shoe bases.

TABLE 2

SUMMARY OF STATE SURVEY

								COSTS			NEW CONCEPTS					ACCIDENTS		
STATE	DATE RECIEVED	DRAWINGS SUBMITTED	TYPE SUPPORT NOW BEING USED	MAX. MOUNTING HEIGHT (FT.)	SUPPORT LOCATION (FT.)	LUMINAIRE SIZE (WATTS)	MAX. LUMINAIRE ARM LENGTH (FT.)	BASE ($)	SUPPORT ($)	REPLACEMENT ($)	DRAWINGS	TYPE	MATERIAL	TRAFFIC (VEH./MI.)	RAN-OFF-ROAD	FATAL W/LUM. SUPT.	FATALITIES (PER ACCIDENT)	NOTES
ALABAMA	10/23/67	NONE	AL. POLE ON SHOE BASE	---	-----	-----	15.0	---	------	---	---	------	---	750,000,000	133 (1966)	0	0	-------
ALASKA	11/24/67	NONE	NO DETAILS	---	-----	-----	---	---	------	---	---	------	---	-------	---	---	---	NEW CONCEPT UNDER DEVELOPMENT, NO DETAILS
ARIZONA	4/15/68	YES	T-BASE AL 356 T4 SG 70A-T6. SLOTTED SLIP PLATE (TTI)	50	11'OR LESS	750	---	75	150-250	350	---	------	---	2,658,457	415	0	0	
ARKANSAS	4/8/68	NONE	------	---	-----	-----	---	---	------	---	---	------	---	747,636,435	175	0	0	
CALIFORNIA	4/11/68	YES	T-BASE ASTM 356 SG 70A-T4 OR T6	400	10'	700 ASA H35-18NA	15.0	25-50	150-175	100	---	------	---	27,717,000,000	15,662	28	1	316 INJURY ACCIDENTS, 444 PERSONS INJURED.
COLORADO	4/18/68	YES	T-BASE ASTM B-26 SG 70A-T6	40.0	10'	700	10.0	(30'MH)	420 (40'MH)	70	---	------	---	-------	---	---	---	-------
CONNECTICUT	5/13/68	NONE	T-BASE 6061-T6 OR 6063-T6 SHOE BASE	40.0	4'-20' FROM SHOULDER	1000	15.0	250	250	125	---	*	---	2,512,211,130	991	6	1	*HIGH LEVEL ILLUMINATION
DELAWARE	-----	----	------	---	-----	-----	---	---	------	---	---	------	---	-------	---	---	---	-------
FLORIDA	4/9/68	YES	T-BASE AL. 356-T4 SG 70A-T6 AL. POLE ON SHOE BASE STEEL T-BASE W/AL. INSERT	---	4'FROM PVMT.	400	15.0	---	525	**	YES	TRANS. & INSERT 356-T4 SG 70A	---	2,491,636,000	1,095	1	1	**MAINTENANCE BY LOCAL AUTHORITIES
GEORGIA	10/8/67	NONE	T-BASE	---	-----	-----	---	70	240	120	*	*	*	1,299,000,000	---	---	---	*NO NEW DESIGN CONCEPTS CONTEMPLATED
HAWAII	11/13/67	NONE	AL. POLE ON SHOE BASE AL. POLE ON AL. T-BASE STEEL POLE ON AL. T-BASE	---	2' 12' FROM PVMT.	-----	---	50	180	630	NONE	*BREAK-AWAY ANCHOR BOLTS	---	85,000,000	3	0	0	*WELD-RITE CO. 4417 OAKPORT ST., OAKLAND, CALIF.
IDAHO	11/3/67	NONE	AL. POLE ON SHOE BASE	---	-----	-----	15.0	---	274	243	*	*	*	372,000,000	---	---	---	*ALL FUTURE LUMINAIRE SUPPORTS TO BE ALUMINUM ON SHOE BASE.
ILLINOIS	10/27/67	YES	6063-T6 AL. TUBE 6061-6062-T6 AL. EXTRUSION CAST AL. T-BASE	46	14'-18' FROM PAVEMENT 8' TO CURB	-----	15.0	---	385-500	75-100	*	*	*	4,515,000,000	913	6	1.0	*NO NEW CONCEPTS CONTEMPLATED.
INDIANA	4/10/68	YES	STEEL OR AL. POST CAST AL. T-BASE	40	20'-30' FROM PAVEMENT	400 AT 30' M.H. 1000 AT 40' M.H.	25.0	---	------	---	---	------	---	3,061,000,000	---	---	---	-------
IOWA	4/18/68	YES	CAST AL. T-BASE	40	15' FROM PVMT.	400	15.0	85	190	---	*	*	*	-------	---	---	---	*INCREASE DISTANCE FROM PAVEMENT
KANSAS	10/24/67	YES	6063-T6 POLE, ASTM B-108-SG 70A-T6 T-BASE. ASTM B-108-SG 70A-T6 INSERT SSA-F	35	10'-15' FROM PAVEMENT	-----	0-15	100 INSERTS	900-1100	---	*	*	*	-------	187	7	9	*NO NEW CONCEPTS CONTEMPLATED.
KENTUCKY	4/11/68	YES	STEEL POLES AL. T-BASE AL POLES AL. T-BASE ASTM B-108 OR B-26 SG 70A-T6	40	UP TO 30' FROM PAVEMENT EDGE	400-700	0-25	75	140 (ST. 30'MH) 310 (ST. 40'MH) 375 (AL. 40'MH)	390	*	*	*	-------	---	---	---	*NO NEW CONCEPTS CONTEMPLATED.
LOUSIANA	10/19/67	YES	STEEL SHOE BASE W/ INSERT B-108 SC 70A T6 T-BASE	415	15' FROM PAVEMENT	700	15.0	---	------	---	*	*	*	-------	---	---	---	*NO NEW CONCEPTS CONTEMPLATED.
MAINE	4/26/67	YES	T-BASE	40	2'6" FROM SHOULDER	-----	10-15	---	500 (POST & BASE)	175	*	*	*	490,000,000	4.71	0	0	*NO SPECIFIC DETAILS PRESENTED.
MARYLAND	4/22/67	NONE	STEEL, CAST AL. INSERTS OR T-BASE	40	30' FROM PAVEMENT	700	30	165 (700 W) 165 (400 W)	309-352 (700 W) 224-273 (400 W)	750 (700 W) 674 (400 W)	---	------	---	2,181,308,322	1,028	10	1.1	-------

								COSTS			NEW CONCEPTS					ACCIDENTS		
STATE	DATE RECIEVED	DRAWINGS SUBMITTED	TYPE SUPPORT NOW BEING USED	MAX. MOUNTING HEIGHT (FT.)	SUPPORT LOCATION (FT.)	LUMINAIRE SIZE (WATTS)	MAX. LUMINAIRE ARM LENGTH (FT.)	BASE ($)	SUPPORT ($)	REPLACEMENT ($)	DRAWINGS	TYPE	MATERIAL	TRAFFIC (VEH./MI.)	RAN-OFF-ROAD	FATAL W/LUM. SUPT.	FATALITIES (PER ACCIDENT)	NOTES
MASSACHUSETTS	4/15/68	YES	AL POLE B-235-GS10A-T6 AL SHOE BASE OR T-BASE	50	14' FROM PVMT	1000	15.0	100-125	325-475	150	YES	*	STEEL	-------	0	11	0	*80'± TOWER LIGHTING
MICHIGAN	4/23/68	YES	AL. T-BASE ASTM B-26 OR B-108 SG 70A-F, SLOTTED STEEL PLATE (GM)	45	12' ON RAMP 16'-8" ON FWY	400-1000	17.0	30	500-900 W/FDN.	---	*	*	*	4,437,000,000	---	---	---	*NOW USING G.M. PROVING GROUND BASE.
MINNESOTA	4/15/68	YES	AL. (6063 OR 6061-T6) W/ 3337-T6 T-BASE STRAIN-LESS (16GH TY 304)	40	14 FROM PAVEMENT	400	12.0	---	AL. 200 SS 200	AL. 45	---	------	---	--------	---	---	---	----------
MISSISSIPPI	5/21/68	YES	AL OR STEEL POLE W/A356 T6 CAST AL OR A-126-42 CL A. (GREY IRON CASTING T-BASE)	50	16' FROM PAVEMENT	275-400	15.0	---	795 W/BASE	150	*	*	*	--------	---	---	---	*THE CAST-IRON CAN BE CONSIDERD A NEW CONCEPT.
MISSOURI	4/9/68	YES	AL. POLE SHOE BASE AL. T-BASE (B-108-66 SG 70A-T6) STEEL POLE SHOE BASE AL T-BASE B-108-66 SG 70A-T6	30	10' FROM PAVEMENT	400	15.0	350 W/BASE	250	250	---	-------	---	11,183,227	813	0	0	----------
MONTANA	10/18/67	YES	AL POLE (AL 6063-T6) CAST AL. 356 ALLOY SHOE BASE	47	10 FROM SHOULDER	-----	15.0	---	500	---	*	*	*	333,000,000	---	---	---	*NO NEW CONCEPTS CONTEMPLATED
NEBRASKA	---	---	-----	---	-----	-----	---	---	-----	---	---	-------	---	--------	---	---	---	----------
NEVADA	10/27/67	YES	Fy=40,000 PSI 11GA STEEL POLE 6" AL INSERT	---	6 FROM SHOLD 10 FROM PVMT	-----	15.0	25	140	90	YES	INSERT	AL. ALLOY	--------	---	---	---	----------
NEW HAMPSHIRE	10/27/67	YES	AL. POLE ON AL SHOE BASE	---	-----	400	---	125	375	---	*	*	*	367,000,000	4	0	0	*NO NEW CONCEPTS CONTEMPLATED.
NEW JERSEY	4/9/68	YES	6063-T6 SHAFT-ASTM B-108 AL T-BASE	26	4.5' FROM SHOULDER	250	15.0	24	93	275	*	*	*	35,535,000,000	0	0	0	*NO NEW CONCEPTS CONTEMPLATED
NEW MEXICO	4/8/68	YES	(ASTM B-108-62T SG 70A-T6) T-BASE (ASTM 356-T4) 6" INSERT ON STL. & AL. POLES	45	2' FROM SHOULDER	400-1000	18.0	45 INSERT	500	---	NO	NONE	---	--------	---	2	---	----------
NEW YORK	4/18/68	NONE	6063-T6 AL SHAFT W/CAST AL. T-BASE	30	14' FROM EDGE OF PVMT.	400	15.0	---	400-650 W/BASE	---	---	*	---	56,349,000,000	---	---	---	*ALL FUTURE SUPPORTS TO BE ALUMINUM
NORTH CAROLINA	8/7/68	YES	AL POLE ON 356-T6 SHOE BASES, STEEL POLES ON 356-T4 T-BASES	32	12' FROM EDGE OF PVMT.	500	15.0	---	700 COMPLETE	---	*	*	*	26,616,000,000	591	---	1.18	*SHOE BASES AND FRANGIBLE T-BASES
NORTH DAKOTA	4/9/68	YES	*STEEL OR AL WITH STEEL OR AL. T-BASES OR SLIP BASE (TTI)	40	2' FROM SHOULDER	700	15.0	---	* 297 (250W) 310 (400W)	---	YES	TTI SLIP BASE	STEEL	276,136,096	100	0	0	* INCLUDES METALLIC POLE, BASE AND MAST ARM, LAMP, LUMINAIRE, INTERNAL WIRING & LABOR, MATERIAL & EQUIPTMENT FOR INSTALLATION.
OHIO	6/17/68	YES	STEEL OR AL SHAFT WITH (ASTM B-26 OR B-108 SG 70A-T6) T-BASE	50	12'-30' FROM EDGE OF PVMT.	400-1000	30.0	80-160	320-800	---	---	---------	---	-------	406	1	---	T-BASE NOT CONSIDERED FEASIBLE FOR ARM LENGTHS OVER 25' OR M.H. IN EXCESS OF 40'
OKLAHOMA	11/1/67	YES	STEEL POLES (fy=48,000 PSI) W/AL T-BASE (356F OR B-108 SG 70A-T6	40	6-16 FROM PAVEMENT EDGE ON LEFT 10-16 FROM PAVEMENT EDGE ON RIGHT	400	15.0	55	218-290 COMPLETE	200	NO	NONE	---	*	*	*	---	*NONE
OREGON	4/10/68	YES	STEEL POLE W/SLIP BASE OR AL. T-BASE	50	30 FROM SHOULDER	700-1000	15.0	---	------	---	YES	TTI SLIP-BASE	STEEL	1,754,370,000	544			
PENNSYLVANIA	4/17/68	YES	STEEL AND AL. POLES ON AL T-BASE	45	12 FROM PAVEMENT	400-1000	30.0	---	AL 295 STEEL 250	350	NO	*SLIP-BASE	---	2,640,234,070	---	1	1	*NOT TTI OR GM DESIGN
RHODE ISLAND	4/10/68	NONE	AL POLE ON AL SHOE BASE	35	6'-15" FROM PVMT.	400	15.0	---	-----	---	---	-----	---	-------	---	---	---	--------
SOUTH CAROLINA	4/10/68	NONE	AL POLE ON AL SHOE BASE	30	4' FROM SHLDR.	400	12.0	---	-----	---	NO	NONE	---	854,143,800	97	0	0	
SOUTH DAKOTA	4/2/68	NONE	*	---	-----	-----	---	---	------	---	NO	NONE	---	--------	---	---	---	*AS OF THIS DATE NO LIGHTING INSTALATIONS ON THE INTERSTATE SYSTEM.
TENNESSEE	4/5/68	NONE	CAST AL T-BASE ON ALL SUPPORTS NOT PROTECTED BY GUARDRAIL.	45	20' FROM EDGE OF PVMT.	700	15.0	---	-------	---	NO	NONE	---	1,374,000	296	---		---------
TEXAS	4/4/68	YES	AL. T-BASE AND INSERTS W/STEEL POLE AL. POLE W/SHOE BASE W/BARRIER	50	18 FROM EDGE OF PVMT.	400-1000	12.0	20-80	130-200	---	---	50' M.H.	---	--------	---	---	---	50' MH W/1000 W LUM. BEING USED MORE
UTAH	4/29/68	YES	AL T-BASE W/STEEL OR AL POLES SLIP BASE W/STEEL POLE	48	20' FROM EDGE OF PVMT.	-----	20.0	---	------	---	---	GM SLIP BASE	---	1,818,425 PER DAY	11	---	---	*NO INSTALLATION ON INTERSTATE TO DATE
VERMONT	10/20/67	YES	AL. (6063-T6 OR ASTM B-221) OR A242 POLES W/AL. (356 ALLOY) T-BASE	---	-----	-----	---	PART OF POST COST	600	---	NO	NONE	---	--------	---	---	---	----------
VIRGINIA	10/23/67	YES	AL POLE ON AL. SHOE BASE	30	12 FROM PAVEMENT	250	15.0	PART OF POST COST	365	---	NO	T-BASE	HAPCO OR UNION METAL		1,481	0	0	----------
WASHINGTON	-----	YES	STEEL POLE W/SHOE BASE OR AL. T-BASE.	30	12' FROM PAVEMENT	400	16.0	---	-----	---	---	------	---	--------	---	---	---	--------
WEST VIRGINIA	4/11/68	YES	AL T-BASE OR AL. POLE W/SHOE BASE AL BASE OR AL POLE W/SHOE BASE	30	-----	-----	---	---	-----	---	NO	NONE	---	--------	---	1	1	--------
WISCONSIN	4/11/68	NONE	AL T-BASE W/AL STEEL POLES OR AL INSERT W/STEEL T-BASE	50	4' FROM SHLDR.	400-1000	24.0	54	782 (50' MH) 437 (32' MH)	---	---	-----	---	--------	---	1	1	*COMPLETE INSTALATION
WYOMING	4/9/68	YES	AL. POLE W/AL. SHOE BASE	40	15' FROM PVMT.	400-1000	20.0		500	700	---	-----	---	130,000,000	1,479	1	3	*NEW CONCEPTS CONTEMPLATED
DISTRICT OF COLUMBIA	10/25/67	NONE	AL. T-BASE OR AL. INSERT.	---	-----	-----	---	43	-----	---	---	*	---	178,000,000	---	2	2.5	*NEW CONCEPTS CONTEMPLATED

CHAPTER TWO

RESEARCH FINDINGS

FINDINGS FROM FULL-SCALE TESTS

A total of 11 tests were conducted: 10 were for the purpose of concept evaluation, and one (Test 538–1) was to further the state-of-the-art in the collision dynamics of luminaire supports. Table 3 lists (according to the concept groupings) the supports that were subjected to full-scale tests.

Frames from the high-speed motion picture film at selected times during the collision events for the tests appear in Appendix D.

Table 4 gives the pertinent data for each test, including the vehicle response and damage. Two types of sensors were used to determine vehicle velocity data: electronic switchstrips and high-speed motion picture films. The velocity data in Table 4 (V_i, V_f, ΔV_f, ΔV_{lc}) were derived from the film data. Only the film-derived data are shown, for two reasons: (1) these data were felt to be more reliable than the electronic-derived data and (2) a continuous time-velocity record could be obtained using the film information, whereas only information at specific points in time was available with the electronic-derived data. Comparison of the data calculated from the electronic sensors and other pertinent test data appear in Appendix A.

The velocity, ΔV_{lc}, is the change in vehicle velocity calculated at the time the vehicle lost contact with the support. The vehicle deformation is the total crushing and does not include any recoverable deformation. The vehicle dollar damage was obtained from estimates made by an independent licensed auto damage appraiser. The vehicle decelerations shown are the average of two accelerometers which were mounted on the vehicle.

All tests except Test 538-1 (the prestressed concrete support) produced safe collisions. The prestressed concrete shaft behaved essentially as a fixed object, completely stopping the vehicle.

Table 5 gives the response of the support as reflected in its rotation about its longitudinal axis, observed damage, and coordinates of the point farthest from the vehicle line of travel. The X coordinate indicates the lateral movement of the shaft toward the traveled lanes. In all cases, the steel shafts (Tests 538-6, 7, 13, 8, and 10) were bent when the mast arm hit the ground. This appeared to be caused by a high bending moment induced at the lower mast arm mounting flange. This did not appear to be a problem with the stainless steel davit arm shaft (Test 538-9) or the aluminum shafts (Tests 538-4, 11, 12, and 5). This is possibly due to the lower mass and high material yield stress. It should be noted that the carbon steel shafts had 15-ft arms, and that the arms on the aluminum and stainless steel supports were 10 ft in length. Note that the lateral translation of the support (X coordinate) for the aluminum shafts (Tests 538-11 and 12) can be quite large. This is due to the rebound of the shaft when it hits the ground. This was not noted in Test 538-4 owing to the high collision resistance and subsequent low trajectory of the shaft (see Figs. D-6, D-7, and D-8).

The shaft fell along a line in the direction of vehicle motion in all cases, even though considerable lateral translation may have occurred. In each test, the structure experienced clockwise (when viewed from the top) angular motion about the post longitudinal axis. This always occurs for the support with the single luminaire arm, owing to the torques about the principal axes of inertia.

It should be recognized that the results of these tests are for a specific set of collision circumstances. Although the responses are indicative of what to expect in the greatest majority of collisions, anomalies could occur with various vehicle types, angles of collision incidents, roadside terrain, etc. One should not be surprised if every collision, with supports similar to those tested, does not produce identical results.

FINDINGS FROM LABORATORY AND ANALYTICAL INVESTIGATIONS

Laboratory Tests

Laboratory tests were conducted on the various base concepts to obtain basic data on their static and dynamic behavior (see Appendix B). Impact tests yielded information on the dynamic load-deformation properties for the two types of cast aluminum transformer bases, the cast aluminum shoe base with integral riser, and the progressive-shear transformer base, from which the fracture energy for each base was calculated. These values were correlated with the full-scale tests with the intent of establishing a test method for the laboratory evaluation of base concepts. The dynamic tests were conducted with a 1,000-lb pendulum falling from an effective height of 14 ft 10 in. The point of contact was 14 in. above the mounting test floor (this dimension was chosen to be compatible with the bumper height of the 1958 Fords used in full-scale tests). Table 6 gives the results of two tests on each sepcimen, and the results of similar tests, conducted by ALCOA, on aluminum shoe base supports (*10*). The ALCOA tests were conducted using a drop weight to fracture the bases. Nominally 25-ft-long poles were attached to the bases, and the pole and base assembly were mounted horizontally for testing.

Base fracture energies derived from laboratory tests were correlated with the results of the full-scale tests to establish the validity of their use as a measure of energy absorbed by the base in a full-scale test. By writing an energy balance equation for the vehicle, base, and support system, the change in vehicle velocity could be calculated. This calculated velocity was compared with the measured velocity

TABLE 3

SUMMARY OF TESTS [a]

CONCEPT	TEST NO.	BASE MATERIAL	MANUFACTURER IDENT.	SHAFT HT. (FT)	SHAFT MATERIAL	SHAFT CONFIG.	MOUNTING HEIGHT (FT)	MAST ARM (FT)	COLLISION VELOCITY (MPH) [b]	REMARKS
Frangible transformer base	538-6	Cast al. B-108-62T SG70AT6	A.B. Chance UDP-46	35	Steel	Straight	40	15	43.8	Comparison of basic concept
	538-13	Cast al. A356-T6	A.B. Chance UDP-521	35	Steel	Straight	40	15	39.5	Comparison of basic concept
Progressive-shear base	538-9	201 Stainless	Millerbernd SDS-9-400	40	Steel	Davit	40	9	37.4	Comparison of basic concept
	538-7	201 Stainless	Millerbernd SDS-9-400	35-5″	S. steel	Straight	40	9	43.1	New design mast arm type stainless shaft
	538-8	Galvanized sheet steel	Millerbernd Type B	35	Steel	Straight	40	15	44.0	Comparison of basic concept
Cast aluminum shoe base	538-4	Cast al. A 356-T6	Kerrigan 709 028	37	Al.	Straight	40	10	37.7	Heavy wall shaft
	538-11	Cast al. A 356-T6	HAPCO 50706-063	37-2″	Al.	Straight	40	10	40.8	Heavy wall shaft
	538-12	Cast al. A 356-T6	HAPCO 50706-063	37	Al.	Straight	40	10	39.1	Thin wall shaft reinforced against buckling
	538-5 [c]	Cast al. A 356-T6	Kaiser AT-50	28	Al.	Straight	30	6	42.2	New concept of cast shoe base
Slip base	538-10 [d]	Steel A 441	Tex. Trans. Inst.	35	Steel	Straight	40	15	28.0	Comparison of basic concept
—	538-1	—	Union Metal 810-V	37	Prstr. Conc.	Straight	35.75	10	38.8	State-of-the-art

[a] All supports used 50-lb simulated luminaires; all vehicles were 1958 Fords.
[b] From film data.
[c] 30-ft mounting height as opposed to 40-ft in other tests.
[d] 28 mph collision velocity.

TABLE 4

SUMMARY OF VEHICLE RESPONSE

TEST NO.	VEH. WT. (LB)	VEH. VEL. (MPH) [a] V_i	V_f	ΔV_f	ΔV_{lc}	t_{lc} [b] (SEC)	VEH. DEFOR. (IN.)	VEH. DAMAGE ($)	VEH. g (AVG. OF 2)
538-6	3580	43.8	36.7	−7.1	−5.6	0.069	14	397	14.7
538-13	3340	39.5	32.5	−7.0	−5.7	0.140 [a]	16	459	8.9
538-9	3480	37.4	30.3	−7.1	−7.0	0.123	16	491	10.8
538-7	3880	43.1	35.3	−7.8	−6.5	0.167	16	427	15.0
538-8	3620	44.0	37.3	−6.7	−5.9	0.080	15	427	10.1
538-4	3700	37.7	28.3	−9.4	−9.3	0.098	20	838	15.0
538-11	3580	40.8	33.7	−7.1	−6.0	0.105	17	484	5.9
538-12	3940	39.1	31.8	−7.3	−6.6	0.182	16	548	8.7
538-5	3820 [c]	42.2	38.2	−4.0	−2.4	0.075	11	382	8.8
538-10	3340 [d]	28.0	22.1	−5.9	−3.7	0.084	9	383	6.5
538-1	3660	38.8	0	−38.8	—	0.524	17	1601	—

[a] From film data; V_i = vehicle velocity at contact; V_f = vehicle velocity at rear tapeswitch set; ΔV_{lc} = change in vehicle velocity at loss of contact; and ΔV_f = change in vehicle velocity at rear tapeswitch.
[b] t_{lc} = time after impact when contact was lost.
[c] 30-ft mounting height.
[d] Note 28 mph collision velocity.

TABLE 5

SUMMARY OF SHAFT RESPONSE

TEST NO.	COORDINATE OF SUPPORT POINT FARTHEST FROM VEH. TRACK [a]			ROTATION OF ARM (°) [c]	DAMAGE	
	POINT	X (FT)	Y (FT)		SHAFT	MAST ARM
538-6	Q	7	45	200	Slight bow	Total
538-13	P	7.5	5	180	Slight bow	Total
538-9	R	15	25	200	None	None
538-7	P	9	13	210	Slight bow	Severe bend
538-8	P	7	11	190	Slight bow	Total
538-4	R	7	15	180	Fractured, no bow	None
538-11	R	27 [b]	9.5	210	Fractured, no bow	None
538-12	P	7	15	190	Fractured, no bow	Bent
538-5	P	7	16.5	180	Buckled, no bow	None
538-10	P	5	7.5	160	Slight bow	Severe bend

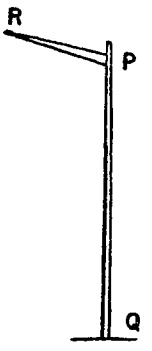

[a] Origin at base of support. X is normal to vehicle track and (+) to left. Y is along vehicle track and (+) on upsteam side of base.
[b] Caused by rebound on ground impact.
[c] In a clockwise direction (when viewed from the top).

TABLE 6

SUMMARY OF STATIC AND DYNAMIC TESTS

DESCRIPTION	LOAD (LB)		$\frac{P_{dyn.}}{P_{static}}$	BASE FRACTURE ENERGY (FT-LB)
	PEAK STATIC	PEAK DYNAMIC		
Cast transformer bases:				
A.B. Chance UDP-521				
Test 1	23800	36702	1.54	8569
Test 2	21800	41700	1.91	10086
Avg.	22800	39201	1.73	9328
A.B. Chance UDP-46				
Test 1	34500	52817	1.51	8764
Test 2	30000	51937	1.73	7267
Avg.	32250	52377	1.62	8016
Progressive-shear base:				
Millerbernd Type B				
Test 1	17700	11040	0.63	6701
Test 2	13800	12375	0.90	8165
Avg.	15750	11708	0.78	7433
Cast shoe w/riser:				
Kaiser AT-50				
Test 1	18200	32547	1.79	6887
Test 2	—	33994	1.82	8270
Avg.	18200	33271	1.81	7579
Cast shoe base: [a]				
Test 1	—	27000	—	10500
Test 2	—	29000	—	11750
Avg.	—	28000	—	11125

[a] These values were obtained from ALCOA tests incorporating full-size poles. See Sharp and Young (*10*).

change from the full-scale test that employed bases for which the base fracture energy had been determined in the laboratory. Table 7 gives the results of the correlations for six tests. Note that the ratio of $\Delta V_{calc.}/\Delta V_{test}$ varies by approximately $\pm 25\%$. This variation can be attributed partly to inherent errors in the determination of the test value of ΔV and partly to the approximate nature of the equation used. Results, however, are within acceptable experimental tolerance and indicate that the laboratory-derived values of base fracture energy represent the energy absorbed in a full-scale test.

Further Development of the Triangular Slip Base

An attempt was made to improve the low-velocity collision response of supports using the triangular slip base. Laboratory model impact tests confirmed that the addition of a riser cone to the base, shown in Figure 17(a), would cause the shaft to have a vertical velocity component. It was anticipated that the added vertical velocity component would increase the maximum height of the support trajectory, and hence would allow the vehicle to clear the falling shaft. A full-scale test (Test 538-10) showed that although the riser cone performed as intended, the desired results were not achieved; the deformed front end of the vehicle restrained the vertical motion.

An analysis was made of the base to determine its resistance to applied shear and torsional moment about the longitudinal axis of the shaft. The resulting equations for the maximum shear and torque are summarized as follows:

For the maximum shear R_T,

$$R_T = R_1 + R_2 + R_3 \tag{1}$$

in which

$$R_1 = \frac{\mu T_1}{\beta}[(\sqrt{3} + \mu)\cos(\phi + \theta) + (\mu\sqrt{3} - 1)\sin(\phi + \theta)] + \mu T_1(\cos\theta + \sqrt{3}\sin\theta); \tag{2}$$

for $0° > \theta \geq 30°$,

$$R_2 = \frac{\mu T_2}{\beta}[\sqrt{3}\sin(\phi + \theta) - (1 + 2\mu)\cos(\phi + \theta)] - 2\mu T_2 \cos\theta; \tag{3}$$

for $\theta = 0°$,

$$R_2 = 2\mu T_2; \tag{4}$$

TABLE 7

CORRELATION OF BASE FRACTURE ENERGY WITH FULL-SCALE TESTS

TEST NO.	K_{test} (g/FT)	$(\Delta V_{lc})_{test}$ [a] (MPH)	β	$K = K_{avg.}$ [b] $(\Delta V_{lc})_{calc.}$ (MPH)	$K = K_{avg.}$ [b] $\frac{\Delta V_{calc.}}{\Delta V_{test}}$	$K = K_{test}$ $(\Delta V_{lc})_{calc.}$ (MPH)	$K = K_{test}$ $\frac{(\Delta V_{lc})_{calc.}}{(\Delta V_{lc})_{test}}$
538-6	12.6	−5.6	1.05	−3.9	0.70	−4.8	0.86
538-13	6.7	−5.7	1.26	−5.5	0.97	−4.7	0.83
538-8	6.8	−5.9	1.20	−5.1	0.86	−4.6	0.78
538-11	8.8	−6.0	1.46	−6.1	1.01	−6.1	1.01
538-12	6.5	−6.6	1.25	−4.6	0.70	−5.4	0.82
538-5	9.9	−2.4	1.09	−2.5	1.02	−2.7	1.06

[a] From film data.
[b] $K_{avg.} = 8.8$.

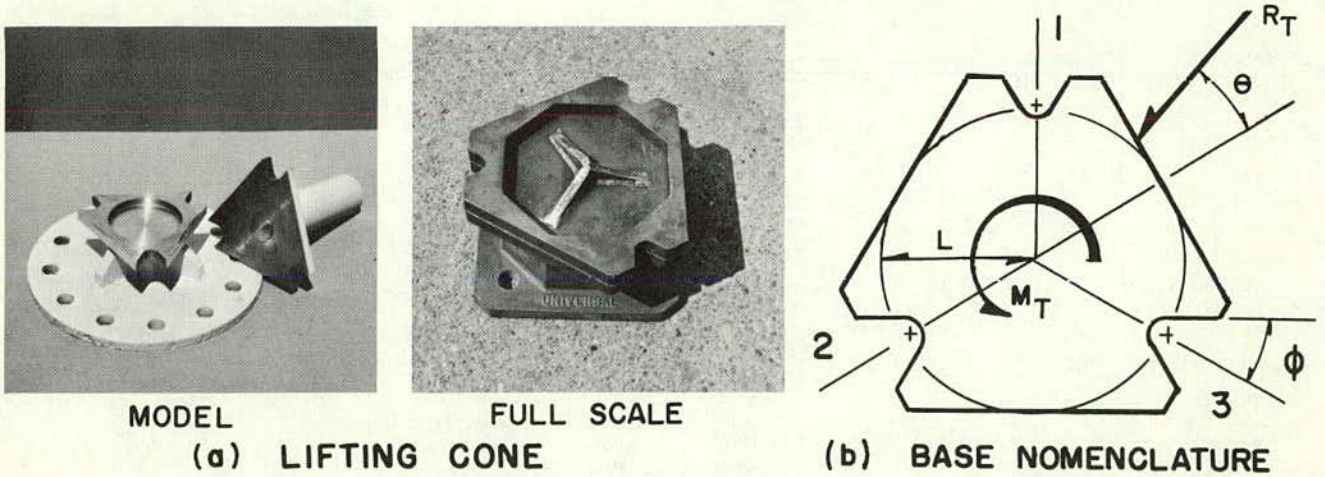

Figure 17. Triangular slip base.

and

$$R_3 = \frac{\mu T_3}{\beta}[(\sqrt{3} + \mu)\cos(\phi - \theta) + (\mu\sqrt{3} - 1) \sin(\phi - \theta)] + 2\mu T_3 \sin(30 - \theta) \quad (5)$$

In these equations,

μ = coefficient of friction;

T_1, T_2, T_3 = force in bolts 1, 2, and 3 (lb);

ϕ = slot angle;

θ = angle of applied force; and

$\beta = (\sin\phi - \mu\cos\phi)$.

For the maximum torque, M_T,

$$M_T = \frac{2\mu}{\beta}(T_1 + T_2 + T_3)[L\cos\phi + \mu(L\sin\phi - d/2)] \quad (6)$$

TABLE 8

EFFECT OF ϕ AND θ ON R_T AND M_T[a]

	R_T FOR		
θ	ϕ=20	ϕ=25	ϕ=30
0°	8.790T	4.970T	3.527T
30°	7.593T	4.151T	2.850T
M_T	84.84T	45.74T	30.97T

[a] $T_1 = T_2 = T_3 = T$; $\mu = 0.25$; $L = 6$ in.; and $d = 3/4$ in.

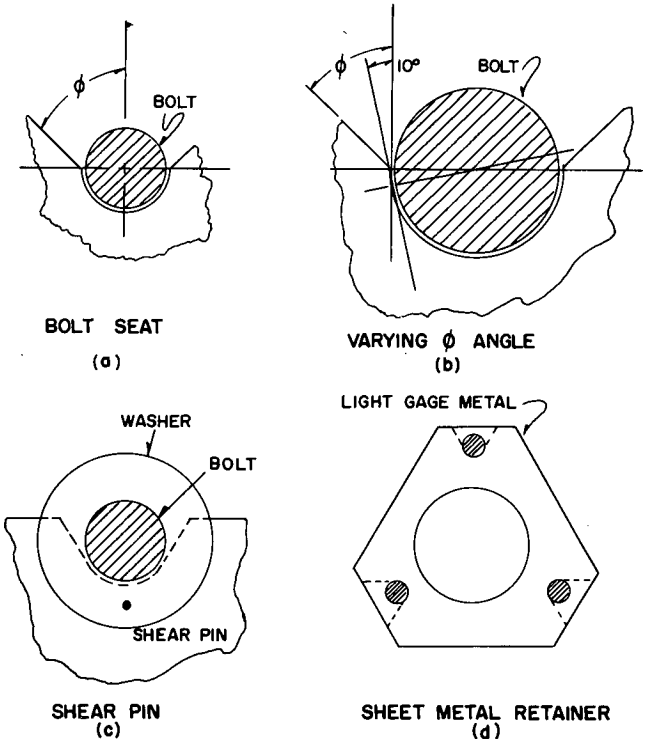

Figure 18. Modifications to slip base.

in which

L = radius of bolt circle (in.);

d = diameter of bolt (in.);

M_T = torque (in.-lb); and

T_1, T_2, T_3 = force in bolts 1, 2, and 3 (lb).

Table 8 gives the effects of ϕ and θ on R_T and M_T. It can be seen that as the slot angle ϕ becomes smaller the resistances increase. In the design of a base of this type it is desired to have the smallest possible value of R_T and the largest M_T. This requires that the slot angle or the bolt preload, or both, be varied to supply the resistance to the design torque. Because it is desired to have the smallest possible R_T, it is not practical to reduce ϕ to much less than 30°. Alternatives for increasing M_T without appreciably affecting R_T must be sought when high torsional loads must be registered.

It has been suggested that the slot be modified as shown in Figure 18(a). This solution is not practical because, under the action of a shear load, no scissor action could take place until either the bolt or plate was galled sufficiently to develop it. This would destroy the intended function if the support is to be reused after a collision.

Another solution is shown in Figure 18(b). This configuration would allow scissor action but would have the advantage of a small ϕ angle in the initial stages of slip (as given in Table 8, the value of M_T is increased as ϕ is decreased). Once the base slips, the ϕ angle would be larger and hence R_T would decrease. This solution would provide for a high torsional resistance but would not affect the value of R_T significantly. The alternatives will probably be required for those supports which support long mast arms and unusually large luminaires (those with a large aerodynamic profile).

Base Fracture Energy

The energy which would be absorbed to separate the base is dependent on the bolt forces, T_1, T_2, and T_3; the coefficient of friction, μ; the angles ϕ and θ; the depth of the slot; and the diameter of the bolts. The slot depth and bolt diameter determine the movement of the upper plate when the bolts disengage. Static laboratory tests have indicated that the bolt loads and the coefficient of friction vary as the plates slip. Therefore, it is considered conservative to consider the energy absorbed as

$$BFE \cong R_T(\phi, \theta, \mu, T)\left[\frac{S - (d/2)}{12\cos\phi}\right] \quad (7)$$

in which

$R_T(\phi, \theta, \mu, T)$ = peak resistance from Eq. 1;

BFE = base fracture energy (ft-lb);

T = nominal bolt load (lb);

S = depth of slot (in.); and

d = diameter of bolt (in.).

Consideration of Joint "Walking"

There has been some concern over the "walking" of the joint caused by wind-induced shaft vibrations. Two solu-

tions have been employed with the Cambridge base as tested by the Road Research Laboratory (*4*, p. 24). The first employs a shear pin through the washer and into the plate, as shown in Figure 18(c). The second, shown in Figure 18(d), uses a light-gauge metal retaining plate which is torn under the action caused by collision.

MATHEMATICAL SIMULATION

Rigid Body Model

Response of two models was investigated. The first model studied assumed the post structure to be a rigid body under the action of constant and time-varying forces, and the vehicle to be a spring-mass system having a single degree-of-freedom and capable of contacting the post at any angle in its plane of travel. The spring is assumed to be massless and incapable of restitution. The rigid mass and its velocity simulate the momentum of the vehicle. The energy absorbed by the vehicle is obtained from the spring force-deformation relationship.

Vehicle simulation is a vital part of the over-all problem, but present research is concerned mainly with the development of a model to simulate the response of the support structure.

The complete development of the rigid body model and the correlation of this model with crash test results have been previously reported (*11*).

Elastic Model

The second model studied was taken to be elastic and was obtained by using the matrix displacement method and a finite element formulation. The post system was idealized as an assemblage of beam elements. Each beam element was taken to have 12 degrees of freedom so that out-of-plane motion could be studied. The analysis was linear and is valid for small post rotation. It was assumed that the linear equations would apply as long as the post structure and the impacting vehicle were in contact. The post rotations become quite large after contact is lost, and a linear analysis is no longer valid.

The computer coding for this model allows for the determination of dynamic stresses and of natural frequencies of vibration.

Verification of the Mathematical Models

To obtain information to validate the models, a testing program was conducted. The test that was used for the purpose of correlation (Test 538-2) involved a 20-ft 4-in. OD steel pipe with a wall thickness of 0.24 in. and a base exhibiting breakaway characteristics. A simulator was used as the collision vehicle (see Fig. 19). Instrumentation employed to obtain the results of the test consisted of accelerometers on the simulator and high-speed photography.

Table 9 gives the results of the crash test and compares them with those obtained from the models. These results apply at the time when the post and vehicle lost contact. Table 10 gives a comparison of test and model results when the rigid-body model is used to simulate the trajectory of the structure after it has lost contact with the vehicle. Data

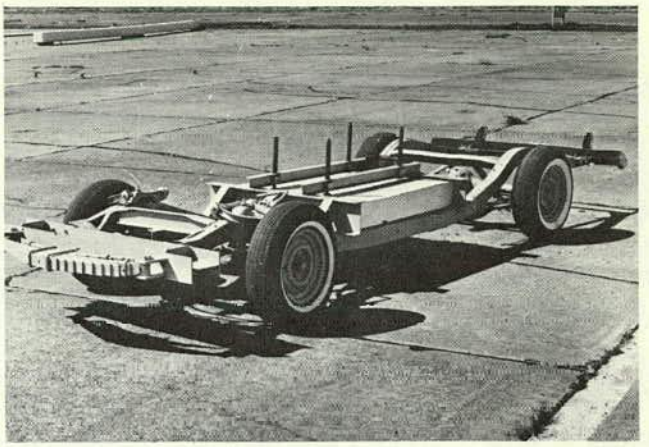

Figure 19. Vehicle simulator.

obtained from the elastic model were used as initial conditions to the rigid-body equations of motion that follow.

The results in Table 9 reveal that, as expected, the elastic model gives more accurate representation of the initial part of the event. However, the rigid model also gives satisfactory results that can be used to describe the response of the post structure. In addition, the rigid model requires much less computer time.

The results obtained from the first test were for a case exhibiting planar motion. To validate the models for the case of nonplanar motion, the results of Test 538-10 were used. These results are given in Tables 11 and 12.

The films of Test 538-10 showed that the post first loses contact with the vehicle after 40.0 millisec. The vehicle then apparently catches up with the post after a few additional milliseconds and the post seems to ride the front end of the vehicle until contact is finally lost after a total elapsed time of 84 millisec. The elastic model predicted similar initial contact time but contact with the vehicle was never regained. The rigid model predicted a single contact time of 86.4 millisec. It must be emphasized that idealization of the vehicle as a single degree-of-freedom system can introduce considerable error. This is more apparent when a full-size vehicle is employed; a considerable part of the discrepancies given in Tables 11 and 12 can be attributed to this. The values of the post rotation angle at the mass center given in Table 11 for the test and the elastic model represent the inclination of the post toward the vehicle as seen by the high-speed cameras. The rotation given for the rigid model corresponds to the Eulerian angle and gives a true measure of the inclination of the post for the assumptions made.

Table 12 gives a comparison of test results obtained when the rigid model is used to simulate the overall behavior of the post system. The results apply when the post strikes the ground on its return path after impact has occurred. The values of XX_P, XX_R, ZZ_P, ZZ_R, and YY_P correspond to coordinates of the Points P and R (see Table 5) when contact with the ground is made. The values missing in Table 12 could not be obtained from film data.

TABLE 9

COMPARISON OF RESULTS FOR TEST 538-2
AT TIME POST AND VEHICLE LOSE CONTACT

ITEM	VEHICLE VELOCITY (FPS)		VEHICLE TRANSLATION (FT)	POST ROTATION ANGLE AT MASS CENTER (°)	CONTACT TIME (MILLISEC)
	INITIAL	DECREASE			
Test	54.0	1.5	3.86	15.5	61
Elastic model	54.0	1.41	3.16	14.6	59.12
Rigid model	54.0	1.30	2.91	13.0	54.60

TABLE 10

COMPARISON OF RESULTS FOR TEST 538-2
AT TIME POST STRIKES REAR OF VEHICLE

ITEM	VEHICLE TRANSLATION (FT)	POST ROTATION ANGLE AT MASS CENTER (°)	TRANSLATION OF TOP OF POST (FT)	TIME TO HIT VEHICLE (MILLISEC)	TERMINAL CONDITION
Test	21.1	121	1.8	433	Post hits rear of vehicle with point 4.6 ft from top.
Model	20.5	123	0.4	391	Post hits rear of vehicle with point 4.6 ft from top.

TABLE 11

COMPARISON OF RESULTS FOR TEST 538-10
AT TIME POST AND VEHICLE LOSE CONTACT

ITEM	VEHICLE VELOCITY (FPS)		VEHICLE TRANSLATION (FT)	POST ROTATION ANGLE AT MASS CENTER (°)	CONTACT TIME (MILLISEC)
	INITIAL	DECREASE			
Test	41.1	2.7	1.6	2.2	40
		5.6	3.1	7.5	84
Elastic model	41.1	4.6	1.5	6.0	38.6
Rigid model	41.1	2.7	3.4	5.8	86.4

TABLE 12

COMPARISON OF RESULTS FOR TEST 538-10
AT TIME POST HITS GROUND

ITEM	X_P[a] (FT)	Z_P (FT)	X_R (FT)	Z_R (FT)	Y_P (FT)	TIME TO HIT GROUND (MILLISEC)	TERMINAL CONDITION
Test	−4.3	—	5.4	—	−9.2	1285	Post hits ground with Point R
Rigid model	−5.9	4.2	4.5	—	−10.8	1210	Post hits ground with Point R

[a] X, Y, Z is a fixed right-handed coordinate system having X in the direction of vehicular travel, Z vertical and its origin at the initial position of the base.

From the results of these two tests, it may be concluded that within satisfactory engineering accuracy the phenomenological behavior of a luminaire support structure impacted by a vehicle can be predicted from the models. The rigid-body model gives a good overall description of the event, while the elastic model gives a more accurate representation over the initial part of the motion. The linear equations derived for the response of the elastic post do not apply after contact with the vehicle is lost, because the rotations of the post are quite large.

Discussion

The correlation of the mathematical models with data obtained from the full-scale crash tests demonstrates the feasibility of the application of the models to the luminaire support post problem. Because the model vehicle is highly idealized, a very close correlation cannot be expected. In any case, the general behavior of the actual system can be simulated with the models discussed.

The time increment required to numerically integrate the equations of the elastic model is quite small. This small time increment, coupled with the large number of simultaneous equations necessary to solve the system, means considerable computer time and a high expense to solve a problem. In the cases considered, it was found that it usually took about 10 min of computer time to solve the elastic system for the initial part of the motion; in this same computer time, at least six complete problems using the rigid-body model were solved.

FINDINGS FROM A PARAMETER STUDY OF THE COLLISION DYNAMICS OF LUMINAIRE SUPPORTS

The many variables that affect the response of a vehicle and support in a collision cannot be economically explored by full-scale testing methods. For this reason, a mathematical model which simulates the response of the vehicle and support has been formulated and programmed for solution on a digital computer.

Two mathematical models were developed, as previously explained. Validation of these models showed that the rigid-body model gave satisfactory results. Because of its simplicity and economy of computer time it was used in the parameter study. The model can be used to study the effects of the various vehicle and support parameters without having to resort to full-scale collision tests.

For the parameter study which was conducted, four luminaire supports, three vehicle weights, three vehicle collision velocities, two angles of approach, and five base fracture energies were used. The supports were 30- and 40-ft mounting height aluminum or steel shafts with 15-ft mast arms supporting a 50-lb luminaire (see Fig. 20). Vehicle speeds were varied from 15 to 60 mph; vehicle weights were varied from 2,500 to 4,500 lb. Collision angles (angle measured from the normal to the plane of the luminaire support arm) were 5° and 15°. Base fracture energies were varied from 750 to 15,000 ft-lb.

For low-velocity collisions (15 mph) the support will fall either in front of the vehicle (with a secondary collision

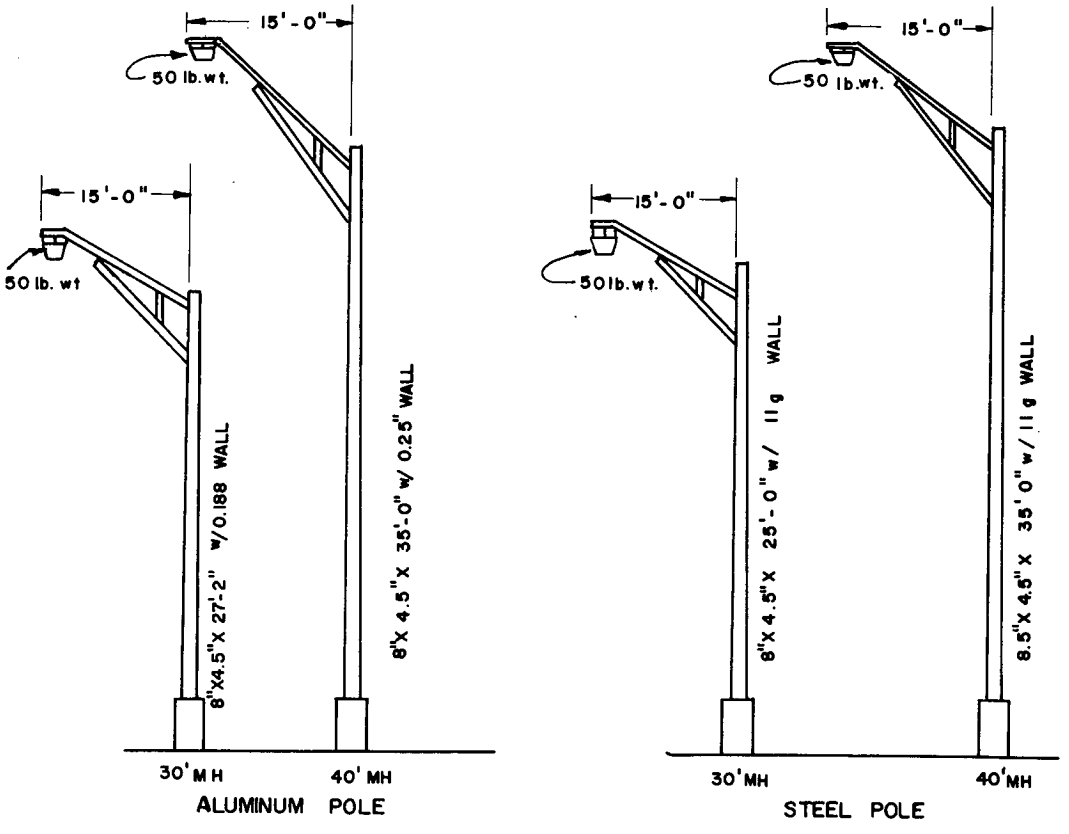

Figure 20. Parameter study supports.

occurring) or across the hood and passenger compartment. The change in vehicle velocity increases with the base fracture energy, and is practically independent of the type of shaft. The vehicle decelerations increase with increased base fracture energy. For the most severe collision (a 2,500-lb vehicle, a 40-ft mounting height steel support, and a base fracture energy of 9,000 lb) the vehicle will experience a 15.0 mph velocity change and 17 g deceleration. This is in the range in which passenger injury may occur. Although the occurrence of passenger injury at 15 mph may be reduced by decreasing the base fracture energy, the support will always fall on the vehicle. Obviously, in this case lightweight supports will produce less of a hazard to the vehicle passengers.

For 30 mph collisions, the study shows that the 30-ft supports (both steel and aluminum) will clear the vehicle in all cases, but the 40-ft supports have a tendency to hit the vehicle after first contacting the ground with either the top of the shaft or the end of the mast arm. In the cases where the rebounding pole strikes the vehicle, the point of contact is normally near the rear of the vehicle, away from the passenger compartment. The velocity change increases approximately linearly with increased fracture energy, exhibiting larger changes with the heavier supports.

For a collision velocity of 45 mph, all supports will clear the vehicles. The change in vehicle velocity varies linearly with an increase in base fracture energy.

When a support is struck, it tends to rotate in a clockwise direction about its longitudinal axis (viewed from the top) and tends to fall in a line roughly parallel to the vehicle path and displaced toward the roadway. The maximum translation occurs in the low-velocity collisions. The likelihood of the support falling into the traveled lanes can be minimized if the support is located a distance equal to the mast-arm length from the pavement edge.

Curves were constructed which present the results of the parameter study. These curves can be used to determine the vehicle velocity change and the support response. The vehicle velocity for which the falling support will not present a hazard for vehicle occupants can be determined from the curves. Figure 21 shows the curve for a 3,500-lb vehicle in collision with a 30-ft mounting height steel support with bases exhibiting base fracture energies varying from 750 to 15,000 ft-lb. The shaded zone represents the limiting vehicle collision for a non-hazardous support response. A non-hazardous response is considered to occur when the falling support does not strike in the vehicle passenger area, but the base may hit the trunk after the top of the support initially strikes the ground. Velocities which fall to the left of this zone indicate hazardous collisions; those to the right indicate collisions in which the support will clear the vehicle. The change in vehicle velocity must also be checked to insure that it is not excessive. Note the influence of the base fracture energy on the change in vehicle velocity. The curves indicate that if the vehicle possesses enough kinetic energy after base fracture to produce a non-hazardous support response, a safe collision (from the standpoint of vehicle response) will result. Curves similar to Figure 21, covering the results of the parameter study, appear with the design criteria in Chapter Three.

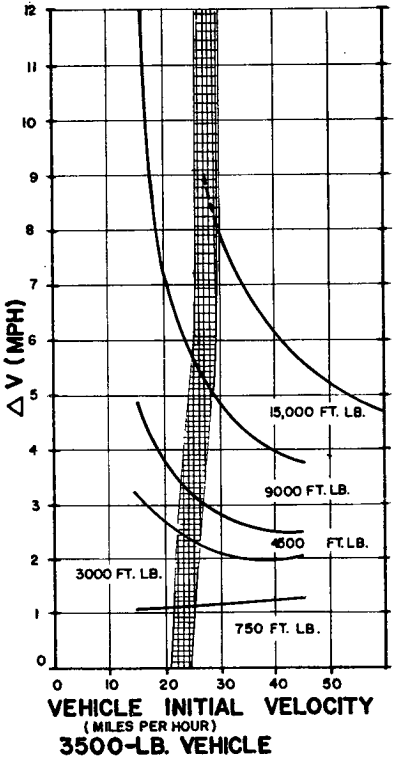

Figure 21. Predicted response: vehicle vs 30-ft steel support.

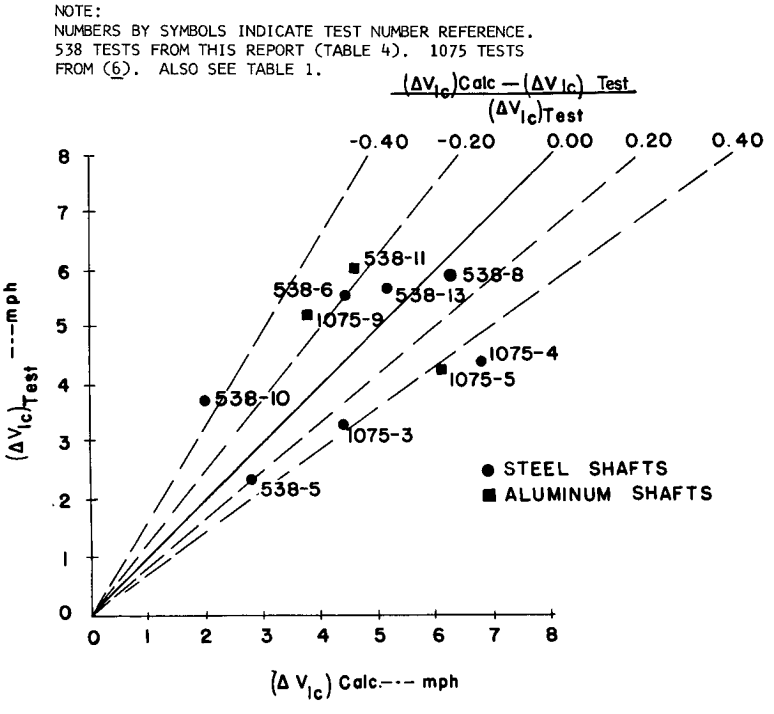

Figure 22. Correlation of parameter study with full-scale test data.

Curves of the type shown in Figure 21 (see Figs. 24 through 27) were used to correlate the mathematical model with the results of 10 full-scale tests. Figure 22 shows the comparison of the calculated velocity change with those observed. Note that four tests fall within 10% prediction accuracy, three fall within 40%, and the remaining three are slightly greater than 40%.

Although previous sections show that the model can accurately predict the collision dynamics for a specific test (using support and vehicle data for the specific test), Figure 22 shows the range in results when tests of varying parameters are compared with the curves generated for the specific variables in the parameter study.

FINDINGS FROM COST-EFFECTIVENESS STUDY

The major intent of the economic study was to provide a method of improving the economic analysis of roadway illumination. In particular, cost data are presented which center on lighting costs as related to various bases that are being used, with emphasis on the breakaway concepts. A method is presented which is general in nature and can be used as a design tool for computing lighting costs.

The study investigated initial costs, accident costs resulting from vehicles colliding with light poles, and normal maintenance costs. The accident costs were further broken down as to structural damage to the pole and base, damage to the vehicle, and injury costs to the occupants. Current cost data surveys were made from available literature and from interviews with personnel of the Texas Highway Department and the Texas Turnpike Authority. Data from the full-scale collision tests were also used.

A systems approach may be used to deal with the various parameters which are encountered in an economic analysis so that the parameters can be considered in perspective. Expressions were developed which relate roadside illumination to the major contributing factors and can be used to compare lighting systems on the basis of cost-effectiveness.

Details of the economic study appear in Appendix C. Its application to the cost-effectiveness of various pole and base concepts, used in conjunction with a hypothetical study, is given in Table 13. The table gives the total costs per mile of roadway (one way) occurring over the design life (assumed to be 20 yr) of the lighting system, discounted to present values at a discount rate of 5%. Direct costs are those the highway departments must assume directly; they include initial and maintenance costs but exclude vehicle accident costs. Direct plus indirect costs consist of highway department costs plus accident costs.

TABLE 13

COST-EFFECTIVENESS OF VARIOUS SUPPORTS FOR HYPOTHETICAL STUDY

POLE AND BASE	COSTS ($) DIRECT	DIRECT + INDIRECT
(*a*) Steel Pole		
Steel shoe base	34,630	64,960
Alum. transformer base	35,660	55,440
Steel transformer base	35,610	62,880
Stainless steel progressive-shear base	36,150	57,780
Carbon steel progressive-shear base	35,640	55,410
Slip base	35,690	51,180
(*b*) Aluminum Pole		
Alum. shoe base (thin wall)	37,940	60,340
Alum. shoe base (thick wall)	37,940	66,180
Alum. transformer base	38,950	54,440
Slip base	39,490	53,610

CHAPTER THREE

INTERPRETATION, APPRAISAL, AND APPLICATION

CONCEPT EVALUATION

The four basic concepts were first evaluated on the basis of the results of Tests 538-6, 13, 8, 4, 11, and 10. Once this had been accomplished, the other variations and modifications to the concepts were considered.

The tests were conducted under conditions as similar as possible. It is important to remember, at this point, that because similar supports, vehicles, and vehicle collision speeds were used in Tests 538-6, 13, and 8, the variations in response can be attributed directly to the base employed. In Test 538-10 the support shaft and mast arm were identical to those in Tests 538-6, 13, and 8, but the vehicle velocity was 28 mph instead of a nominal 40 mph. Because a 28 mph collision is more severe than a 40 mph collision (lower vehicle kinetic energy, hence less available to produce breakaway and subsequent motion of the support), the results are compared on an equal basis with the other tests. If the results show that the base performs satisfactorily when compared on this basis, it will perform satisfactorily under higher impact speeds.

Comparisons of the concepts are made, using the following values:

1. Change in kinetic energy/initial kinetic energy ($\Delta KE_{ic}/KE_i$)—this ratio expresses the amount of work done in deforming the vehicle, making the base break away and setting the support in motion.

2. (Vehicle deformation)^2/initial kinetic energy ($d^2 \times 10^5/KE_i$)—this ratio represents vehicle deformation. It is a measure of the work done in deforming the vehicle and reflects the amount of the total available energy absorbed by the vehicle.

3. Direct damage assessment ($)—these figures are the direct costs of repairing the vehicle and, as such, are a good measure of collision severity.

4. Change in velocity/initial velocity ($\Delta V_{ic}/V_i$)—this ratio is a measure of impulse (momentum) which is corrected for variations in initial vehicle velocity. It is not a good measure of collision severity if impulse times of the various collisions under consideration are significantly different. However, because it has gained some acceptance as a measure of breakaway support collision severity, it is included.

These calculated values, or severity ratios, *are intended as possible indicators of collision severity and are not necessarily the true or only indicators.* However, if any one test consistently shows high severity ratios, the ranking of the collision severity can be established on a basis that will be relative to all the tests under consideration. Furthermore, because one of the concepts evaluated herein (cast aluminum transformer base with a steel shaft) has been established by accident statistics as safe, the *relative safety of all concepts tested* can be compared to it.

All of the following calculations which employ velocity data were made using data derived from high-speed film records (see Table 4). Electronic means were also used to obtain these data (see Appendix A). It was felt, however, that the film data were more reliable, due to the accuracy of the film speed (time base) and the resolution of the film (distances could be measured to the nearest 0.5 in.). Also, all data could be taken from a media that was relatively consistent for all tests, whereas the electronic data were subject to calibration errors, limited observation time, vehicle suspension idiosyncrasies, etc.

Table 14 gives the severity ratios calculated for six tests of the four basic concepts: (1) cast aluminum transformer bases (Tests 538-6 and 13); (2) progressive-shear transformer base (Test 538-8); (3) cast aluminum shoe bases (Tests 538-4 and 11); and (4) the triangular slip base (Test 538-10). Table 15 gives a ranking of the ratios; the most severe is indicated by 6. If each individual severity ratio is given a weight of 1, a Severity Index can be calculated using the following equation:

TABLE 14

SEVERITY RATIOS, SIX BASIC TESTS

TEST NO.	$\frac{\Delta KE_{ic}}{KE_i}$	$\frac{d^2 \times 10^5}{KE_i}\left(\frac{\text{IN.}^2}{\text{FT-LB}}\right)$	VEHICLE DAMAGE ($)	$\frac{\Delta V_{ic}}{V_i}$
538-6	0.245	0.594	397	0.128
538-13	0.268	1.020	459	0.144
538-8	0.252	0.666	427	0.134
538-4	0.434	1.583	838	0.254
538-11	0.271	1.010	484	0.147
538-10	0.246	0.645	383	0.132

TABLE 15

RANKING OF SEVERITY RATIOS,[a] SIX BASIC TESTS

TEST NO.	$\frac{\Delta KE_{ic}}{KE_i}$	$\frac{d^2 \times 10^5}{KE_i}\left(\frac{\text{IN.}^2}{\text{FT-LB}}\right)$	VEHICLE DAMAGE ($)	$\frac{\Delta V_{ic}}{V_i}$	SEVERITY INDEX
538-6	1	1	2	1	0.208
538-13	4	5	4	4	0.708
538-8	3	3	3	3	0.500
538-4	6	6	6	6	1.000
538-11	5	4	5	5	0.792
538-10	2	2	1	2	0.292
Ranking	4, 11, 13, 8, 10, 6	4, 13, 11, 8, 10, 6	4, 11, 13, 8, 6, 10	4, 11, 13, 8, 10, 6	4, 11, 13, 8, 10, 6

[a] Ranking of 6 indicates most severe collision.

Severity Index =

$$\frac{\Sigma \text{ Severity Ratio Ranking}}{(\text{No. of Severity Ratios})\ (\text{Max. Severity Ranking})}$$

The ranking on the basis of the Severity Index is given in Table 15. The Severity Index ranking can be used only as a method of comparing the *relative severity of the concepts tested,* and should *not* be used as a safety indicator.

Consider the severity ratios for the 10 tests given in Table 16. Table 17 gives the ranking of these ratios. The individual rankings are shown at the bottom of the table, as is the ranking using the Severity Index. Table 18 summarizes the Severity Index ranking and lists the supports for ease of reference. Note how the four supports, not included in the basic six, fit into the ranking. The stainless steel davit support with progressive-shear base (Test 538-9) and the modified aluminum shaft with an A356-T6 shoe base (Test 538-12) had Severity Indices that fell between the Severity Indices of the two aluminum shafts of the basic set of tests. The stainless steel mast or shaft with progressive-shear base (Test 538-7) fell between the cast aluminum transformer base and the carbon steel progressive-shear transformer base. The least severe of all of the tests in the series was the aluminum shaft with a cast shoe base with integral riser (Test 538-5).

Table 19 correlates the maximum dummy acceleration (transducer in chest cavity) with the observed response and the Severity Index. In the three tests with the highest Severity Index, both dummies made contact with the interior of the vehicle. In the fourth highest (Test 538-11) only the driver dummy hit the steering wheel. In these four tests the change in vehicle velocity at loss of contact was in excess of 6.0 mph, and the duration of impact was in excess of 0.093 sec.

As a guide for making a determination of occupant injury as determined by the dummy response, reference is made to the work of Patrick (*12*), Blamey (*13*), and

TABLE 16

SEVERITY RATIOS, TEN TESTS

TEST NO.	$\frac{\Delta KE_{lc}}{KE_i}$	$\frac{d^2 \times 10^5}{KE_i}\left(\frac{\text{IN}^2}{\text{FT-LB}}\right)$	VEHICLE DAMAGE ($)	$\frac{\Delta V_{lc}}{V_i}$
538-6 [a]	0.245	0.594	397	0.128
538-13 [a]	0.268	1.020	459	0.144
538-9	0.341	1.094	491	0.187
538-7	0.282	0.737	427	0.151
538-8 [a]	0.252	0.666	427	0.134
538-4 [a]	0.434	1.583	838	0.254
538-11 [a]	0.271	1.010	484	0.147
538-12	0.268	0.881	548	0.160
538-5 [b]	0.115	0.370	382	0.057
538-10 [a, c]	0.246	0.645	383	0.132

[a] Six basic tests.
[b] 30-ft mounting height support; all others 40-ft M.H.
[c] Vehicle collision velocity, 28 mph; all others at ± 40 mph.

TABLE 17

RANKING OF SEVERITY RATIOS, TEN TESTS

TEST NO	$\frac{\Delta KE_{lc}}{KE_i}$	$\frac{d^2 \times 10^5}{KE_i}\left(\frac{\text{IN}^2}{\text{FT-LB}}\right)$	VEHICLE DAMAGE ($)	$\frac{\Delta V_{lc}}{V_i}$	SEVERITY INDEX
538-6 [a]	2	2	3	2	0.235
538-13 [a]	5	8	6	5	0.600
538-9	9	9	8	9	0.875
538-7	8	5	4	7	0.600
538-8 [a]	4	4	5	4	0.324
538-4 [a]	10	10	10	10	1.000
538-11 [a]	7	7	7	6	0.675
538-12	6	6	9	8	0.725
538-5 [b]	1	1	1	1	0.100
538-10 [a, c]	3	3	2	3	0.260
Ranking	4, 9, 7, 11, 12, 13, 8, 10, 6, 5	4, 9, 11, 13, 12, 7, 8, 10, 6, 5	4, 12, 9, 11, 13, 8, 7, 6, 10, 5	4, 9, 12, 7, 11, 13, 8, 10, 6, 5	4,9, 12, 11, 13, 7, 8, 10, 6, 5

[a] Six basic tests.
[b] 30-ft M.H. support; all others 40-ft M.H.
[c] Vehicle collision velocity 28 mph; all others at ± 40 mph.

TABLE 18

SUMMARY OF SEVERITY INDEX RANK, TEN TESTS

TEST NO.	SEVERITY INDEX	DESCRIPTION
538-4[a]	1.000	Aluminum shaft with A 356-T4 shoe base
538-9	0.875	Stainless steel davit arm shaft with progressive-shear base
538-12	0.725	Modified aluminum shaft with A 356-T6 shoe base
538-11[a]	0.675	Aluminum shaft with A 356-T6 shoe base
538-13[a]	0.600	Cast aluminum transformer base with steel shaft
538-7	0.600	Stainless steel mast arm shaft with progressive-shear base
538-8[a]	0.324	Carbon steel progressive-shear transformer base with steel shaft
538-10[a, c]	0.260	Triangular slip base with steel shaft
538-6[a]	0.235	Cast aluminum transformer base with steel shaft
538-5[b]	0.100	Aluminum shaft with cast shoe base with integral riser

[a] Six basic tests.
[b] 30-ft M.H. support; all others 40-ft M.H.
[c] Vehicle collision velocity 28 mph; all others at ± 40 mph.

TABLE 19

COMPARISON OF SEVERITY INDEX RANK AND DUMMY RESPONSES, TEN TESTS

		DUMMY RESPONSE			
TEST NO.	SEVERITY INDEX	PEAK g	DRIVER HIT STEERING WHEEL	PEAK g	PASSENGER HIT DASHBOARD
538-4	1.000	12.3	Yes	3.9	Yes
538-9	0.875	9.0	Yes	1.3	Yes
538-12	0.725	8.3	Yes	2.8	Yes
538-11	0.675	5.3	Yes	1.8	No
538-7	0.600	3.4	No	1.4	No
538-13	0.600	9.3	No	1.6	No
538-8	0.324	9.0	No	2.7	No
538-10	0.260	4.0	No	1.3	No
538-6	0.235	3.5	No	2.3	No
538-5	0.100	5.5	No	1.0	No

others. These investigators have indicated that head and chest impact injuries occur when the head velocity, measured relative to the vehicle, exceeds 11 mph. Because many other factors enter into the determination of injury, no attempt is made to assess whether injuries would have occurred. However, inasmuch as the relative velocities of the dummies could not exceed the change in vehicle velocity, none of which exceeded 9.3 mph, the likelihood of serious injury to live occupants was small.

Discussion

The various concepts are rated by their Severity Index in the previous section. As noted previously, the support bases were oriented so that the most severe collision occurred (except for the aluminum shoe base supports, which have no preferred orientation). A different ranking probably would have resulted if the orientations had been more favorable, as explained in the following.

Four tests were conducted using aluminum supports with cast shoe bases. One support (Test 538-12) was modified by stiffening the lower portion of the shaft, and one (Test 538-5) employed a cast shoe base with an integral riser which stiffened the shaft against crushing. The Severity Index ranking showed that the conventional aluminum supports (Tests 538-4, 11, and 12) were among the most severe. Because these supports have uniform base properties, they do not have a preferred orientation and, hence, collision angles greater than 0° would not have affected their Severity Index appreciably.

Test 538-12 showed that stiffening the lower portion of a conventional aluminum shaft did not decrease its relative position in the ranking.

Test 538-5 demonstrated the desirable features that can be obtained with a cast shoe base with integral risers. The riser stiffens the shaft against crushing and transmits the shear to the base, which fractures, with very little over-all

deformation of the shaft in the area of bumper contact. This base must be contacted in the stiffened area in order to function as in the test. If the applied force is above the riser (20 in.), the shaft will crush and the behavior will be similar to that of the conventional shoe base aluminum supports.

The supports with progressive-shear bases fell roughly in the middle of the Severity Index ranking, with one notable exception (Test 538-9). In this test the base deformed, forming a ramp, which caused the vehicle to override it. This had the effect of driving the base down into the ground, increasing its resistance to motion. This action occurred after the button welds in the impacted face had failed. This behavior was not as pronounced in Test 538-7, with a resultant lower ranking. Both these bases had eight button welds per face. Note that the carbon steel progressive-shear transformer base (Test 538-8), which had six button welds per face, did not ramp, and fell much lower in the ranking. *All of these bases would have produced less severe collisions if they had been hit on one edge, the most favorable orientation.*

Two types of cast aluminum transformer bases were tested. The type used in Test 538-6 had flat faces; that in Test 538-13 had rounded faces. When struck by the vehicle bumper, the flat face of the base distributed the load to the corner columns, with the resultant failure occurring at the bottom edge near the mounting lugs. The base broke cleanly. The transformer base with rounded faces behaved differently, which probably influenced its response. The bumper penetrated the base before fracture occurred in the bottom edge of the base. Considerable tearing was evidenced by the mangled base. *Both of these bases would have exhibited lower rankings if contact had been made on one edge.* The edge serves as a stiffener which transmits load directly to the mounting lug. Failure would therefore occur at a lower load due to the fact that bending resistance is supplied by only one mounting lug at the corner. For aluminum transformer bases to operate effectively, they must be contacted by the vehicle.

The Severity Index of the triangular slip base fell in the range of the aluminum transformer bases. Note that this test (Test 538-10) was conducted at 28 mph. The ranking would indicate that a 28 mph collision with this type of base is only slightly more severe than a collision with an aluminum transformer base at 43 mph. This means that its Severity Index would be lower for a higher collision velocity. The optimum collision angle for this type of base is 30°, measured from a line through one slot and the geometric center (see Table 8). With the base oriented for a collision along this line, the resistance would have been approximately 24% less, resulting in a slightly lower Severity Index.

The Severity Index ranking can be used only as a method of comparing the relative severity of several tests and should not be used as a safety indicator. In the four most severe collisions, the dummies contacted the interior of the vehicle. However, it is not felt that serious injuries would have resulted.

DESIGN CRITERIA

The following criteria for the design of safe luminaire supports have been developed from the findings of the various phases of the study. A thorough understanding of the conceptual principles of breakaway base supports and prudent application of the design criteria are essential.

The Support

A breakaway base is essential for a safe luminaire support installation.

As a first consideration, the base must be designed primarily to support the static and wind-induced loads with a suitable factor of safety. The breakaway features are secondary to this. However, because the response of the support and vehicle are influenced primarily by the breakaway features, the following should be carefully considered and prudently applied:

1. The base fracture energy (BFE) of any base under consideration should be determined by a reliable means, either by laboratory tests or analytical calculations.
2. If the base is of a frangible material (such as the aluminum transformer base) it must be constructed in such a way that the vehicle bumper makes contact with it, rather than with the supported shaft. (Automobile standards should be consulted to determine bumper heights.)
3. The lowest base fracture energy should be used which is consistent with static and wind strength requirements.
4. The initial tension or preload in the clamping bolts of slip-type bases should be sufficient to balance the static loads, plus a suitable factor for wind loads. In any event, the resistance, R_T and M_T, and the base fracture energy (BFE) should be checked by Eqs. 1, 6, and 7. Provisions should be made to prevent joint "walking."
5. Concrete foundations should be constructed so as to be level with the surrounding ground surface.
6. If the base is of the slip type, the supported shaft must possess sufficient strength to resist crushing or denting in the vehicle contact area (existing ASTM A-245 Grade C, 11-gauge steel shafts appear to be adequate).
7. If a base has properties that depend on its orientation, it should be positioned so that the direction of least resistance will coincide with the most probable vehicle approach angle. This is of primary importance if low-velocity collisions are the major accident expected. The preferred orientation for accepted base concepts is shown in Figure 23. Due consideration should be given to aesthetics.
8. In those cases where low-velocity collisions are most probable, the base fracture energy must be a minimum; and the shaft should be as light in weight as possible.

Support and Vehicle Response

Because most bases are standard items for which fracture properties can be cataloged, the selection of a base should be based on the vehicle and support response for the worst anticipated collision. This can be accomplished by reference to Figures 24 through 27, which show the responses of four supports to collisions by three vehicles. Enter the figure which most nearly fits the support under consideration with a given vehicle velocity. For the base fracture

energy under consideration determine the maximum vehicle velocity change. Check to see whether the velocity is to the right or left of the zone lines: if to the right, a non-hazardous collision will result; if to the left, the support will fall on the vehicle in the passenger compartment area. If the support shaft is heavy, consideration must be given to the consequences which could occur. In these cases a lightweight shaft should be used.

The severity of the collision is gauged by the velocity change and the vehicle deceleration which is obtained from Figure 28. If the velocity change exceeds 6.0 mph, there is a possibility of minor passenger injury. Velocity changes larger than 12 mph should be avoided.

The encroachment of the fallen support onto the traveled lanes can be checked by referring to Figures 29 and 30. This possibility will usually occur in low-speed collisions.

Mounting Height

Supports that have mounting heights greater than 40 ft and bases with fracture energies greater than 9,000 ft-lb should be considered with caution, because they may be severe for low-velocity collisions.

APPRAISAL AND APPLICATION

In this study an attempt was made to evaluate the various devices currently in use to enhance the safety of luminaire supports. The data generated from full-scale tests provide a scale (Severity Index) by which to evaluate the relative performance of the various concepts. The curves, developed from the parameter study using a mathematical model, provide the means for evaluating the collision response of selected supports (shaft and base) when struck by a range of vehicles.

Efforts were made to develop a laboratory technique which can be used to efficiently establish a parameter (base fracture energy) that would reflect the performance of a particular base in a full-scale collision. The base fracture energy is a measurable parameter which, when obtained under standardized procedures, and used in conjunction with curves similar to Figures 23 through 30, will enable the designer to evaluate its effectiveness as a safety feature for luminaire supports.

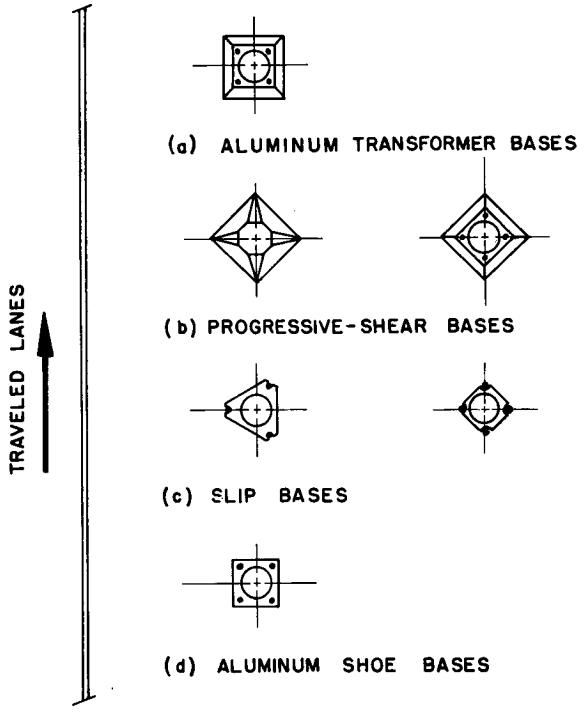

Figure 23. Preferred base orientation.

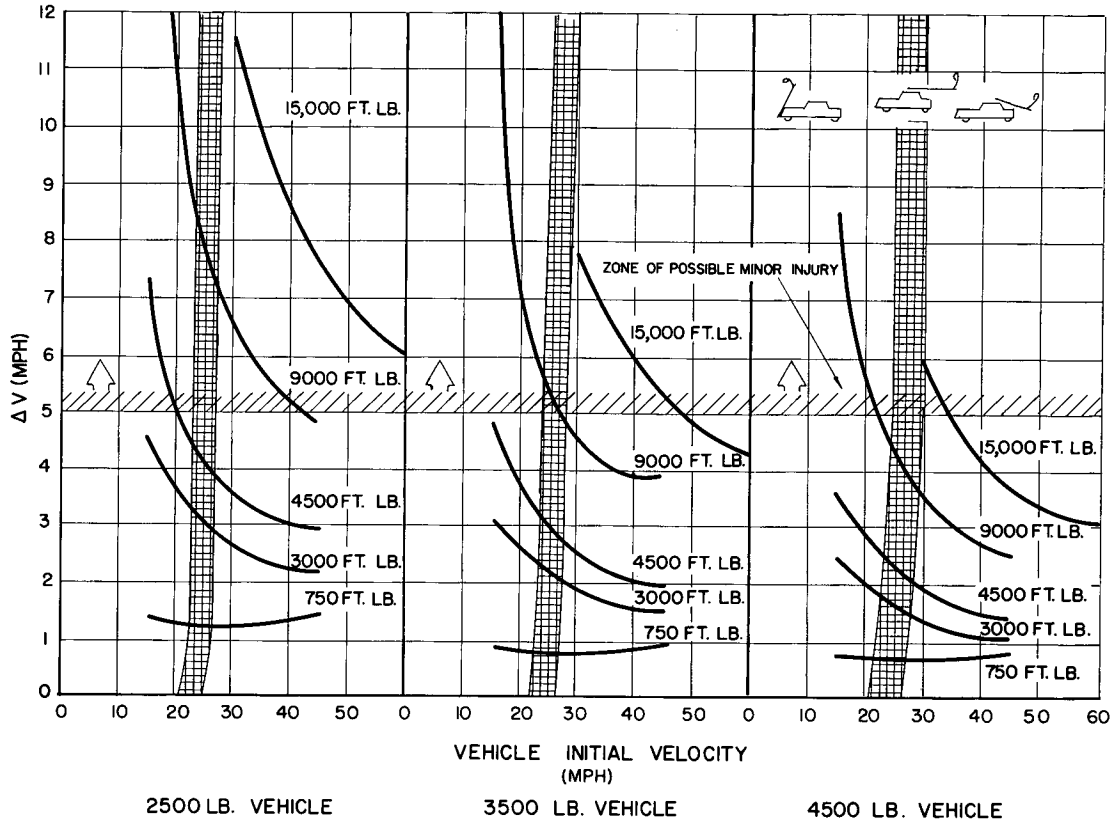

Figure 24. Predicted response: vehicles vs 40-ft aluminum support.

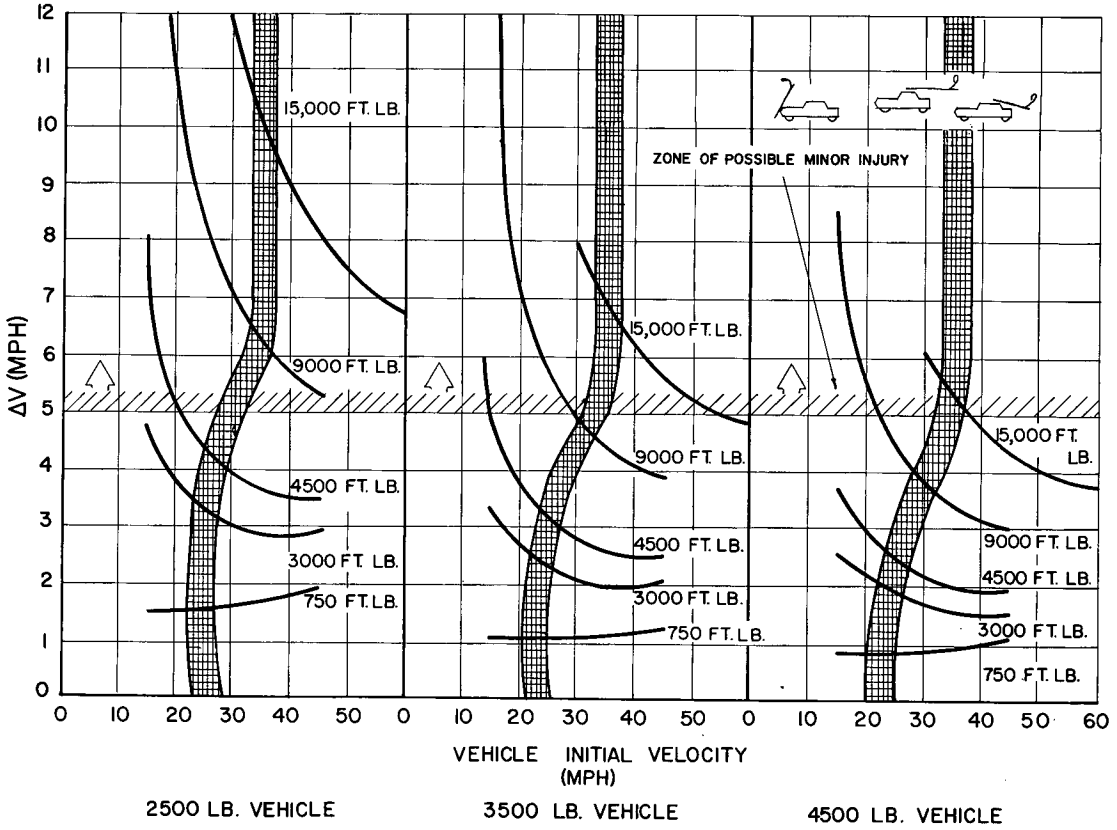

Figure 25. Predicted response: vehicles vs 30-ft aluminum support.

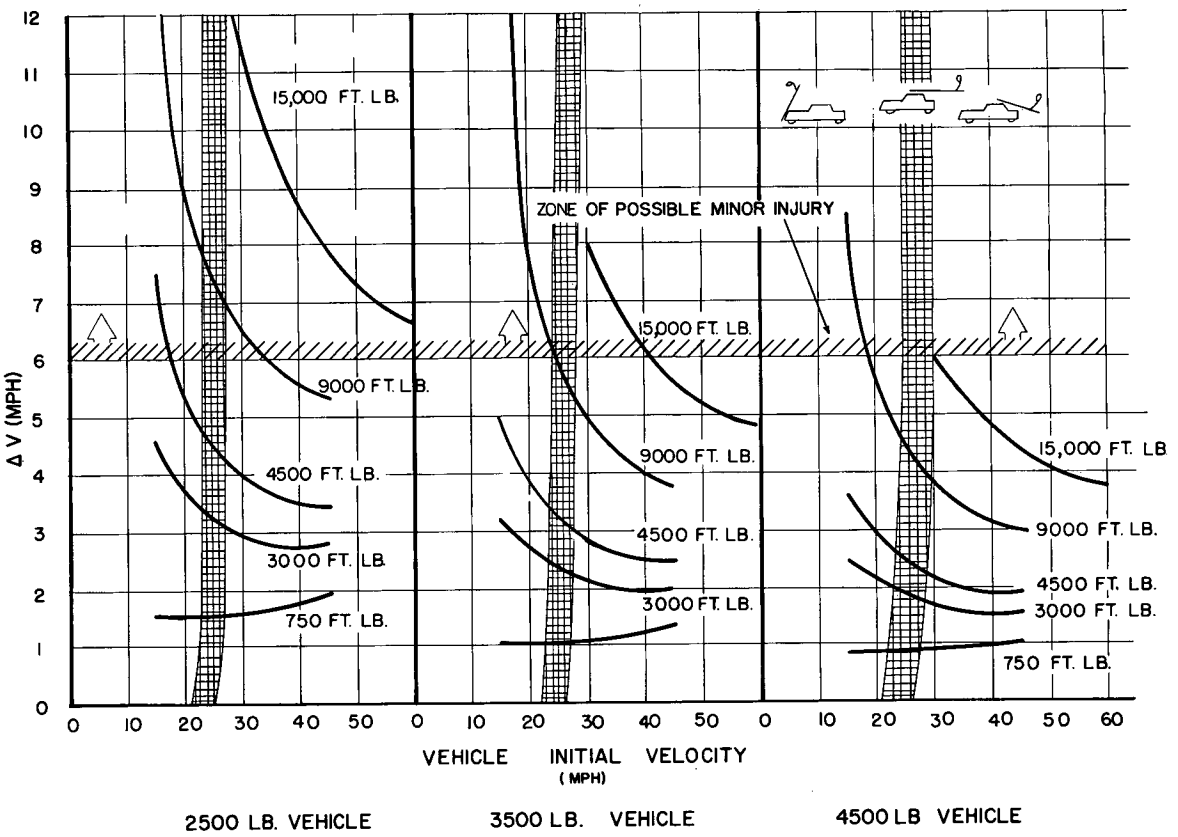

Figure 26. Predicted response: vehicles vs 30-ft steel support.

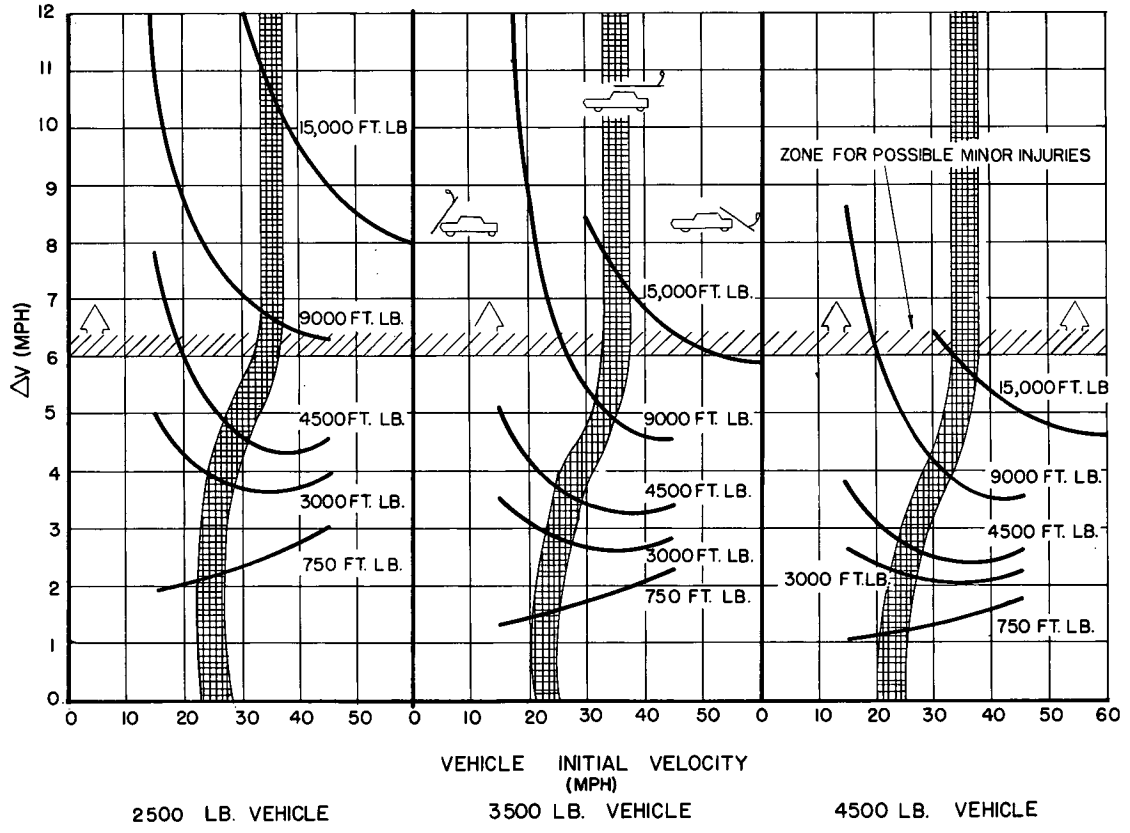

Figure 27. Predicted response: vehicles vs 40-ft steel support.

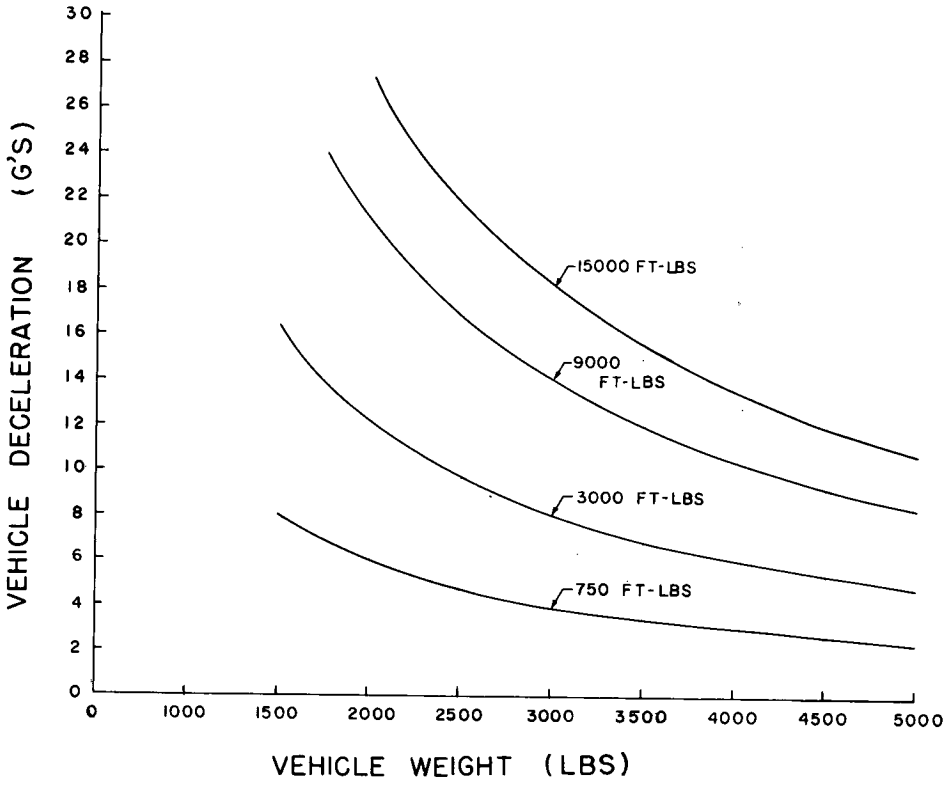

Figure 28. Vehicular deceleration as a function of vehicle weight.

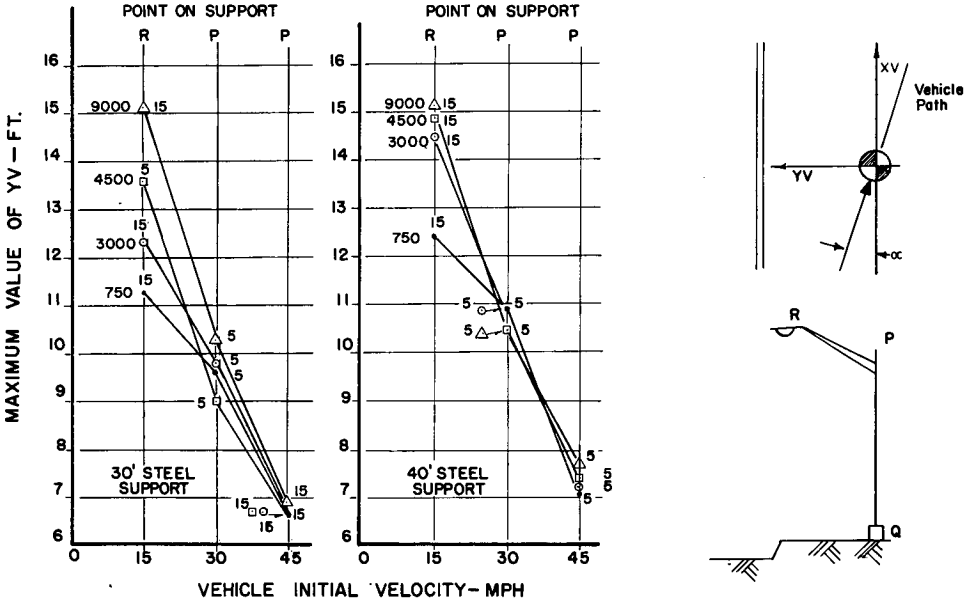

Figure 29. Maximum translation, aluminum supports.

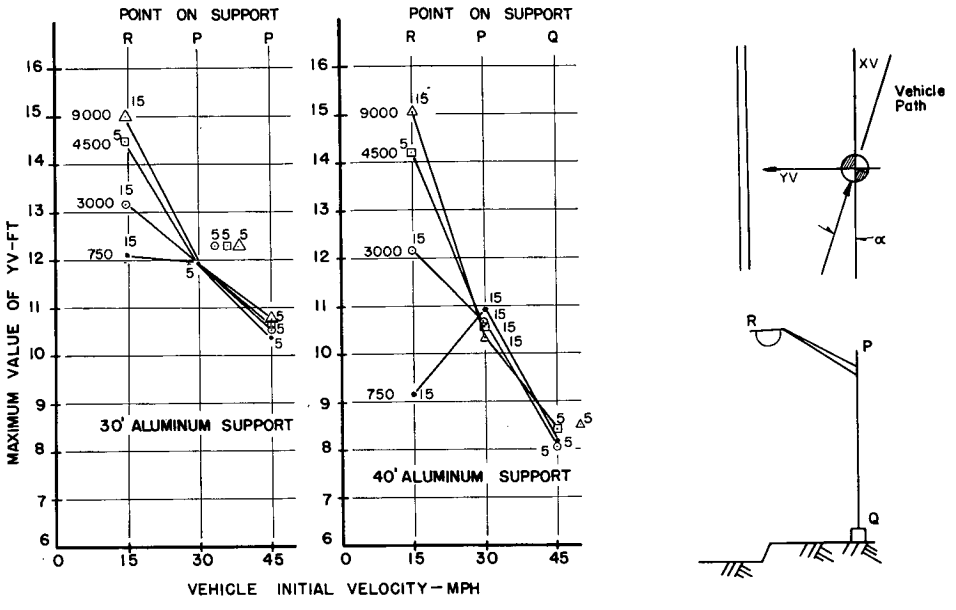

Figure 30. Maximum translation, steel supports.

CHAPTER FOUR

CONCLUSIONS AND SUGGESTED RESEARCH

CONCLUSIONS

This study has shown that the collision response of a vehicle and luminaire support can be predicted with acceptable accuracy. Design criteria have been formulated which, if prudently applied, will result in a design that will yield adequate safety.

It has been established that the response of a support depends primarily on the resistance of the base (measured by its fracture energy), and to a lesser extent on the support size (for standard steel and aluminum poles) and the vehicle weight. For more massive concrete luminaire supports, the weight of the support pole is certainly a primary consideration. For base designs that are orientation-sensitive, the direction of least resistance should coincide with the most probable angle of collision. Care should be exercised in the orientation of the base, especially where low-velocity collisions are probable.

Low-velocity collisions (20 mph or less) are the most hazardous. There is danger from vehicle deceleration and from the falling shaft. Where low-velocity collisions are most probable, lightweight supports and bases possessing the lowest base resistance should be used.

Tests and analytical studies have shown that bases which use the slip principle have the lowest base resistance of all concepts studied to date. Although the use of this type of base will not alleviate the possibility of the support falling on the vehicle in low-velocity collisions, it will significantly influence the deceleration and velocity change of the vehicle, which will greatly reduce the probability of injury.

The study has shown that with normal aluminum or steel supports (30- and 40-ft mounting heights) the danger of a hazardous collision decreases with an increase in vehicle collision velocity. The lower limit for a low-hazard collision (from the standpoint of the support falling on the vehicle) is approximately 35 mph.

For larger supports (50-ft mounting height and higher) it appears that more hazardous collisions (from the standpoint of the support falling on the vehicle) can occur with collision velocities as high as 45 mph. This limit could be reduced somewhat by using bases with low base fracture energies.

Highway and traffic engineers must recognize that these conclusions are based primarily on the results of studies conducted with an idealized mathematical model (correlated with full-scale collisions), and for frontal impacts only. Under conditions which exist in actual roadside collisions, anomalies can arise and different types of collisions

can occur. It is felt, however, that adherence to the principles set out will yield adequate safety.

A method is presented in Appendix C by which the cost-effectiveness of a lighting installation can be determined.

SUGGESTED RESEARCH

All full-scale collision tests which have been conducted—those presented in the literature and those conducted in this study—were frontal impacts. The behavior of supports in this type of collision is understood and can be predicted with acceptable accuracy. However, collisions which involved vehicles hitting a support in a broadside attitude have not been adequately studied. Collisions of this type are worthy of future study. The vehicle collision and crush characteristics are different when impacts occur in this attitude, and the impact forces are applied higher up on the support, which could result in significantly different collision behavior. Vehicle occupants are also much more vulnerable to injury when loads are applied normal to the longitudinal axis of the vehicle. The crushing which occurs on side impacts can be large, causing the deformed vehicle metal to encroach into the passenger compartment. It is therefore suggested that studies be initiated to develop crash-testing techniques for such side impacts. Full-scale tests should be conducted to yield data on side collisions, and these data should be used to verify and modify the mathematical model for use in predicting the behavior under this type of collision.

A lower limit for breakaway action should be defined; i.e., that speed at which the damage to the vehicle and occupant is potentially less with the luminaire support remaining in place than that which might occur if the pole fell on the vehicle. This decision will necessarily have to be based on a cost-effectiveness approach; this will require more data than are now available.

Standard laboratory tests and analytical techniques should be established for determining the base fracture energies for various bases.

Further parameter studies should be conducted to extend the results of this study. A wider range of luminaire support parameters is needed to cover all types of supports in use.

To make cost-effectiveness studies more meaningful, additional information is needed on the nature and frequency of vehicle encroachments for different types of highways, traffic, and weather conditions. Additional data are needed on the average cost of collisions with luminaire supports (costs on vehicle damage, personal injury, and lighting installation damage). Such information should be included in accident reporting and records and should provide costs for collisions with supports with the various combinations of bases, shafts, and mounting heights.

The economic model that was developed can be used, *with cost data applicable to the locale under study*, to determine the cost-effectiveness of various types of supports.

REFERENCES

1. "Fatal Accidents on Completed Sections of the Interstate System, July—December 1966." Circular Memo. to Regional Fed. Hwy. Administrators and Division Engineers. J. D. Lacy, Director, Office of Traffic Oper., Bur. of Public Roads, p. 12 (June 13, 1967).
2. WALKER, A. E., and HIGNET, H. J., "Break-away Lighting Column." *Highways and Public Works*. Vol. 35, No. 1689, p. 3 (May 1967).
3. MOORE, R. L., *Single Vehicle Accidents in Relation to Street Furniture*. 6th Internat. Study Week, Traffic Eng., Salzburg (1962).
4. HIGNET, H. J., *High Speed Impact Test on a 40 ft. Lighting Column Fitted with a Break-away Joint*. RRL Report LR67, Crowthorne, p. 24 (1967).
5. EDWARDS, T. C., *Multi-directional Slip Base for Break-away Luminaire Supports*. Research Report 75-10, Texas Transportation Institute (Aug. 1967).
6. ROWAN, N. J., and KANAK, E. W., *Impact Behavior of Luminaire Supports*. Research Report No. 75-8, Texas Transportation Institute (Oct. 1967).
7. Personal correspondence with Mr. Eric Nordlin, Materials and Research Dept., Calif. Division of Highways, Sacramento (Mar. 1968).
8. SPICOLA, J. A., "Break-away Light Poles." *Traffic Digest and Review*, p. 5 (Sept. 1967).
9. Personal correspondence with Millerbernd Mfg. Co., Winsted, Minn.
10. SHARP, M. L., and YOUNG, R. F., *Falling Weight Impact Tests of Lighting Standards*. Report No. 12-68-8, Aluminum Co. of America, p. 9 (Feb. 1968).
11. MARTINEZ, J. E., *An Analytical Solution of the Impact Behavior of Luminaire Support Assemblies*. Research Report 75-9. Texas Transportation Institute (Aug. 1967).
12. PATRICK, L. M., MERTZ, H. J., and KROLL, C. K., "Knee, Chest, and Head Impact Loads." *Proc. 11th Stapp Car Crash Conf.*, Anaheim, Calif., p. 116 (Oct. 10-11, 1967).
13. BLAMEY, C., "Results from Impact Tests on Telegraph Poles." *Highway and Bridges*, 32(1576), pp. 7-8, 13 (1964).
14. PRYOR, W. T., "Progressive Uses of Aerial Surveys for

Highways." Presented at the Environmental Eng. Conf., ASCE, Dallas (Feb. 1967).
15. EMORI, R. I., "Analytical Approach to Automobile Collisions." *SAE Paper 680016,* Auto. Eng. Cong., Detroit (Jan. 8, 1968).
16. CASSEL, A., and MEDVILLE, D., "Economic Study of Roadway Lighting." *NCHRP Report 20* (1966).
17. THOMPSON, J. A., and RANSLER, B. I., "Economic Study of Various Mounting Heights for Highway Lighting." *Hwy. Res. Record No. 179* (1967) pp. 1-15.
18. RECHT, J. L., *How to Do a Cost-Benefit Analysis of Motor Vehicle Accident Countermeasures.* National Safety Council, Chicago (1966).
19. LAZENBY, J. G., *Progress Report on The Design Concept and Field Performance of Break-away Devices for Illumination Poles in Texas.* Fort Worth (1967).
20. HUTCHINSON, J. W., and KENNEDY, T. W., *Medians of Divided Highways—Frequency and Nature of Vehicle Encroachments.* Univ. of Ill. Engineering Experiment Station Bull. 487, Urbana (1966).
21. MICHIE, J. D., and CALCOTE, L. R., "Location, Selection, and Maintenance of Highway Guardrails and Median Barriers." *NCHRP Report 54* (1968).
22. "Highway Guardrail: Determination of Need and Geometric Requirements." *HRB Spec. Rep. 81* (1964).
23. STONEX, K. A., "The Single-Car Accident Problem." *SAE Paper 811A,* Auto. Eng. Cong., Detroit (Jan. 13-17, 1964).

APPENDIX A

CONCEPT EVALUATION—FULL-SCALE TESTS

Four basic concepts were chosen for evaluation. A total of 11 tests were conducted: 10 were for the purpose of concept evaluation, and one was to further the state-of-the-art in the collision dynamics of luminaire supports.

The tests on supports with non-integral bases (Tests 538-6, 13, 8, and 10) used identical steel poles, mast arms, simulated luminaires, vehicles, impact speeds, and instrumentation; only the bases were varied.

In Tests 538-4 and 11, the supports were identical except for the design of the cast shoe base. The support used in Test 538-12 had the same physical dimensions as Tests 538-4 and 11 except that the wall thickness was thinner (0.188 in.) and was reinforced against crushing in the bottom 24 in. of the shaft. The support of Test 538-5 was shorter (28 ft compared with 37 ft) and employed a cast aluminum base (A356-T6) with an integral riser which extended 12 in. into the shaft.

The slip base had the same configuration discussed in Chapter One, but was modified by including a 20° ramp on the base plate to give the shaft an initial upward impulse at impact. See Figure 17(a).

Test 538-1, a prestressed concrete support, was solely to further the state-of-the-art.

The bases of the supports tested were oriented in such a way that the most severe collision would result. Orientation of the bases to their most desirable position would have lowered their Severity Index (Chapter Three), and might have changed their relative ranking. However, inasmuch as there can be no control over the collision angle in real accidents, it was felt that the most undesirable orientation would be the basis on which the comparisons were made.

Shoe bases are not orientation-sensitive.

INSTRUMENTATION

For the test series, instrumentation was used that would yield the information necessary to make a comparison of the various concepts on the basis of vehicle deceleration, change of velocity, time of contact between the vehicle and the test article, peak lap-belt force, and peak accelerations of the anthropomorphic dummies simulating the driver and front-seat passengers. This information was obtained using electronic transducers (accelerometers and switchstrips) and high-speed photography.

Electronic Instrumentation

Table A-1 lists the transducers, their location, and function.

The accelerometers were mounted on a steel block which was welded to the frame rail of the vehicle, behind the front passenger seat, in the area where a seat-belt mounting would be attached. The dimensions of the mounting block were chosen so that its resonant frequency did not influence the data. Accelerometers of two types (strain gauge and piezoelectric crystal) were used.

Two anthropomorphic dummies were used in all tests except Test 538-1 (the prestressed concrete shaft). The dummies were Alderson Research-type P1-50-AU fiftieth percentile males. The articulated joints of the dummies were adjusted to simulate a moderately tense condition. An attempt was made to torque the joints to simulate muscle tone, but this did not prove effective, owing to the low torques (10 in.-lb) required. The dummy placed in the driver's seat was restrained by a standard lap belt (Sears, Roebuck Model 6437-d). This belt was instrumented to measure the belt-force history during the duration of the

TABLE A-1

ELECTRONIC INSTRUMENTATION

TRANSDUCER	MANUFACTURER	MODEL	SENSITIVITY PER VOLT	LOCATION	PURPOSE
Accelerometer	CEC	4-280-0002	42.2 g	Vehicle frame	Deceleration of vehicle
Accelerometer	Statham	A69TC-100	25 g	Vehicle frame	Deceleration of vehicle
Accelerometer	Statham	A69TC-100	200 g	Chest cavity of dummy	Acceleration of dummy
Accelerometer	Statham	A5A-25-350	25.0 g	Chest cavity of dummy	Acceleration of dummy
Force transducer	Strainsert Co.	½-13NCX 2¼"	1000 lb	Seat-belt force transducer (driver dummy)	Seat-belt force
Switchstrips	Tapeswitch Corp. of America	Controflex Ribbon Switch 131 (A)	—	See Fig. A-1 See Fig. A-2	1. Velocity sensors 2. Contact switches

collision event. Accelerometers were placed in the chest cavities of both dummies and were mounted with their sensitive axis normal to the spine line.

Velocity sensors were made of two sets of switchstrips placed 3 ft apart (Fig. A-1) and located in front and behind the target. Figure A-1(a) is a schematic of the circuitry used for these sensors.

The time at which the vehicle made first contact with the test article was sensed by placing a switchstrip on the target at the vehicle bumper height, as shown in Figure A-2(a). The time at which mutual contact between the vehicle and the test article was lost was sensed by another switchstrip placed higher on the shaft of the support so that it would make contact with the upper part of the vehicle hood. These switchstrips are shown in Figure A-2(a). Note that the upper switch was covered by a strip of heavy rubber to insure that it would not be cut by the deformed front end of the vehicle.

Data Reduction from Electronic Instrumentation

The electronic pulses from the various electronic transducer sensors were recorded on magnetic tape in analog form. One channel of the seven available channels was used to record a 500 Hz sinusoidal timing signal. For analysis, the tape was replayed at a speed less than that used for recording. A Honeywell Visicorder, Model 1508, oscillograph was used to record the playback signals. By reducing the playback speed of the tape recorder, the time base of the oscillogram could be varied by controlling its recording paper speed. To limit the playback frequency response, the signals from these accelerometers were filtered, on playback, using 10 Hz and 20 Hz active filters (Analog Devices, Models 701-10 and 701-20). This is equivalent to passing 80 Hz and 160 Hz signals respectively at an 8/1 record/playback ratio. The optical galvanometers used in the oscillograph were chosen to have frequency responses in excess of 160 Hz (Honeywell Models M400-350, and M 1650).

The frame accelerometers were used to obtain peak vehicle deceleration, velocity, and displacement. The velocity of the vehicle can be obtained as a function of time by integration of the acceleration pulse. The vehicle displacement can also be obtained by double integration of the acceleration pulse. Figure A-3 shows the numerical integration technique used in the reduction of the accelerometer data. The data were manually digitized and automatically punched on data-processing cards using the Gerber Digital Data Reduction System, Model GDDRS-3B-2. The integration technique was programmed for computation on a digital computer.

Information on vehicle velocity was also obtained from the velocity-sensing switch sets. These switch sets indicate the passage of the vehicle wheel, which was recorded on magnetic tape. Because the switches in a set are spaced 3 ft apart, the velocity is obtained by measuring the elapsed time (from the oscillogram) for a wheel to traverse this set. These switch sets were placed so as to obtain the initial velocity before impact and the final velocity after loss of contact between the vehicle and the test article (see Fig. A-1).

The total time of contact was determined from the two sets of switchstrips placed on the test article (see Fig. A-2). As shown in Figure A-2(a), the time between closing of the first switch and opening of the second is the total contact time.

Photographic Instrumentation

Table A-2 gives a summary of the cameras used in this series, the function of each camera, and other photographic data. Figure A-4 shows the location of each camera. The prime instrumentation cameras were located so as to obtain high-resolution film on the event up to separation of the test article and the vehicle, close-up view of the action of the base of the test article, and wide-angle coverage of the total event. No data were taken from the documentary films.

To insure that the high-resolution cameras would cover the event from initial contact to separation, two cameras were used with an overlapped field of view (Fig. A-5).

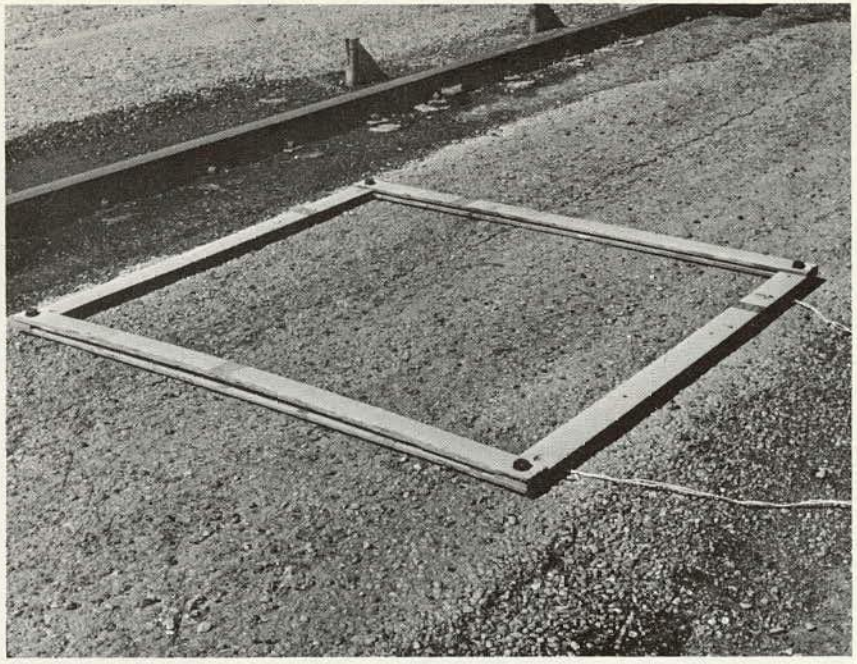

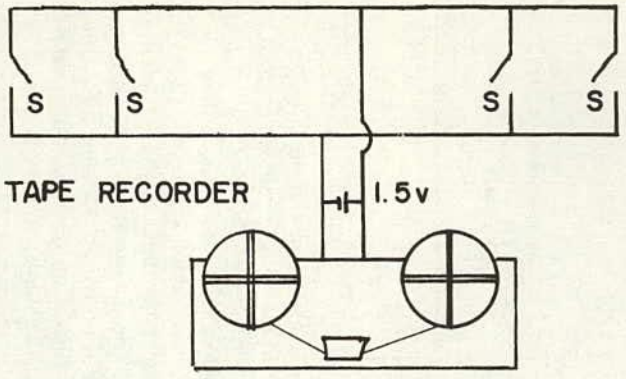

(a) SCHEMATIC CIRCUITRY

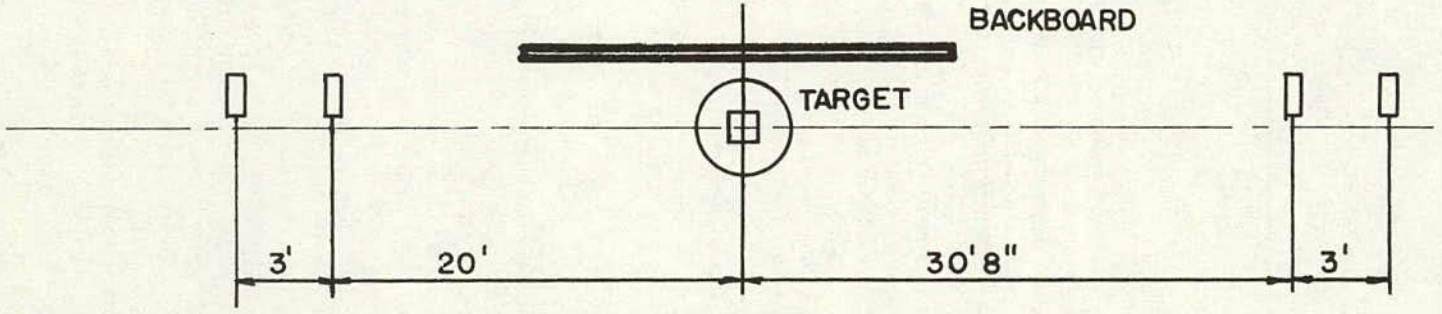

(b) LOCATION OF SWITCH SETS

Figure A-1. Velocity sensors.

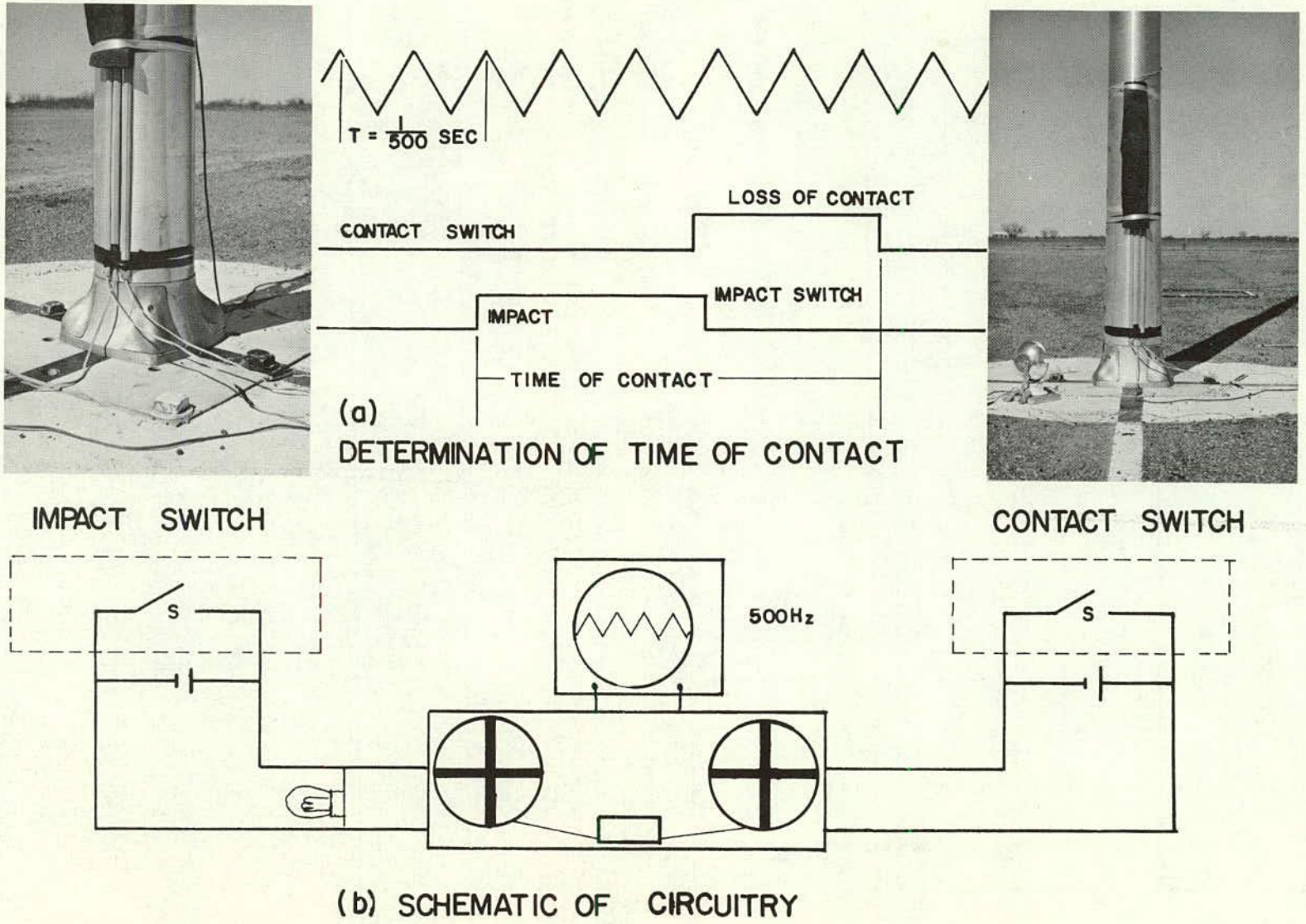

Figure A-2. Impact and contact switchstrips.

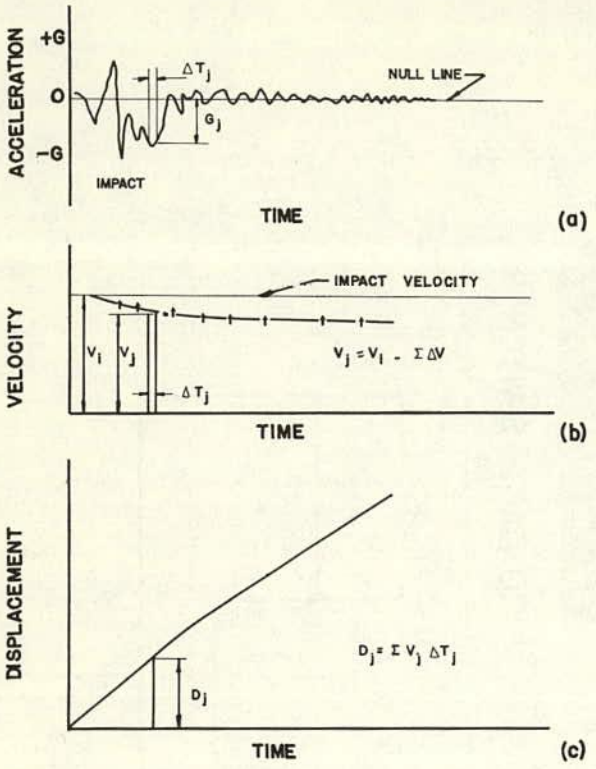

Figure A-3. Crash vehicle accelerometer analysis by numerical integration.

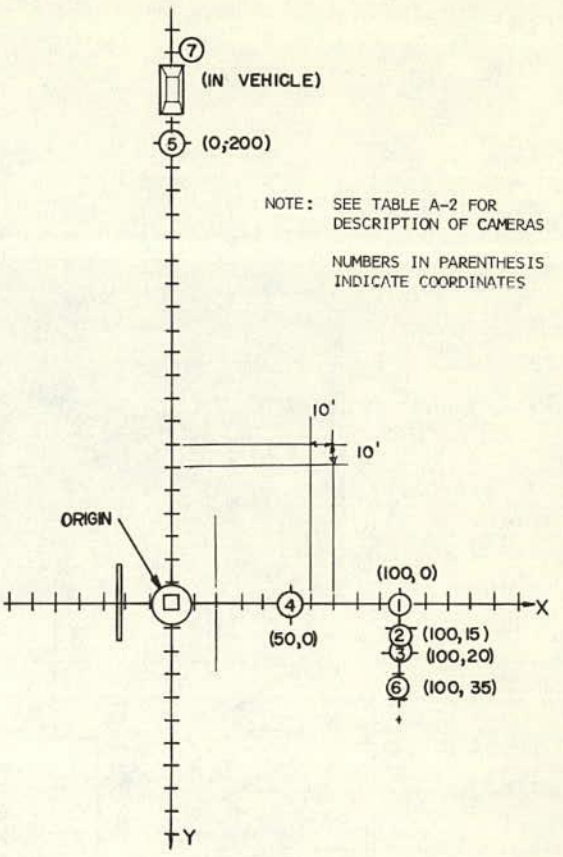

Figure A-4. Location of cameras.

Synchronization of these two films was accomplished by a switch-activated flash bulb. The switch for the flash bulb was placed so that when the flash was activated a reference point on the vehicle was in the field of view of both cameras. The instant of impact was recorded on both cameras by a switch-activated flash bulb. The switch was placed on the test article at bumper height (see Fig. A-2).

All high-speed cameras were equipped with timing lights which placed marks on the edge of the film at a specified frequency (60 Hz for the FASTAX and 100 Hz for the HYCAM). These marks were subsequently used to establish the speed of the film.

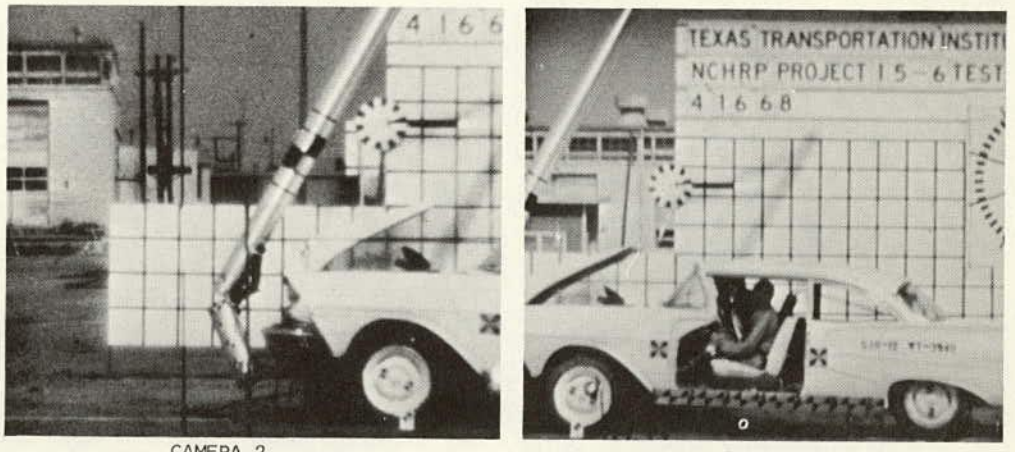

Figure A-5. Camera synchronization.

TABLE A-2

PHOTO INSTRUMENTATION

CAMERA NO.	TYPE AND MANUFACTURER	LENS (MM)	FILM	NOMINAL FILM SPEED (PPS)	CAMERA FUNCTION
1	3-M FASTAX WF-3T	50	Kodak EF Type 7241	1000	Record data camera (field of view overlapped with No. 2)
2	HYCAM Red Lake Lab. K20S4E	50	Kodak EF Type 7241	1000	Record data camera (field of view overlapped with No. 1)
3	HYCAM Red Lake Lab. K20S4E	12.5	Koday EF Type 7241	1000	Wide-angle view of total event
4	Photo-Sonics Traid Corp. 16 mm—1B	75	Koday EF Type 7241	1000	Close-in view of support base
5	Bolex H-16	25	Ektachrome Commercial Type 7255	128	Record support behavior from up track
6	Bell & Howell 200 EE	25	Ektachrome Commercial Type 7255	24	Panned vehicle from oblique overhead position
7	Fairchild N-6	35	Kodachrome II	64	Inside vehicle to observe dummies and support

Figure A-6 shows a typical test vehicle with targets and stadia boards mounted. The vehicles were painted a flat white (Latex Interior); the targets and stadia boards were black on a pastel tan background. Targets of two sizes were used: 4 in. x 4 in., and 6 in. x 6 in. Tests showed that these color combinations and configurations gave the highest possible resolution in the subsequent data analysis. The particular target configuration used was taken from recommendations made by the Bureau of Public Roads Aerial Surveys Branch (*14*). The horizontal stadia board below the front door gave a distance reference for the data analysis.

Data Reduction from Photographic Instrumentation

The primary sources of data in this method of instrumentation are the two high-speed cameras (Cameras 1 and 2, Table A-2). The film record of the event makes possible methodical and detailed analysis of the sequence of the action, frame by frame. The instrument used in the manual digitizing of the time-displacement data was the Vanguard Motion Analyzer (a Model M-16CD projection head mounted on a Model A-11D projection case). This instrument, equipped with a frame counter, permits horizontal and vertical measurements on an enlarged, rear-projected image of the film. Time reference marks, placed on the film by a timing light in the camera, made it possible to accurately determine the speed of the film. A second time reference, a large sweep-hand clock, was mounted in the photographic background. This clock was driven by a constant-speed motor which was calibrated after each test with a tachometer. This clock provided a visual reference by which the film speed obtained from the timing lights could be checked. The stadia board, divided into 3-in. increments, mounted on the side of the test vehicle, established the distance measurement reference. The following method was used in obtaining time-displacement records:

1. Two reference points were established—one on the vehicle (a target mounted for this purpose), and the second a fixed point (usually a vertical line on the background).
2. The film was advanced frame by frame and the change in distance between the two reference points was measured (the Vanguard Analyzer is capable of measuring to the nearest 0.001 in.; however, the resolution of the images on the film prohibited measurement to this accuracy).

Data were taken from the first frame in which the reference mark on the vehicle came into view until such time as the reference mark moved out of the field of view. To obtain as much data as possible from one film, it was necessary to change the vehicle reference from one near the front of the vehicle for the first frames on the film to one near the end of the vehicle for the last frames on the film. The time displacement curve constructed from these data was used to calculate the vehicle velocity at any time. To average out errors in the data which can be caused by small changes in film speed and inherent digitizing errors, the velocities were calculated using the mean slope of the displacement time curve over a 3-ft interval. A 3-ft interval was used because this is identical to the reference distance used in calculating vehicle velocity from the switchstrip sets.

The film data and resultant velocity calculations for each test appear in a following section.

(a) TYPICAL VEHICLE

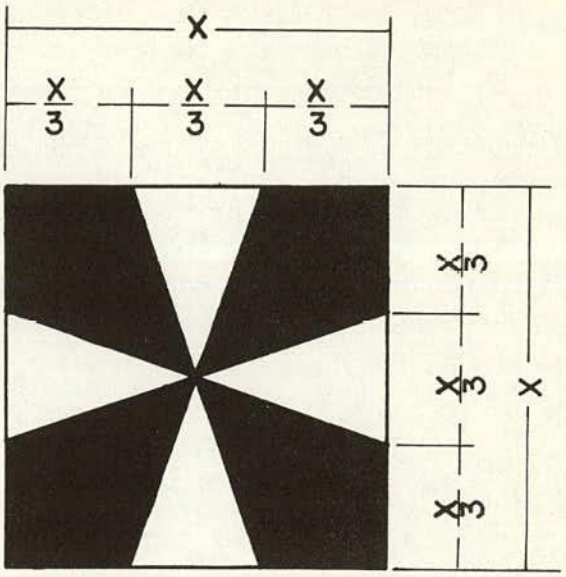

(b) TARGET

Figure A-6. Typical test vehicle.

TEST VEHICLES

All test vehicles used were 1958 Ford Sedans. A choice of vehicles was determined by the availability of a sufficient number of vehicles of one model year in the vicinity of the test facility. Vehicles of any body style (except station wagons and convertibles) were acceptable. Each vehicle was required to be mechanically complete; i.e., to have complete engines and accessories (engines were not required to be in running condition), brakes, and intact body shells.

Vehicle Launch and Guidance

The vehicles were launched by a reverse-tow mechanism, shown in Figure A-7(a). This mechanical linkage allowed the tow vehicle to travel at a speed ½ of that desired for the towed vehicle. A dolly which traveled on a rail kept the vehicle on the proper line to the target. A release mechanism at the end of the rail freed the dolly from the vehicle and the tow line. A steering guide attached to the right front wheel, shown in Figure A-7(b), followed a cable stretched along the path of the vehicle. This guide served

TABLE A-3

SUMMARY OF TEST RESULTS

TEST NO.	VEH. WT. (LB)	VEH. VEL. (ELECTRONIC) (MPH) V_i	V_f	ΔV_f	ΔV_{te}[a]	VEH. VEL. (FILM) (MPH) V_i	V_f	ΔV_f	ΔV_{te}	t_{te}[b] (SEC)	VEH. DEF. (IN.)	VEH. DAMAGE ($)	VEH. g (AVG. OF 2)
538-6	3580	42.5	39.0	−3.5	−5.0	43.8	36.7	−7.1	−5.6	0.069	14	397	14.7
538-13	3340	40.3	33.8	−6.5	−3.9	39.5	32.5	−7.0	−5.7	0.140[c]	16	459	8.9
538-9	3480	36.9	30.2	−6.7	−5.9	37.4	30.3	−7.1	−7.0	0.123	16	491	10.8
538-7	3880	42.3	34.6	−7.7	−4.7	43.1	35.3	−7.8	−6.5	0.167	16	427	15.0
538-8	3620	43.1	36.6	−6.5	−4.3	44.0	37.3	−6.7	−5.9	0.080	15	427	10.1
538-4	3700	37.4	28.3	−9.1	−8.1	37.7	28.3	−9.4	−9.3	0.098	20	838	15.0
538-11	3580	39.5	35.0	−4.5	−4.8	40.8	33.7	−7.1	−6.0	0.105	17	484	5.9
538-12	3940	37.7	31.6	−6.1	−7.6	39.1	31.8	−7.3	−6.6	0.182	16	548	8.7
538-5	3820[d]	41.9	38.0	−3.9	−3.5	42.2	38.2	−4.0	−2.4	0.075	11	382	8.8
538-10	3340[e]	27.6	23.4	−4.2	−1.5	28.0	22.1	−5.9	−3.7	0.084	9	383	6.5
538-1	3660	41.4	0.0	−41.4	—	38.8	0	−38.8	—	0.524	17	1601	—

[a] Best fit of two accelerometers.
[b] t_{te} = time after impact when contact was lost.
[c] From film data; V_i = vehicle velocity at contact (mph); V_f = vehicle velocity at rear tapeswitch set (mph); ΔV_{te} = change in vehicle velocity at loss of contact (mph); and ΔV_f = change in vehicle velocity at rear tapeswitch (mph).
[d] 30-ft. mounting height.
[e] 28 mph collision velocity.

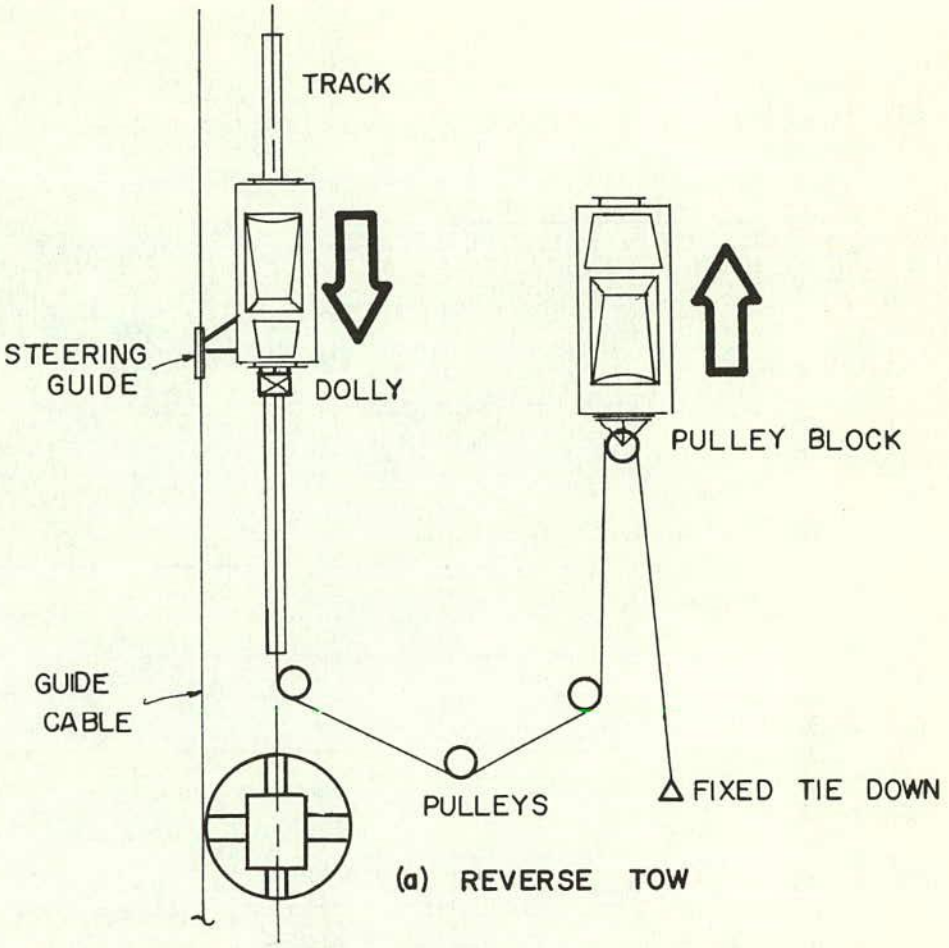

to stabilize the vehicle and insured a central impact. In all but two tests (Tests 538-8 and 538-13) the impact point was on the geometric center of the vehicle.

TEST RESULTS

Table A-3 is a summary of all tests. Velocity values were calculated from two sources—electronic (switchstrips and integration of accelerometer traces) and high-speed film.

The results of each of the 11 tests were collected and ararnged in the following order:

1. Description of support and base.
2. Description of the phenomenological response of the support and vehicle.
3. Post-collision support damage, and position of the support on the ground with respect to the vehicle path.
4. Post-collision vehicle damage, and damage appraisal.
5. Oscillogram of vehicle and dummy accelerometers, and seat-belt force transducer.
6. Time-displacement data reduced from high-speed motion picture films.

The results of Test 538-6, which are typical, appear in this order in Figures A-8 through A-13. Similar data for all other tests are available on request to the Program Director, NCHRP.

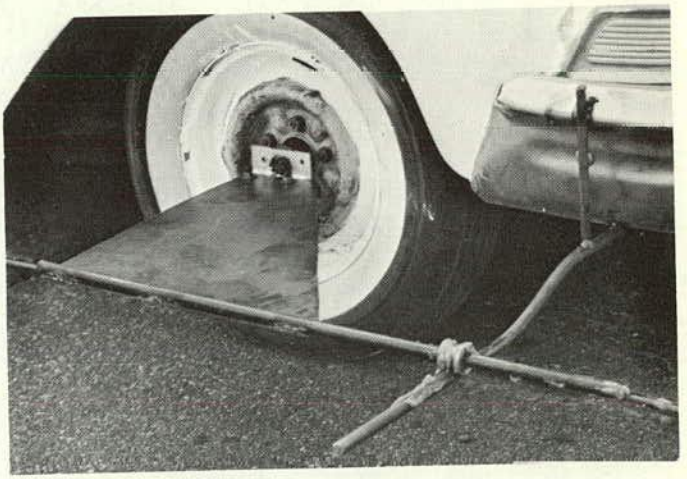

(b) STEERING GUIDE

Figure A-7. Vehicle launch and steering.

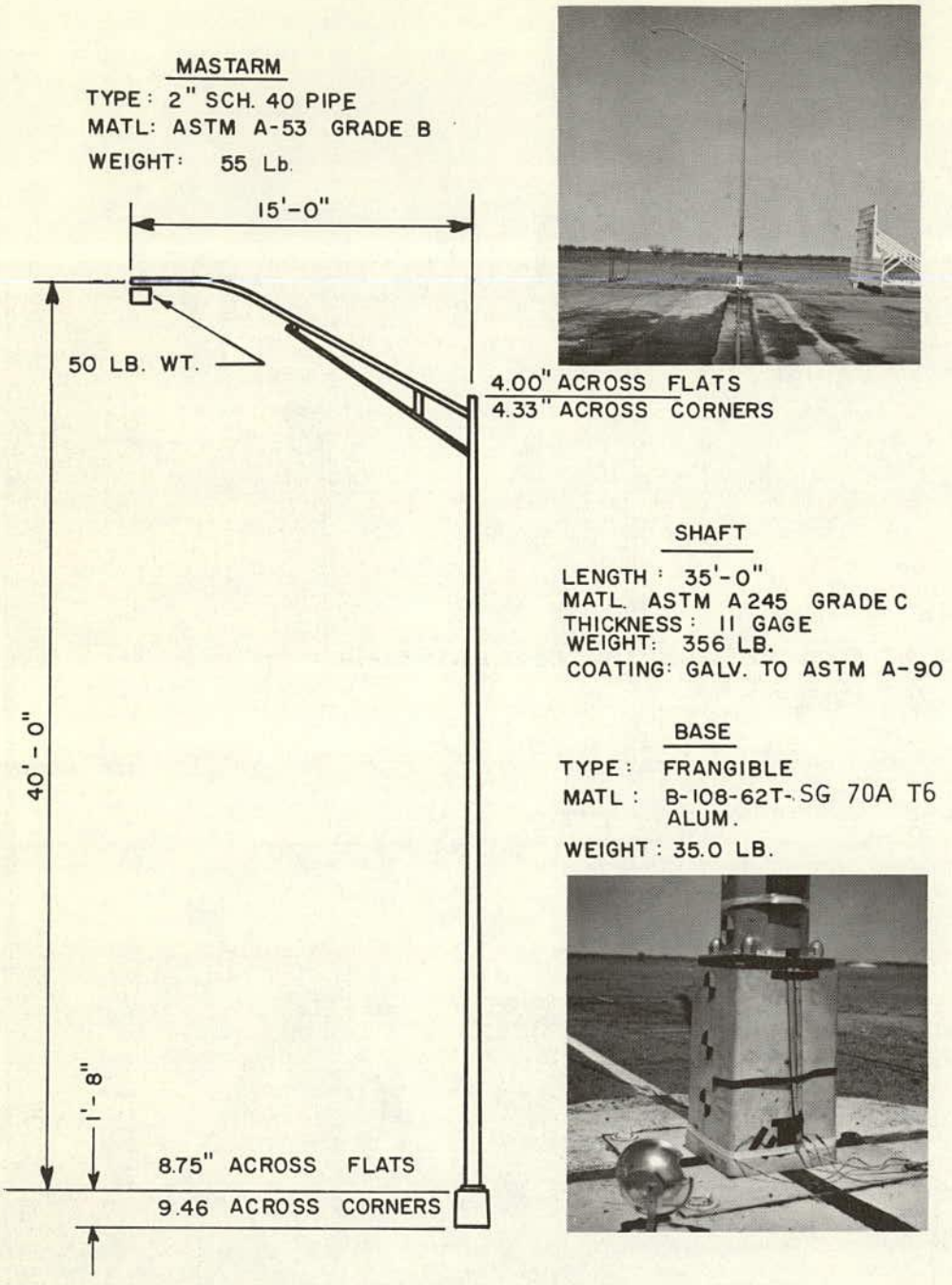

Figure A-8. Test 538-6: support and base.

Test 538-6

Phenomenological Response of Support and Vehicle

The transformer base sheared with a tensile crack initiating in the bottom surface near the mounting lugs. The support lost contact with the vehicle and appeared to reach a maximum altitude in its trajectory of approx. 12 ft. The shaft completely cleared the vehicle and rotated approx. 200° before striking the ground. The shaft was bent on impact with the ground and did not rebound appreciably. The 50-lb weight simulating the luminaire came off the mast arm. The dummies had very little response and did not hit anything in the vehicle interior. The steel shaft did not rebound appreciably on striking the ground. The rebound of steel poles is not as great as that of stainless steel poles.

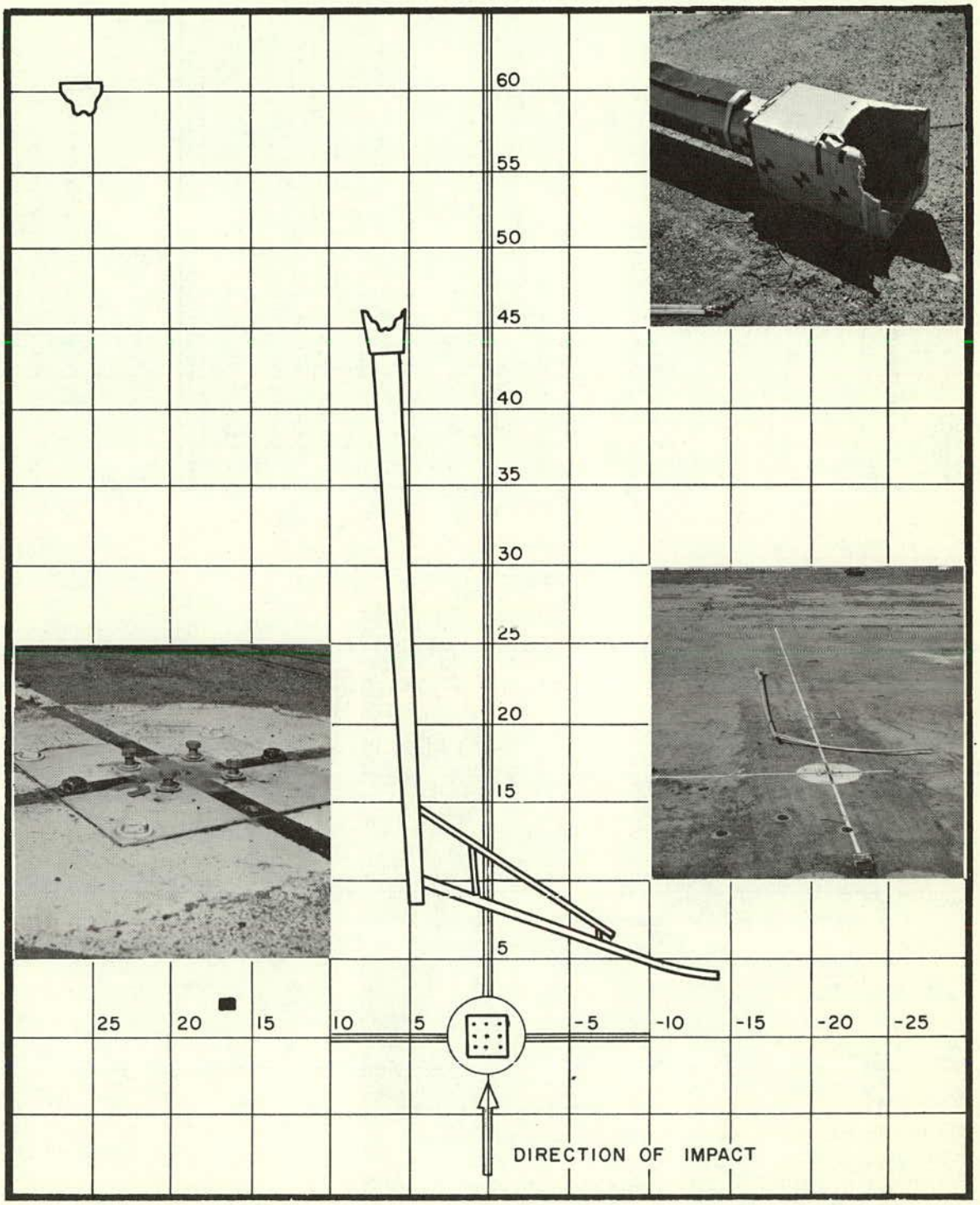

Figure A-9. Test 538-6: post-collision support damage.



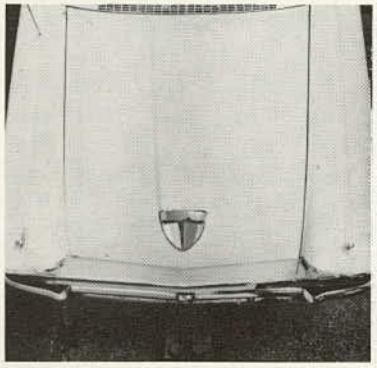
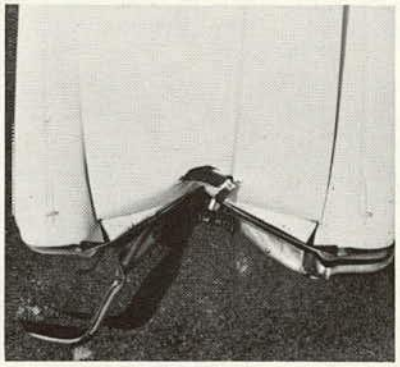

VEHICLE : 1958 FORD
WEIGHT : 3580 LB
DEFORMATION: 14 IN.
DAMAGE EST.: $397

Figure A-10. Test 538-6: post-collision vehicle damage.

R. L. "Dick" Polasek
AUTO DAMAGE APPRAISERS

P. O. BOX 1695
VICTORIA, TEXAS
Phone (512) 575-8382

P. O. Box 255
YOAKUM, TEXAS 77995
Phone (512) 293-2462

P. O. Box 3452
BRYAN, TEXAS 77801
Phone (713) 822-3081

OWNER: — DATE: 4-18 68 APPRAISER R L Polasek
APPRAISED FOR: Texas Transportation Institute (Edwards) SERIAL # 538-6
YEAR 1958 MAKE Ford BODY STYLE 2dr MODEL C/Line MILEAGE LICENSE PJW809

	DESCRIPTION OF REPAIRS AND REPLACEMENTS	HRS. LBR.	Net	PARTS
1	Bumper face bar front	0.9	26 00	—
	" back bar str RIF	0.3		—
	" " " str LIF	0.3		—
1	" rail guard 4F	—		6 70
1	" " " RIF	—		6 70
1	" guard center	—		10 40
1	Grave/ deflector front	0.6		12 70
1	Grill assy.	0.9		17 85
1	" panel upper	1.0		10 90
1	" " " mldg.	—		6 70
1	Radiator support	1.5		20 45
1	" " brace to grill panel	—		1 50
1	Radiator assy.	0.3		74 00
1	" fan blade	0.4		4 40
1	Motor mount LIS	0.5		2 95
1	" " RIS	0.5		2 95
1	Hood panel	1.2		68 50
1	" vent scoop	—		10 00
	Hood hinge align	0.4		—
	Fender str. RIF	1.0		—
	Fender str LIF	1.2		—
	Frame x-member str. front	3.0		—
	Front End Align	1.5		—
	Paint + Materials	5.5	9 00	—
	The Below Signed Agrees Guaranteed Repairs as Per Above Estimates If and When Authorized By Owner.	21.0	35 00	256 70

REPAIR SHOP ACCEPTED BY:
REPAIR SHOP ACCEPTED BY:

LABOR 21.0 HRS. @ 6 00 $ 126 00
35 00
PARTS LESS 10 % $ 25.67 $ 231 03
TAX 5 14

This Is Not An Authorization For Repairs

TOTAL $ 397 17

Figure A-11. Test 538-6: vehicle damage appraisal.

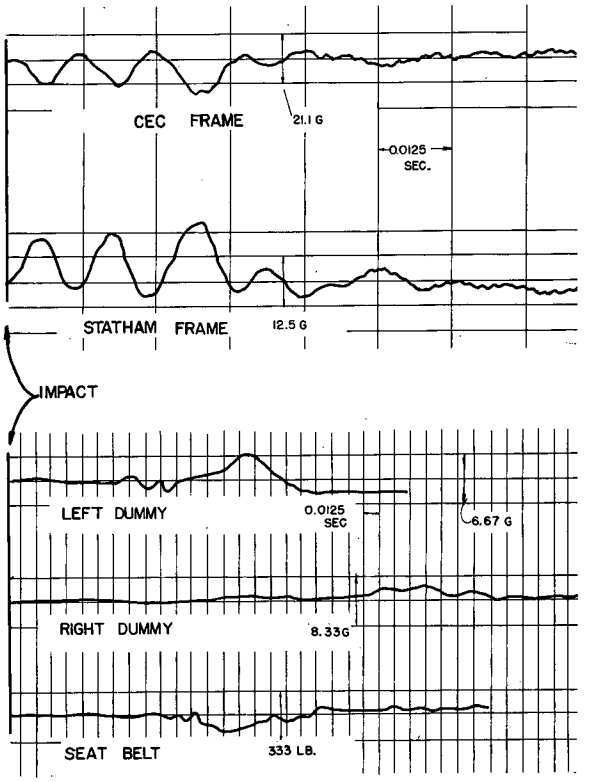

Figure A-12. Test 538-6: vehicle and dummy data.

TEST 538-6

Vehicle: 1958 Ford 2-door Sedan

Vehicle Weight: 3580 lb.

Support: Steel shaft w/20" Alum. transformer base. 41'-8" M.H. w/15'-0" mast arm

Cameras: (1) 3M Co. FASTAX (946 pps) 50 mm lens at f3.5
(2) Red Lake HYCAM, Ser. No. 602 (1079 pps) 50 mm lens at f3.5

Test Date: 3/13/68

Time (Sec. x 10^{-3})		Displacement (ft.)	
5.30		0.34	
10.60		0.68	
15.90		1.02	
21.20		1.36	V_i = 64.2 fps = 43.8 mph
26.50		1.70	
31.80	I	2.04	
37.10		2.37	
42.40		2.70	
47.70		3.04	
53.00		3.38	
58.30		3.72	
63.60		4.06	
68.90		4.37	
74.20		4.67	
79.50		4.96	
84.80		5.25	
90.10		5.54	
95.40		5.84	
100.70		6.14	
106.00	L.C.	6.45	
111.30		6.73	
116.60		7.03	
121.90		7.32	
127.20		7.63	V_{lc} = 56.0 fps = 38.2 mph
132.50		7.91	
137.80		8.21	
143.10		8.51	
148.40		8.82	
153.70		9.12	
159.00		9.42	
164.30		9.72	
169.60		10.01	
174.90		10.30	

TEST 538-6

Time (Sec. x 10^{-3})		Displacement (ft.)	
180.20		10.60	
185.50		10.89	
190.80		11.17	
196.10		11.47	
201.40		11.78	
206.70		12.07	
212.00		12.36	
217.30		12.64	
222.60		12.94	
227.90		13.23	
233.20		13.53	
238.50		13.83	
243.80		14.12	
249.10		14.41	
254.40	Camera (1)	14.72	
259.70		14.99	
265.00		15.29	
270.30		15.58	
275.60		15.87	
280.90		16.16	
286.20		16.47	
291.50		16.73	
296.80		17.03	54.0 fps
302.10		17.31	
307.40		17.60	
308.46	*	17.67	$m = \frac{54.0}{54.5} = 0.993$
313.11		17.93	
317.76		18.19	54.5 fps
322.41		18.44	
327.06		18.69	
331.71		18.94	
336.36		19.20	
341.01		19.43	
345.66		19.69	
350.31		19.95	
354.96	Camera (2)	20.20	
359.61		20.45	
364.26		20.71	
368.91		20.97	
373.56		21.21	
378.21		21.45	
382.86		21.70	
387.51		21.96	
392.16		22.21	

* = reference mark for correlation of cameras

TEST 538-6

Time (Sec. x 10^{-3})		Displacement (ft.)	
387.31		22.46	
391.46		22.73	
395.61		22.96	
399.76		23.21	
403.91		23.46	
408.06		23.72	
412.21		23.98	
416.36		24.21	
420.51		24.47	
424.66		24.72	
428.81		24.98	
432.96	F	25.22	
437.11		25.46	
441.26		25.71	
445.41	Camera (2)	25.95	53.3 fps = 36.7 mph
449.56		26.20	
453.71		26.45	
457.86		26.70	
462.01		26.95	
466.16		27.20	
470.31		27.45	
474.46		27.69	
278.61		27.95	
482.76		28.20	
486.91		28.45	
491.06		28.71	
495.21		28.96	
499.36		29.22	
503.51		29.46	
507.66		29.72	
511.81		29.96	

Figure A-13. Test 538-6: time-displacement data.

APPENDIX B

LABORATORY AND ANALYTICAL INVESTIGATIONS

LABORATORY TESTS

Laboratory tests were conducted on the various base concepts to gain basic data on their static and dynamic behavior. Impact tests yielded information on the dynamic load-deformation properties for the two types of cast aluminum transformer bases, and the cast aluminum shoe base with integral riser. Impact tests of a cast aluminum shoe base, conducted by ALCOA, are included. [Note that the ALCOA test procedure (*10*) is different from that used in this study.] The fracture energy was calculated for each base. Their values are correlated with the full-scale tests with the intent of establishing a test method for the laboratory evaluation of base concepts.

Static tests were conducted on each of the bases to obtain data which could be compared to that from the dynamic tests.

The major developmental work on the triangular slip base has been reported previously (*5*). Analytical studies and laboratory tests were conducted to extend the knowledge of this concept and to explore a modification to enhance its performance in low-speed collisions.

Static Tests

The static tests were conducted using the fixture shown in Figure B-1. In all tests the load was applied 14 in. from the bottom surface of the base by a hydraulic ram acting on a yoke. The load surface of the yoke was 4 in. in diameter. The hydraulic ram was mounted on a roller bearing so that as the base deformed the applied load would continue to act in the plane of the bottom surface of the base. The magnitude of the load was measured with a strain gauge load cell. Displacement of the yoke was measured with a linear differential transformer.

Dynamic Tests

The dynamic tests were conducted by impacting the bases with a ballistic pendulum. The pendulum and a typical test set-up are shown in Figure B-2. The pendulum was fabricated from a length of 12-in. OD pipe and was ballasted with steel-slug aggregate concrete to obtain a total weight of 1,000 lb. The striker head was made of 4-in. OD pipe. The face of the striker head was covered with ⅛-in.-thick rubber gasket material. In all tests the pendulum was dropped from an effective height of 14 ft 10 in. The point

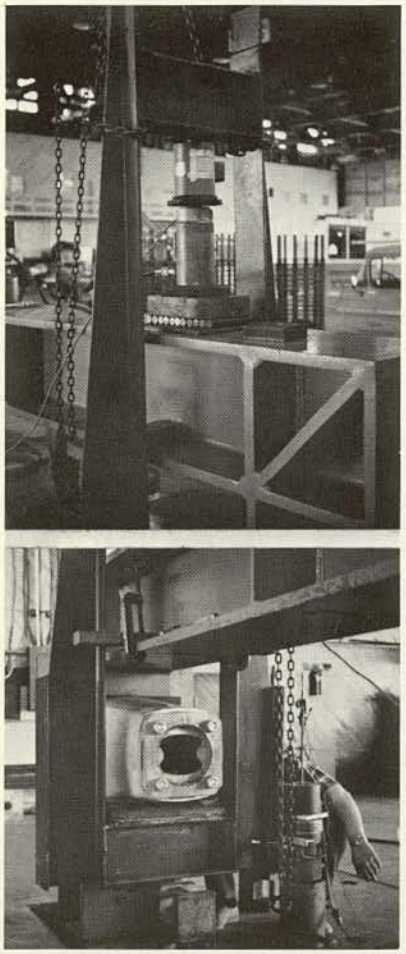

Figure B-1. Static load test fixture.

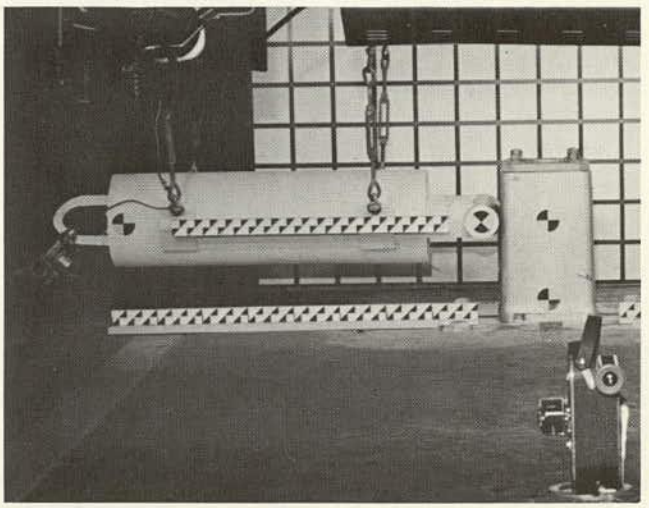

Figure B-2. Ballistic pendulum.

of contact was 14 in. above the mounting plate (this dimension was chosen to be compatible with the bumper height of the 1958 Fords used in the full-scale tests). The pendulum was raised by an overhead hoist and released by an electrically actuated helicopter hook. All of the transformer bases tested had a cast steel mounting plate, identical to the one used on the steel poles in the full-scale tests, bolted to the top surface.

Two types of instrumentation were used. To obtain time-displacement and phenomenological behavior, a Red Lake Laboratory HYCAM camera, operating at 1,500 pictures per sec, was used. The time-displacement information obtained was used to calculate initial velocity. Stadia boards were mounted on the pendulum and in the foreground to supply distance references (Fig. B-2). These boards were graduated in 1-in. increments.

The data-reduction techniques used for these tests are identical to those described in Appendix A.

A crystal accelerometer (Kistler Instruments Corporation Model 808A) was mounted on the longitudinal axis of the pendulum on the rear end plate. A Kistler Instruments Corporation Model 504A charge amplifier was used to amplify and condition the signals. The output of the amplifier was passed through a Kistler Model 544A, 1,000 Hz, 12 db filter before being recorded on magnetic tape. The transducer was calibrated electronically using a 1-volt square-wave signal and the electronics contained within the amplifier. This calibration signal was recorded for subsequent use in the reduction of the data. A 500 Hz sinusoidal signal was also recorded during the test to provide an accurate time reference.

The data from the accelerometer were reduced in a manner similar to that previously explained. Time-displacement information was cross-plotted with deceleration time data (reduced to force-time data) to obtain a force-displacement curve. The energy absorbed by the base to fracture was determined from the area under the curve.

TEST RESULTS

Aluminum Transformer Bases

Two types of aluminum transformer bases were tested. The results of the static and dynamic tests on the base designated as Base A (A. B. Chance UDP-521; this type of base was used in full-scale Test 538-13) are shown in Figures B-3 and B-4, respectively. Figures B-5 and B-6 show the results of the tests for the base designated as Base B (A. B. Chance UDP-46; this type of base was used in Test 538-6). The photographs on the figures show the failure modes.

Note the similarity of the fractures in the static and dynamic tests. For Base A, local crushing occurred at the point of load application. This was caused by the concentration of force on the curved surface. The failure was initiated by a tension crack normal to the bottom edge near the mounting lug. This crack propagated diagonally toward the front face (impacted face). The fracture is not as clean as in the static tests due to the secondary damage done by the passage of the pendulum.

For Base B, the striker of the pendulum made contact parallel to the flat face without crushing. The failure occurred similar to that in Base A. In the static test of Base B the failure was initiated by a tensile crack normal to the bottom surface, with final failure occurring by fracture of the mounting lugs.

Steel Progressive-Shear Transformer Base

The steel progressive-shear transformer base is shown in Figure B-7 (Millerbernd Type B; this type of base was used in Test 538-8). Tests were run with the bases oriented in two different positions. This was necessitated by the fact that the failure load depends on the point of load application. If the base is loaded on the flat side, all six button welds on the face must fail simultaneously. If the load is applied on one edge, the welds fail progressively from the outside toward the center. This orientation results in less total resistance.

Figure B-7 shows the result of the static tests when loaded on the flat side. Note that complete failure did not occur due to excessive deformation (the limits of the loading system were exceeded). When the base was tested dynamically in this orientation, the total input energy of the pendulum (14,800 ft-lb) was absorbed without failure.

Figure B-8 shows the results when the base was loaded on the edge (45° to the flat face). Note that complete failure occurred by a progressive failure of the button welds. The peak resistance occurred when the first weld sheared. The load decreased slightly as the other welds progressively sheared. The load then dropped rapidly, with considerable deformation occurring before the load increased as the welds on the back edge were sheared. Note that the resistance offered by this base when loaded on the edge is considerably lower than when loaded on the flat face.

Aluminum Shoe Base with Integral Riser

The aluminum Kaiser AT-50 base (used in Test 538-5) is a cast shoe base with an integral riser. The shaft is epoxyed to the riser. To simulate the rigidity of the shaft for the dynamic tests, a 30-in. stub shaft was epoxyed to the cast base. Figure B-9 shows the results of the static test. Note that the failure occurred by the initiation of tensile cracks in the flange. In the dynamic tests (Fig. B-10) the failure occurred as a shear failure at the base of the stub shaft. Note that the failures in the two dynamic tests are essentially the same.

Cast Aluminum Shoe Base

The results of two dynamic tests, conducted by ALCOA, are shown in Figure B-11 (*10*). The tests were conducted using an 8-in.-diameter, 0.188-in. wall, 25-ft. aluminum shaft (complete support less mast arm). Two drop hammers were used—1,000 lb in Test 1, and 2,000 lb in Test 2. The impact load was applied through a 6-in. spreader block placed 20 in. above the plane of the base. The shoe bases used in these tests were identical to those used in Tests 538-11 and 12.

The base failed by shearing the fillet welds at the top and

bottom of the base, with a secondary fracture of the shaft at the point of impact. These failures were similar to those experienced in the full-scale collision tests. No static tests were conducted.

Summary of Results

Table 6 is a summary of the results of the dynamic and static tests. Note that the ratios of P_{dyn}/P_{static} indicate that, for the aluminum bases, the dynamic fracture load is ap-

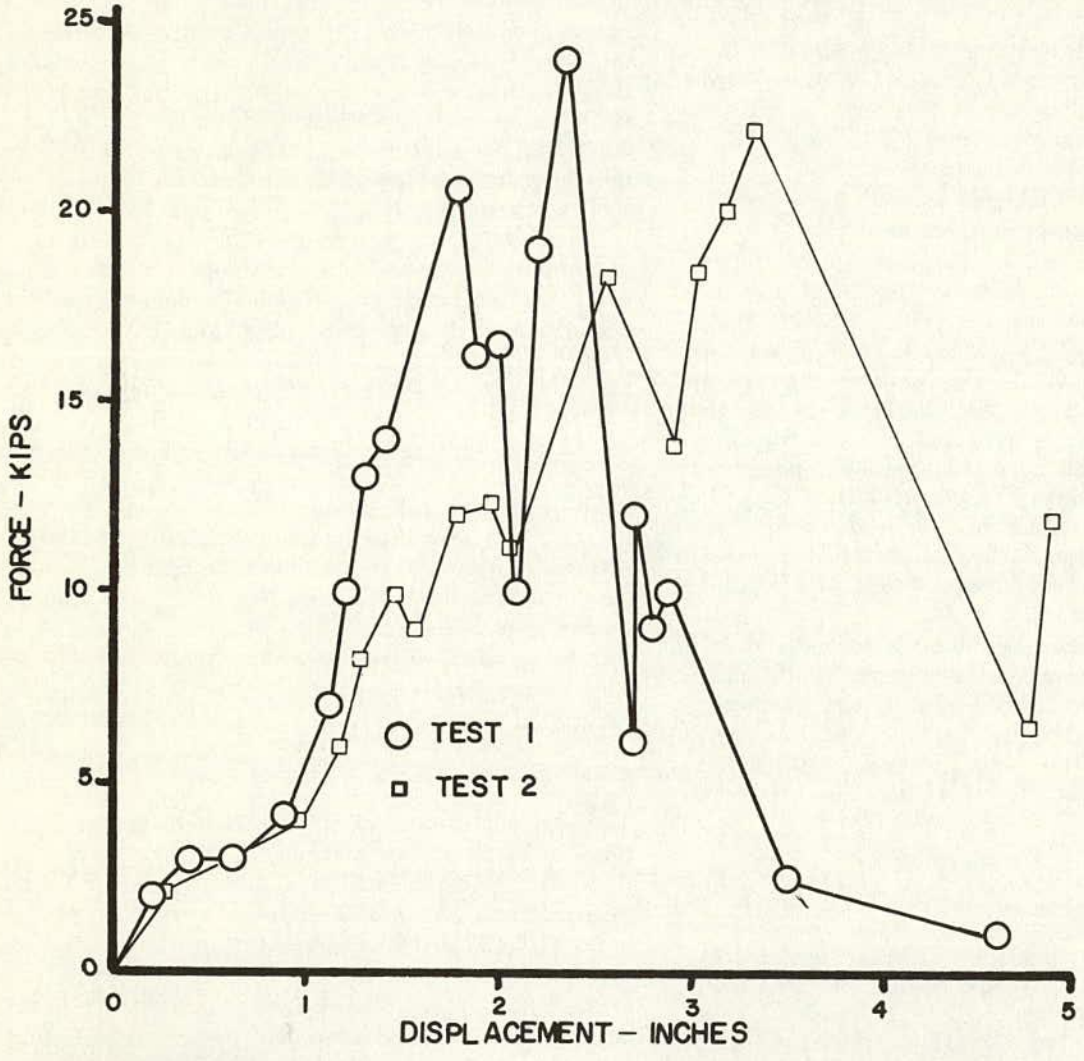

TEST 1

TEST 2

Figure B-3. Static test, aluminum T-*Base A.*

proximately 60% greater than the static fracture load. For the progressive-shear base, the opposite trend is indicated; the dynamic fracture load is 78% of the peak static load. Table 6 also gives the base fracture energy for each test and the average value.

In the tests on the cast shoe bases, two rams of different weights were used (1,000 lb in Test 1, 2,000 lb in Test 2). The drop height of each ram was the same; hence, the energy in Test 1 was 50% of that in Test 2.

CORRELATION OF BASE FRACTURE ENERGIES WITH THE RESULTS OF FULL-SCALE TESTS

The validity of the use of laboratory-derived base fracture energy as a measure of energy absorbed by the base in a

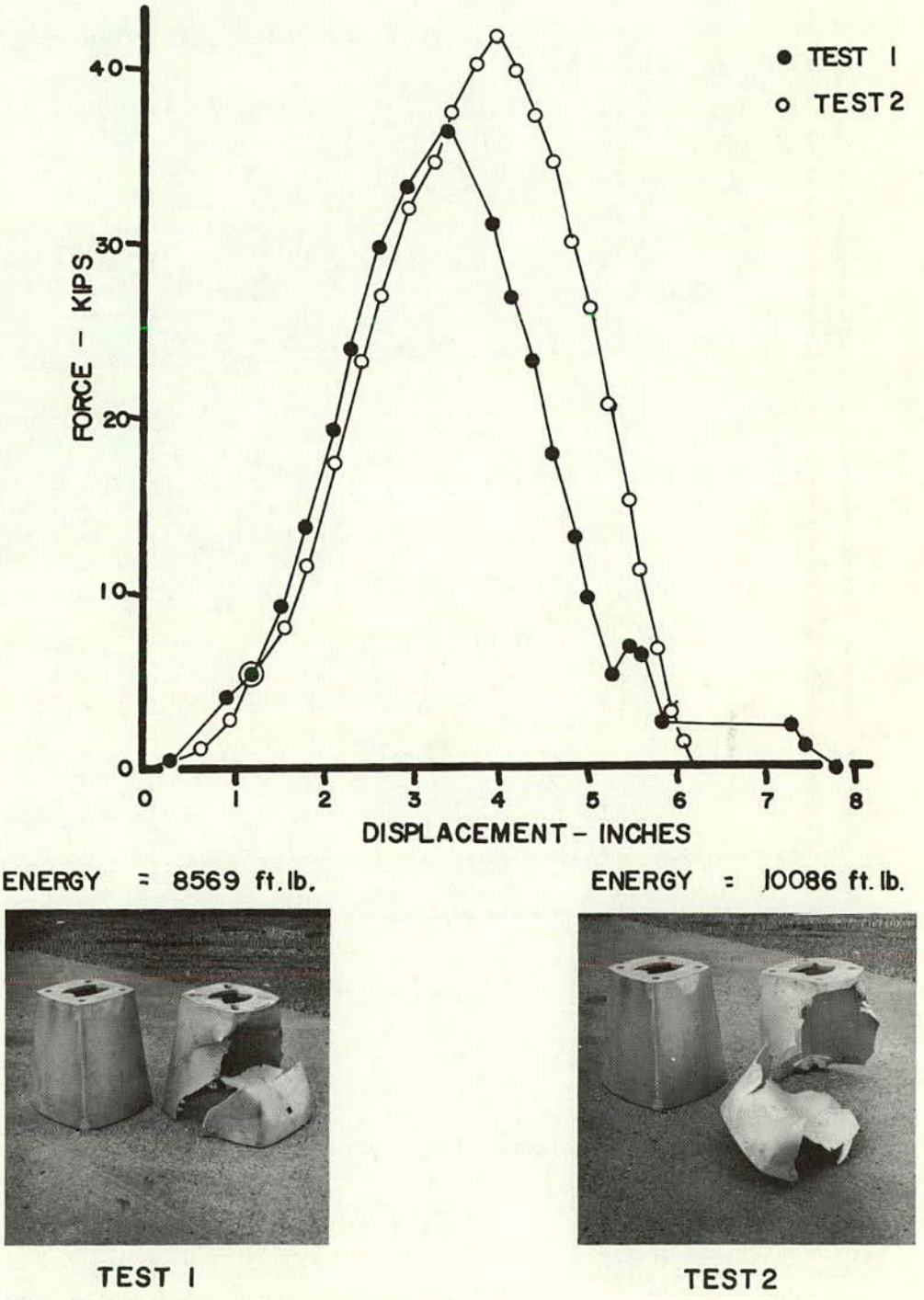

Figure B-4. Dynamic test, aluminum T-Base A.

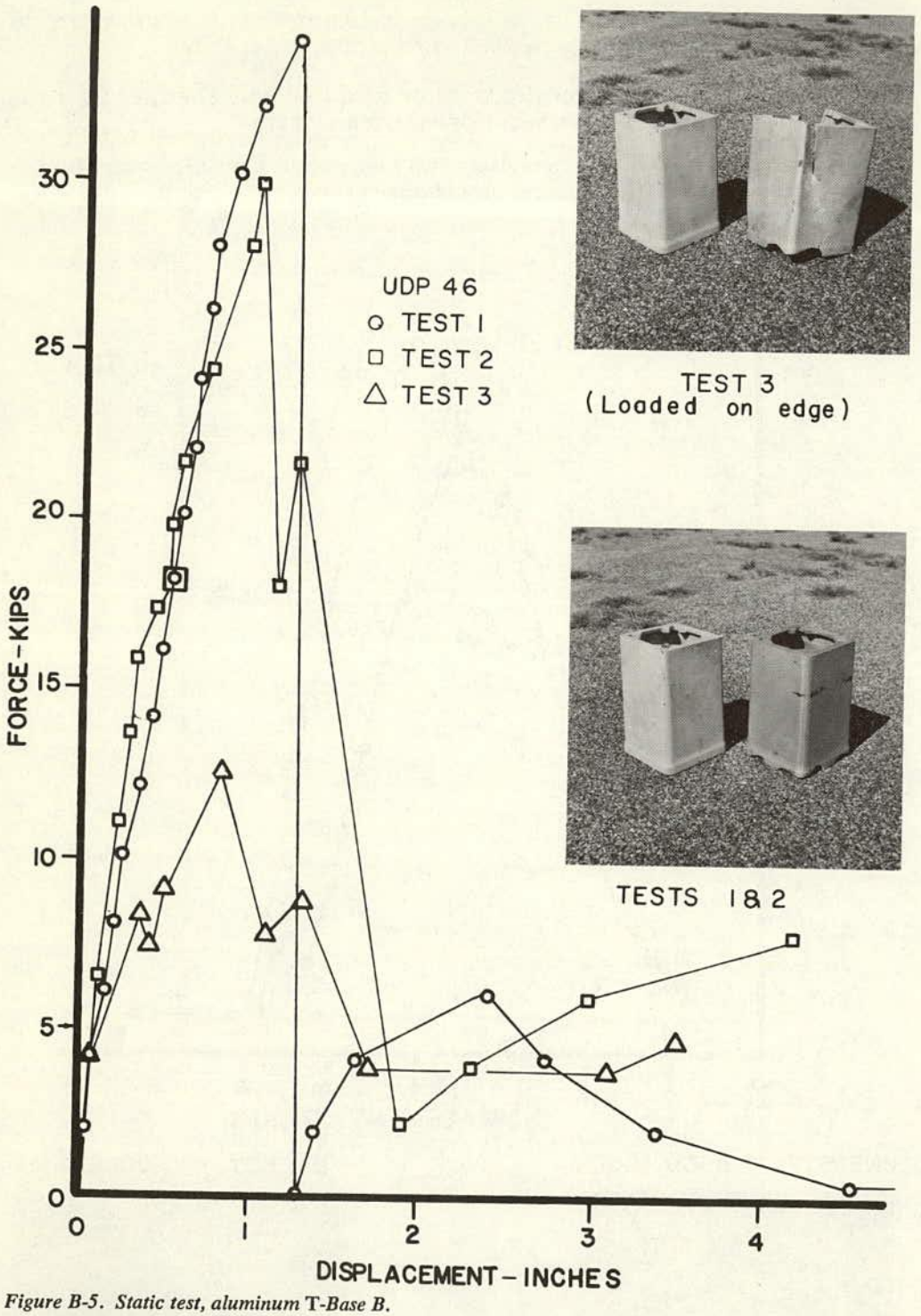

Figure B-5. Static test, aluminum T-*Base B.*

full-scale test can be established as follows. Assume that the vehicle is a single degree-of-freedom spring-mass system. It has been established that the spring, representing the vehicle force-deformation characteristics, can be represented as being linear (*15*, p. 3). The spring stiffness is determined from the peak vehicle deceleration and vehicle deformation using data from full-scale tests.

$$K = g_{max}/d \text{ [=] g/ft} \qquad \text{(B-1)}$$

or

$$k = \frac{g_{max}W}{d} \text{ [=] lb/ft} \qquad \text{(B-2)}$$

in which

g_{max} = peak vehicle deceleration (g);
g = 32.2 ft/sec^2;
W = vehicle weight (lb); and
d = total vehicle deformation (ft).

Also, assume that at the time when the vehicle and support lose contact the support rotational velocity is

$$\omega = \beta V_{lc}/r \qquad \text{(B-3)}$$

in which

ω = rotational velocity of the support shaft about its mass center (rad/sec);
β = multiplying factor to account for the fact that the horizontal component of ω must be larger than V_{lc} for separation to occur; and

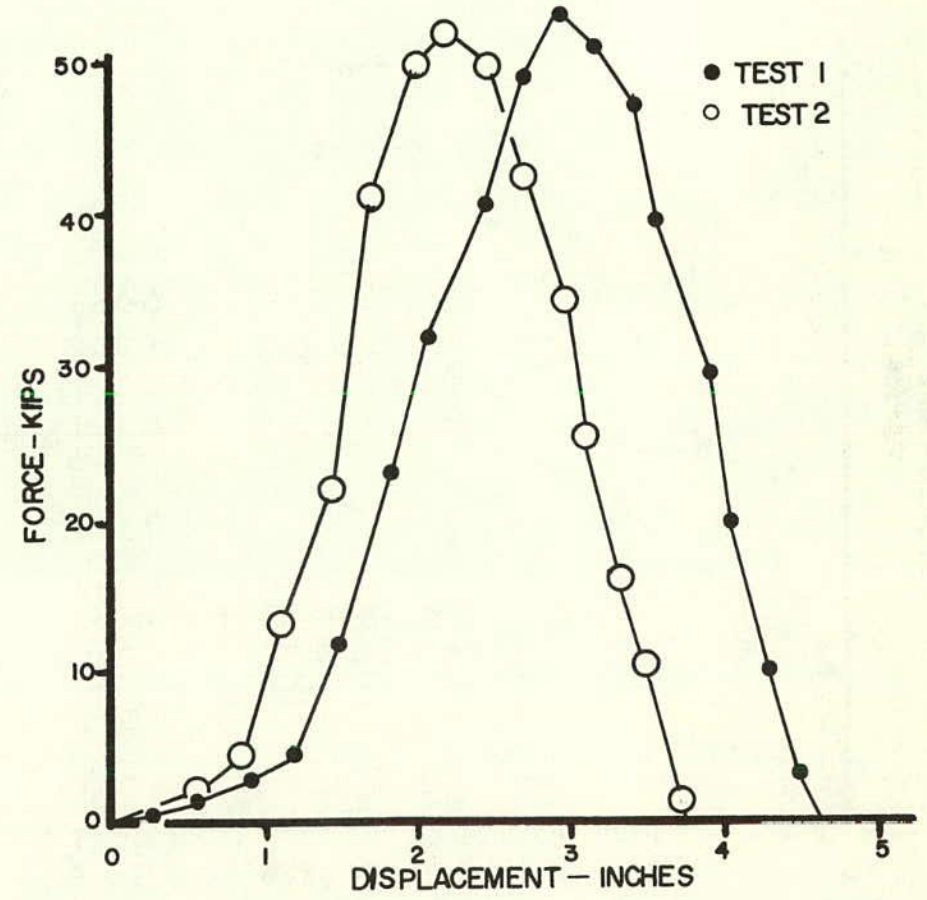

Energy = 8764ft-lb

Energy = 7267ft-lb

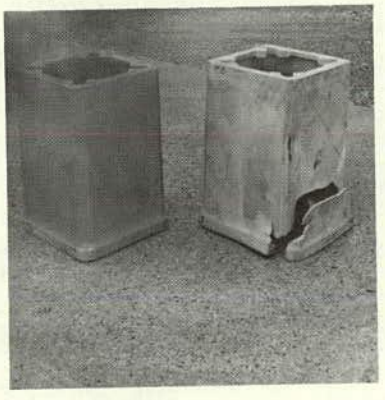

TEST 1

TEST 2

Figure B-6. Dynamic test, aluminum T-*Base B.*

$r =$ distance from base to the mass center of the support (ft).

This relation assumes that rotation, in the direction of vehicle motion, occurs instantaneously about its mass center. By neglecting the out-of-plane rotational and in-plane translational velocities of the support, the following energy balance equation can be written:

$$\frac{1}{2}\frac{W}{g}(V_i^2 - V_{lc}^2) = BFE + \frac{1}{2}kd^2 + \frac{1}{2}I_0\left(\frac{\beta V_{lc}}{r}\right)^2 \quad \text{(B-4)}$$

in which

$V_i =$ initial vehicle velocity (ft/sec);

$V_{lc} =$ vehicle velocity at loss of contact (ft/sec);

$BFE =$ base fracture energy (ft-lb); and

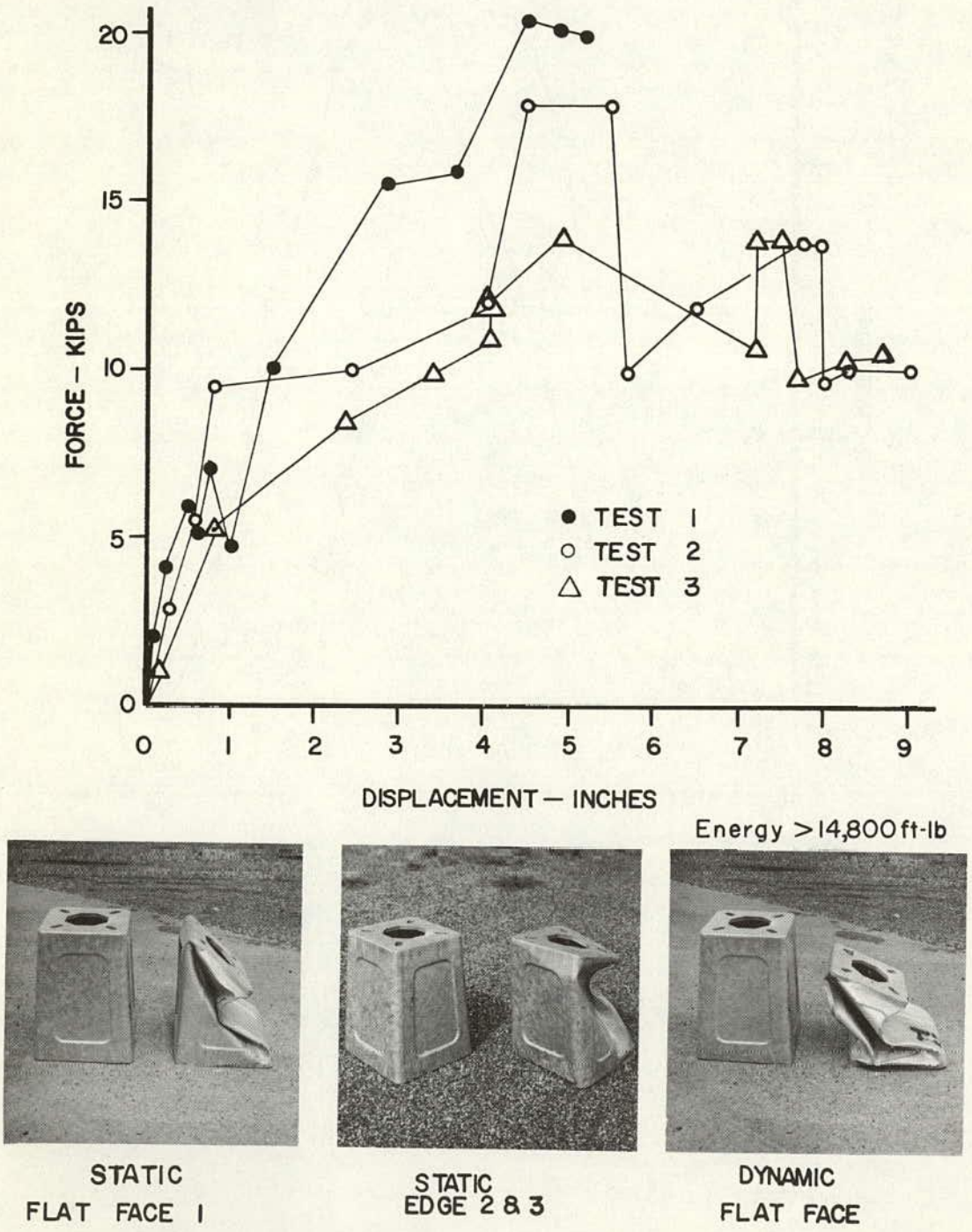

Figure B-7. Static test, steel progressive-shear base.

I_0 = mass amount of inertia about the mass center (ft-lb-sec/rad).

Solving for V_{lc} yields

$$V_{lc} = \sqrt{\frac{2\left[\frac{WV_i^2}{2g} - BFE - \frac{Kd^2}{2}\right]}{\frac{W}{g} + \left(\frac{\beta}{r}\right)^2 I_0}} \qquad \text{(B-5)}$$

By substituting the known information into the right-hand side, the value of vehicle velocity at loss of contact can be calculated. This value is compared with that measured in the full-scale test. If the laboratory-determined values of base fracture energy represent the energy absorbed by the base in the full-scale test, the calculated and measured change in velocity should agree within limits.

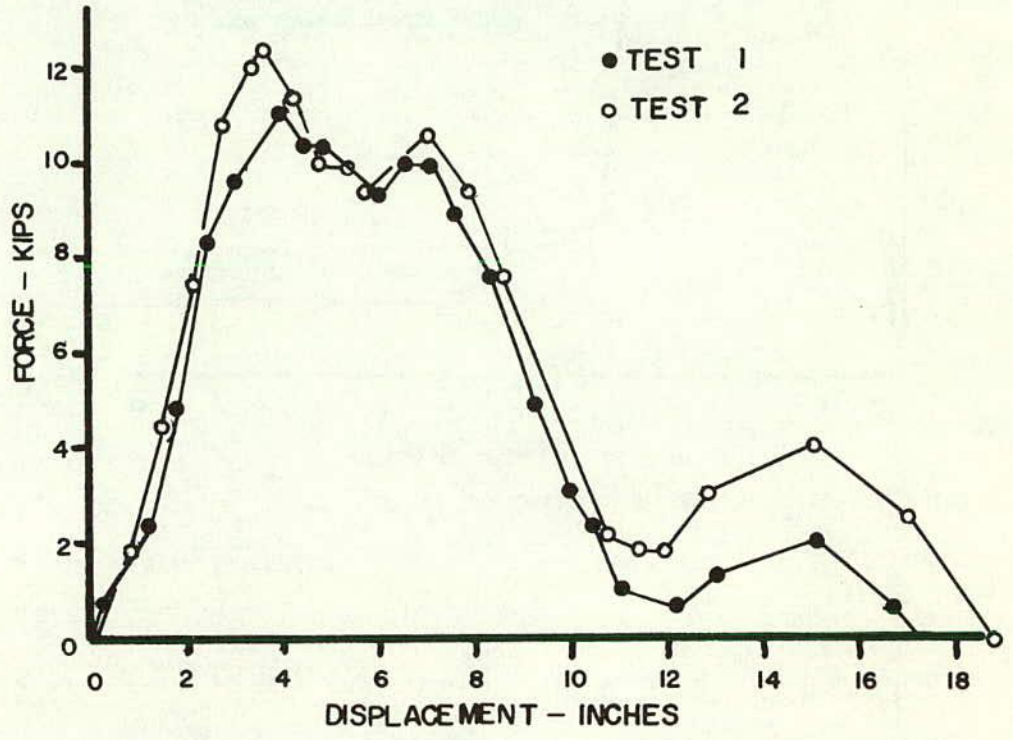

Energy = 6901 ft-lb

TEST 1

Energy = 8766 ft-lb

TEST2

Figure B-8. Dynamic test, steel progressive-shear base.

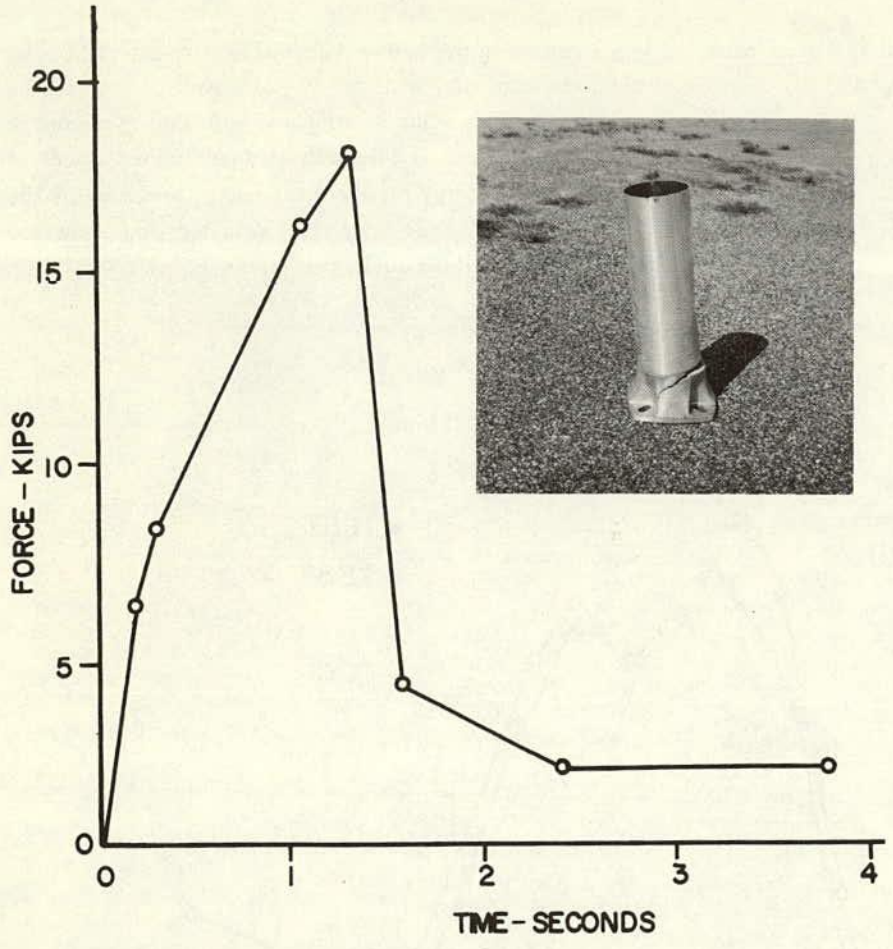

Figure B-9. Static test, aluminum shoe base with riser.

ENERGY = 6886 FT.LB.

TEST 1

ENERGY = 8270 FT. LB.

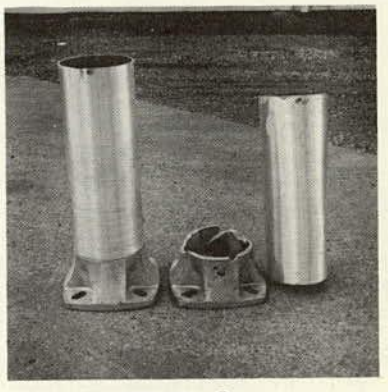

TEST 2

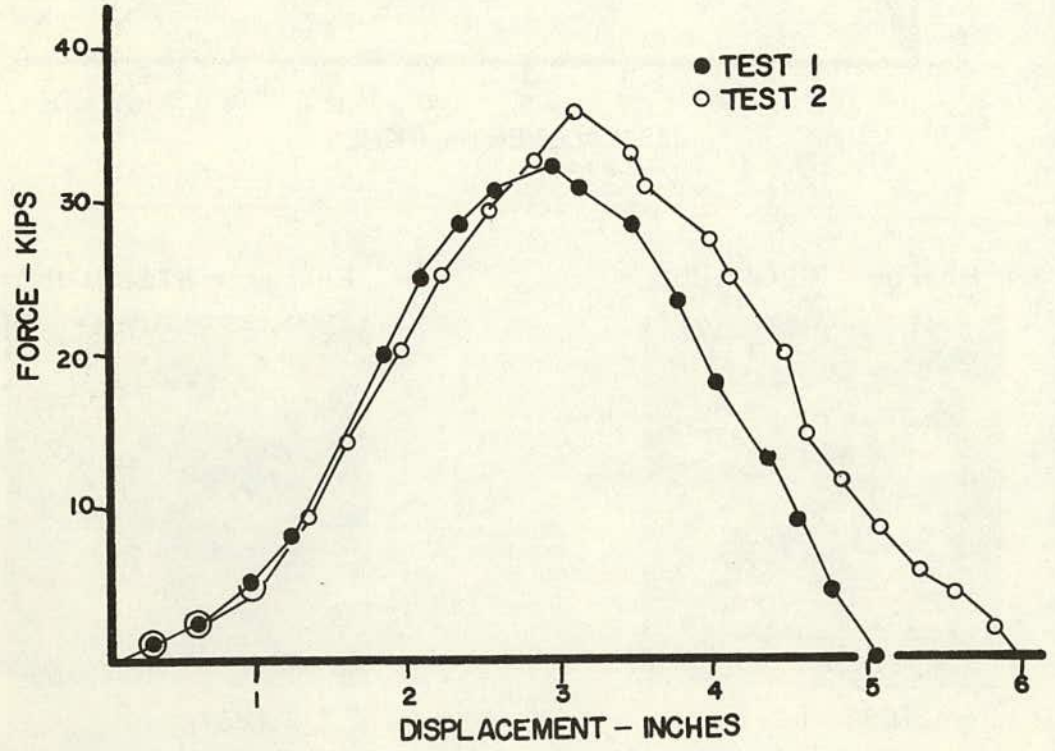

Figure B-10. Dynamic test, aluminum shoe base with riser.

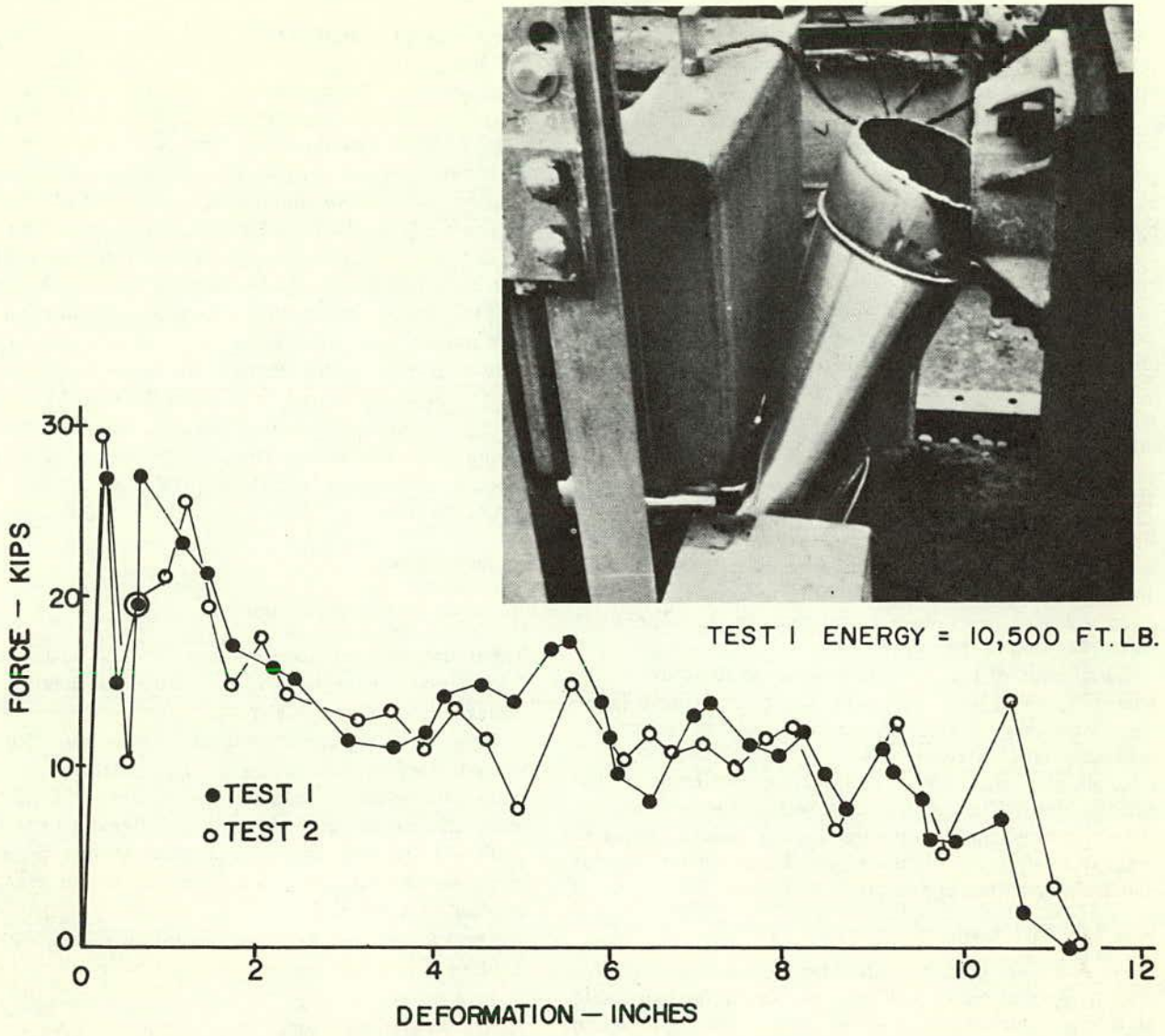

Figure B-11. Dynamic test for aluminum shoe base. (Data and photo courtesy ALCOA.)

APPENDIX C

COST-EFFECTIVENESS STUDY

The major intent of this study was to provide a method for improving the economic analysis of roadway illumination. Cost data are presented which center on lighting costs as related to various bases that are being used, and some that are under consideration for use, with emphasis on the breakaway bases. The cost calculation method presented, however, need not be limited to comparing base costs, and can be used as an over-all design tool.

To obtain current cost data, surveys were made from available literature and by visits to several districts of the Texas Highway Department and the Texas Turnpike Authority. These sources provided valuable information. Data also were obtained from the full-scale tests described in Appendix A.

Under study were initial costs, accident costs resulting from vehicles colliding with light poles, and normal main-

tenance costs. The accident costs were further divided into costs for structural damage to the pole and base, damage to the vehicle, and costs of injury to the occupants.

Expressions were developed which relate roadside illumination costs to major contributing factors. These expressions can be used to compare lighting systems on the basis of cost-effectiveness. The validity of the answers given by these expressions depends on the accuracy of the input data, and, admittedly, some of the input requirements may be difficult to determine. For example, one input parameter is the encroachment rate of vehicles for a given length of roadway. The lack of information in this area and related areas has been due in part to inadequacies in reporting and recording accident data. Measures are now being taken to rectify this situation; with this development, more useful information should become available.

SUPPORT DATA

This section presents cost information for various types of bases and poles, and information on the average cost of accidents with different types of bases and poles. The costs given are used in example calculations in the "Economic Model" section of this appendix.

Initial costs of lighting installations include those of the pole or support, base, pole arm, luminaire, ballast, lamp, foundation, wiring, conduit, trenching, and all other miscellaneous labor and materials.

In addition to the initial costs, there are maintenance and accident costs. The accident costs include those of injuries, vehicle damage, and lighting installation damage. Accident cost information was obtained from Texas accident records and from crash-test appraisals.

Pole and Base Costs

Table C-1 gives costs furnished by the manufacturers for several types of bases with steel or aluminum poles with 10-ft arms and 40-ft mounting height. The costs would vary, depending on quantity, geographic location, and differences in (1) weight (for a given pole type and height), (2) design and weight of bases for a particular base concept, and (3) the amount of discount. However, costs would remain approximately in the same proportions. Because of these variations, the costs given are not meant to be the costs in a particular situation but are intended only to show the relative differences in costs which might be expected. It might be added, however, that these costs agree closely with those given by Cassel and Medville (*16*), who consulted a large number of manufacturers and buyers on the costs of various heights of steel or aluminum poles with shoe or transformer bases.

TABLE C-1

INITIAL COST OF POLE, BASE, AND ARM [a]

POLE AND BASE	COST ($)
(*a*) Steel Pole	
Steel shoe	153
Steel transformer	191
Alum. transformer	192
Carbon steel progressive-shear	192
Steel slip	194
Stainless steel progressive-shear	211
(*b*) Aluminum Pole	
Alum. shoe	281
Alum. transformer	320
Alum. slip	341

[a] For 40-ft mounting height and 10-ft arm.

With 20 to 40 poles per mile, the breakaway bases with steel poles would initially cost about $800 to $1,600 extra per mile, as compared to the steel shoe base. Accident cost savings per mile, due to using the breakaway bases, of an amount significantly greater than this extra cost would justify their use.

Accident Costs

Accident Record Information

There are two primary sources for the accident cost information used in the example calculations herein: Texas accident records, and crash tests.

Most of the accident record information is for 1966 and was collected by Lazenby (*19*). These records cover accidents with lighting installations in the cities of Dallas, Fort Worth, San Antonio, Beaumont, and Houston, and on the Dallas-Ft. Worth Turnpike. Complete information was not given for all accidents; the information that was given appears in Table C-2.

The average costs based on this information are given in Tables C-5 and C-6, and are discussed more fully as follows.

Injury Types and Costs

Table C-3 shows the numbers and types of injuries for four types of pole-base combinations. A type "A" injury is one that entails visible signs of injury, such as a bleeding wound or a distorted member, or one which results in the person being carried from the accident scene. A type "B" injury is one that is visible, such as bruises, abrasions, swelling, limping, and so forth. A type "C" injury is one for which there is no visible injury but for which there is complaint of pain or momentary unconsciousness.

The National Safety Council (*18*) cost values for different types of injury are used in this report. These costs include those of doctor, hospital, medical expenses, and lost work time, but do not include allowance for pain and suffering. The National Safety Council average values for the U.S. for 1967 are given in Table C-4.

The values in Table C-3 indicate that the steel transformer base and the steel shoe base cause considerably more injuries than does the aluminum transformer base. Combining the number of injuries by type from Table C-3 with the cost for each type of injury gives the average injury costs in Tables C-5 and C-6. The average values in Ta-

TABLE C-2

NUMBER OF ACCIDENTS, BY TYPE OF COST INFORMATION

POLE	BASE	NO. OF ACCIDENTS	TYPE OF COST INFORMATION (NO. OF ACCIDENTS)			
			INJURY	VEH. DAMAGE	LIGHTING INSTAL. DAMAGE	ALL THREE
Alum.	Alum. transformer	58	58	48	55	47
Steel	Alum. transformer	19	19	15	15	13
Steel	Steel transformer	37	37	27	31	25
Steel	Steel shoe	35	35	35	35	35

ble C-5 are those obtained when all accidents are used. The average values in Table C-6 are those obtained when only those accidents with complete information on all types of accident costs are used.

Costs of Damage to Lighting Installation

The average cost of damage to the lighting installation generally is higher for breakaway-type bases than for non-breakaway-type bases (see Tables C-5 and C-6). Historical cost information on lighting installation damage is given in Table C-7.

Vehicle Damage Costs

Tables C-5 and C-6 give the average costs per accident for the Texas accident sample.

In addition to the vehicle-damage estimates from accident records, information was provided by the crash tests in the form of cost appraisals (see Appendix A) made by an experienced damage appraiser. The average costs of some of these crash tests are given in Table C-8. To facilitate comparisons of these appraisal costs and the costs from actual accident records, the average accident costs from Table C-5 are included in Table C-8. The only pole and base for which vehicle-damage cost from both crash tests and accident records is available is the steel pole on an aluminum transformer base; the crash-test cost was slightly higher (by $28).

For a vehicle of given weight and velocity, the damage from hitting a luminaire support increases with an increase in base fracture energy. The amount the vehicle is slowed (the decrease in velocity) is related to the deformation—hence, to vehicle damage. The fact that deformation is directly related to the base fracture energy was shown by the crash tests.

This information on the nature of damage, together with the accident record and crash-test information, was used to assign costs of accidents for pole and base types for which accident record information was not available. Table C-9 gives values for accident costs from accident records, and also gives estimated values.

The costs in Tables C-1 and C-9 are used in comparisons in the "Economic Model" section which follows.

TABLE C-3

ACCIDENT-INJURY DATA

POLE	BASE	NO. OF ACCIDENTS	NO. OF INJURIES, BY TYPE[a]		
			A	B	C
Alum.	Alum. transformer	58	2	4	7
Steel	Alum. transformer	19	3	0	2
Steel	Steel transformer	37	12	3	5
Steel	Steel shoe	35	14	9	0

[a] See text for description of injury types.

TABLE C-4

AVERAGE INJURY COSTS, 1967[a]

TYPE OF INJURY[b]	COST ($)
A	1,570
B	1,110
C	515

[a] From National Safety Council (*18*).
[b] See text for description of injury types.

ECONOMIC MODEL

Initial and maintenance costs of many individual lighting configurations are readily available in the literature or can be accurately computed. Average accident costs for several pole and base combinations are presented in the previous section of this appendix. Therefore, the major effort in constructing the model was directed toward obtaining relationships that could be used to predict the number of accidents involving luminaire supports for a given period of time for a given roadway situation. With this expression for accident rate and the cost data per individual installation, total costs can be computed for a complete lighting system.

TABLE C-5

AVERAGE ACCIDENT COSTS, BY TYPE OF COST INFORMATION [a]

POLE	BASE	AVERAGE DAMAGE COST ($) [b] INJURY	VEHICLE	LIGHTING INSTAL.	TOTAL ACCIDENT
Alum.	Alum. transformer	193 (58)	381 (48)	221 (55)	795
Steel	Alum. transformer	302 (19)	400 (15)	313 (15)	1,015
Steel	Steel transformer	669 (37)	501 (27)	231 (31)	1,401
Steel	Steel shoe	913 (35)	541 (35)	103 (35)	1,557

[a] Using each accident for which information is available for a particular type of cost. See Table C-2.
[b] Numbers in parentheses are the numbers of accidents used in that particular average.

TABLE C-6

AVERAGE ACCIDENT COSTS, BY TYPE OF COST INFORMATION [a]

POLE	BASE	AVERAGE DAMAGE COST ($) [b] INJURY	VEHICLE	LIGHTING INSTAL.	TOTAL ACCIDENT
Alum.	Alum. transformer	170 (47)	385 (47)	225 (47)	780
Steel	Alum. transformer	442 (13)	415 (13)	308 (13)	1,160
Steel	Steel transformer	613 (25)	538 (25)	251 (25)	1,402
Steel	Steel shoe	913 (35)	541 (35)	103 (35)	1,557

[a] Using only those accidents for which complete information is available. See Table C-2.
[b] Numbers in parentheses are the numbers of accidents used in that particular average. Costs are from independent data, and cannot be correlated with costs in Table C-5.

Formulation

Definition of Variables

Following is a list of the variables considered in the analysis:

TABLE C-7

AVERAGE COST OF DAMAGE TO ALUMINUM-POLE, ALUMINUM-TRANSFORMER-BASE LIGHTING INSTALLATIONS, FORT WORTH-DALLAS TURNPIKE, 1958-1967

YEAR	NO. OF ACCIDENTS	AVERAGE DAMAGE COST ($) [a]
1958	7	297.87
1959	7	364.21
1960	12	344.64
1961	9	200.56
1962	15	176.25
1963	18	161.99
1964	11	226.15
1965	16	143.98
1966	25	174.39
1967	24	147.17
Total	144	200.13

[a] These are actual repair costs (not estimates), including all direct costs, plus overhead charges (which represent about 5% of the total cost).

C_I = initial cost of individual lighting system; i.e., the pole, base, foundation, wiring, etc.

C_M = normal maintenance cost per year per individual lighting system. This does not include repairs to the installation resulting from vehicles colliding with the pole.

C_{VD} = average vehicle-damage cost resulting from collision with the pole.

C_{OD} = average occupant injury cost resulting from collision with the pole.

C_{ID} = average lighting installation damage cost resulting from vehicle collision with the pole.

C_{TT} = total cost per mile of a lighting system incurred over the useful life of the system.

$C_{TT}' = C_{TT}$ — accident costs.

T = useful life of the lighting installation. At the end of its useful life the installation will be replaced or removed entirely.

L_E = effective length of vehicle (defined further in subsequent sections).

L_S = distance between adjacent individual lighting installations.

L_L = distance from the limits of the designated lane(s) of travel to the base of the light pole.

x = lateral extent of movement of an encroaching vehicle.

N = number of individual lighting installations per mile.

E = number of vehicle encroachments per mile per year.

TABLE C-8

ACCIDENT COSTS FROM CRASH TESTS AND RECORDS, BY TYPE OF POLE AND BASE

POLE AND BASE	ACCIDENT COSTS, PER ACCIDENT ($)			
		ACCIDENT RECORDS		
	CRASH-TESTS VEH. DAMAGE [a]	VEH. DAMAGE	INJURY	LIGHTING INSTAL. DAMAGE
	(a) Steel Pole			
A. Steel shoe	—	541	913	103
B. Alum. transformer	428	400	302	313
C. Steel transformer	—	501	669	231
D. Stainless steel progressive-shear	458	—	—	—
E. Carbon steel progressive-shear	427	—	—	—
F. Slip base	383	—	—	—
	(b) Aluminum Pole			
G. Alum. shoe (thin base wall)	484	—	—	—
H. Alum. shoe (thick base wall)	693	—	—	—
I. Alum. transformer	—	381	193	221

[a] The crash-test vehicle damage estimates were taken as follows: B., from tests 6, 13; D., from tests 7, 9; E., from test 8; F., from test 10; G., from test 11; and H., from tests 4, 12.

TABLE C-9

AVERAGE ACCIDENT COSTS, BY TYPE OF POLE AND BASE

POLE AND BASE	AVERAGE DAMAGE COST ($) [a]			
	VEHICLE (C_{VD})	INJURIES (C_{OD})	LIGHTING INSTAL. (C_{ID})	TOTAL ($C_{VD}+C_{OD}+C_{ID}$)
	(a) Steel Pole			
A. Steel slip	(380)	(195)	(220)	(795)
B. Alum. transformer	400	302	313	1,015
C. Carbon steel progressive-shear	(400)	(300)	(315)	(1,015)
D. Stainless steel progressive-shear	(425)	(350)	(335)	(1,110)
E. Steel transformer	501	669	231	1,401
F. Steel shoe	541	913	103	1,557
	(b) Aluminum Pole			
G. Alum. slip	(350)	(175)	(200)	(725)
H. Alum. transformer	381	193	221	795
I. Alum. shoe (thin base wall)	(450)	(350)	(350)	(1,150)
J. Alum. shoe (thick base wall)	(500)	(650)	(300)	(1,450)

[a] Figures in parentheses are estimates. Other values are from Table C-5.

Encroachment is defined as an unintentional exit from the designated lane(s) of travel.

I = rate of interest.

ADT = average daily traffic.

H = number of impacts occurring over a given length of highway in a given period of time.

S_V = salvage value of individual lighting installation at end of useful life.

θ = angle formed by path of encroaching vehicle with edge of pavement.

As a basis for computation the total cost per mile, C_{TT}, is calculated over the system's useful life. All costs occurring during this period are discounted to present value by use of discount interest rates. The three major types of costs considered were initial, maintenance, and accident due to vehicle collisions.

Initial Costs

Let C_{IT} equal the initial cost per mile of a lighting system. If there are N individual lighting installations per mile,

$$C_{IT} = (N)\ (C_I) \qquad \text{(C-1)}$$

Maintenance Costs

Let C_{MT} equal the maintenance cost per mile of lighting system occurring over the useful life, T, of the system. Discounting future costs to present values at an interest rate of I, C_{MT} is computed by

$$C_{MT} = \sum_{J=1}^{T} \frac{C_M(N)}{(1+I)^J} \qquad \text{(C-2)}$$

If C_M remains constant over the T years, Eq. C-2 can be written as

$$C_{MT} = C_M(N) \sum_{J=1}^{T} \frac{1}{(1+I)^J} \qquad \text{(C-2a)}$$

Let

$$K_T = \sum_{J=1}^{T} \frac{1}{(1+I)^J} \qquad \text{(C-3)}$$

Eq. C-2a can then be written as

$$C_{MT} = C_M(N)\ (K_T) \qquad \text{(C-4)}$$

Accident Costs

Three types of accident cost are considered: vehicle damage, occupant injury, and lighting installation damage.

Let C_{VDT} equal the total vehicle damage per mile of lighting system occurring over the useful life, T, of the system. By discounting future costs to present values at an interest rate of I, C_{VDT} is computed by

$$C_{VDT} = \sum_{J=1}^{T} \frac{C_{VD}\ (H_J)}{(1+I)^J} \qquad \text{(C-5)}$$

in which H_J is the number of collisions occurring in year J. In general, H is a function of J and their relationship must be known before C_{VDT} can be computed.

Before the number of collisions occurring in any given year can be computed, the frequency of encroachments must first be known. Hutchinson and Kennedy (*20*) sought to develop a relationship between the frequency of median encroachment and traffic volume. Figure C-1 shows a curve taken from the report (*20*). This curve, based on averaged data collected from two expressways, is included to indicate the general shape and direction of the volume-frequency relationship that may be expected. Although the encroachment frequency is, in general, a function of many variables, traffic volume seems to be the most influencing factor.

The curve of Figure C-1 has two basic characteristics—a non-linearity in the low-volume range, and linearity in the higher volume range. Reasons are given in the report (*20*) for the particular shape of the curve. Note that the encroachment frequency is based on both directions of travel. If used for roadside frequencies, one-half of the value should be taken, as an approximation.

Regarding the nature of vehicle encroachments, Hutchinson and Kennedy (*20*) investigated the angle of encroachment, lateral extent of encroachment, and total distance traveled during the encroachment. The number of observed

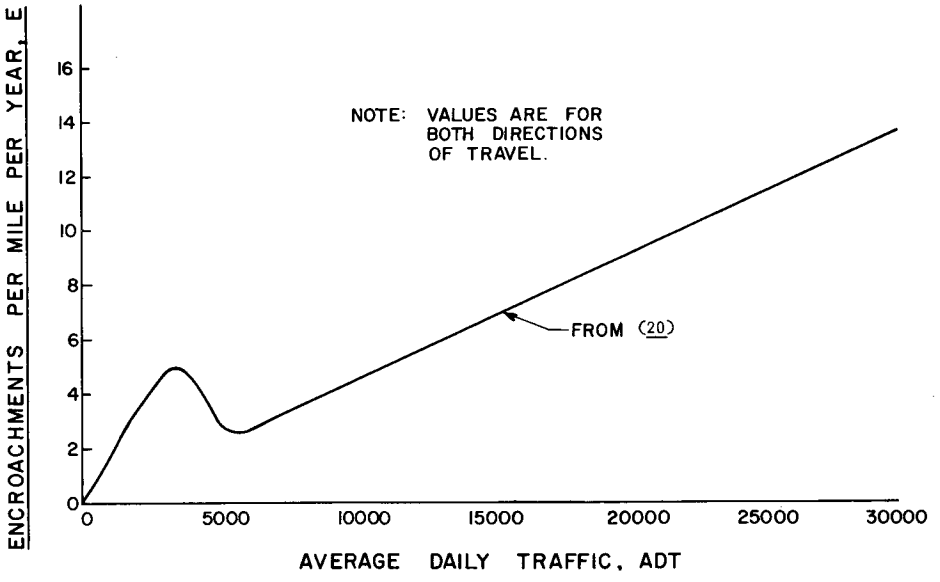

Figure C-1. Median encroachment frequency.

encroachments was in excess of 600 for the roadways considered.

Average values of the previously mentioned parameters were as follows: encroachment angle (°) = 11.0°; lateral extent of travel (ft) = 23.0; and length of travel (ft) = 291.0. Distribution relationships of these parameters were found to be similar to the normal distribution. Ideally, the encroachment angle, lateral extent of travel, length of travel, and velocity of encroachment should all be incorporated into a joint distribution. At present, however, this type of information does not exist. In this analysis, all encroachment angles were represented by an average value. The effects of vehicle velocity are accounted for in the accident cost factors, C_{VD}, C_{OD}, and C_{ID}, which is in effect averaging the velocities of impact. Distribution of lateral travel is discussed in following paragraphs. As more information is developed on joint distributions, it may be possible to increase the accuracy of accident prediction.

Two normal distribution curves for the lateral extent of movement are shown in Figure C-2—one with a standard deviation of 9.0 ft and the other with a standard deviation of 11.0 ft, both having a mean of 23.0 ft. To compute the probability, P, of a vehicle equaling or exceeding a given value of x (say, $x = a$), the following expression is used:

$$P = [1 - \int_{-\infty}^{a} f(x)dx] \qquad \text{(C-6)}$$

Some error is introduced in P by the area to the left of $x = 0$, because P should be zero at $x = 0$. For a given mean, the error increases as the standard deviation increases. For the normal distributions used in this analysis, however, the error will be small and can be ignored.

Figure C-3 shows the actual distribution of lateral movements (*20*) and a normal distribution curve with a standard deviation of 9.0 ft and a mean of 22.0 ft. The median cross-section for which the actual distribution was obtained is shown on the figure.

Figure C-4 is similar to Figure C-3, except the normal distribution has a mean of 23.0 ft. The first normal distribution curve (mean = 22.0 ft) compares favorably with the actual distribution from zero to approximately 17.5 ft of lateral movement. The second (mean = 23.0 ft) compares favorably from approximately 17.5 ft up to 24.0 ft.

Influence of the median cross-section slopes is seen by the changes in the slope of the actual distribution curve. Note that the changes occur at approximately the same lateral distances as changes in the median cross-section slope.

It is felt that the normal distribution can be used to determine the distribution of lateral movements for many roadway conditions. It will have to be modified, however, when there are abrupt changes in the shoulder or median cross-section. A curb, for instance, along the shoulder of the roadway may redirect many encroaching vehicles, especially at low encroachment angles.

Figures C-5 through C-7 show various combinations of normal distributions and are included for reference purposes.

The number of collisions per mile per year can now be computed because the number of encroachments per mile per year, average encroachment angle, pole locations with respect to the roadway, and a means for determining the distribution of lateral movements are known. See Figure C-8; the shaded area represents the path traversed by the encroaching vehicle, with θ equaling the encroachment angle.

Effective length, L_E, is a parameter that accounts for the orientation of the vehicle during the encroachment. If all vehicles left the roadway in a head-on orientation, L_E would equal the vehicle's width. Very little data, statistical or otherwise, were found that could be used to define L_E. Based on limited information obtained from police accident

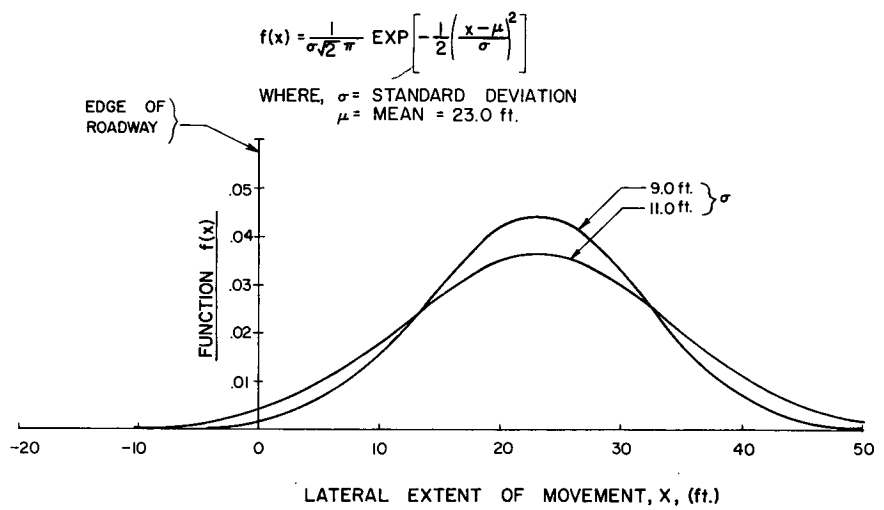

Figure C-2. Normal distribution function of lateral movements.

reports, it seems that L_E could be approximated as the average of the vehicle's length and width.

Once L_E has been determined for individual vehicles, statistical analysis must be applied to determine the distribution of vehicle sizes for a given highway, or it is necessary to resort to an average value for all vehicles. The number and type of vehicles using a given roadway usually are known, and thus the required values should be definable.

The distance from the edge of the pavement to the center of the vehicle is denoted by x. In formulating the problem it was assumed that the effective width of the vehicle was small compared to the length of the encroachment and hence could be set equal to zero. The maximum possible traversable distance along a line connecting adjacent light poles is termed L_D; L_D' is defined as the length of L_D traversed when the vehicle is at x. From geometry

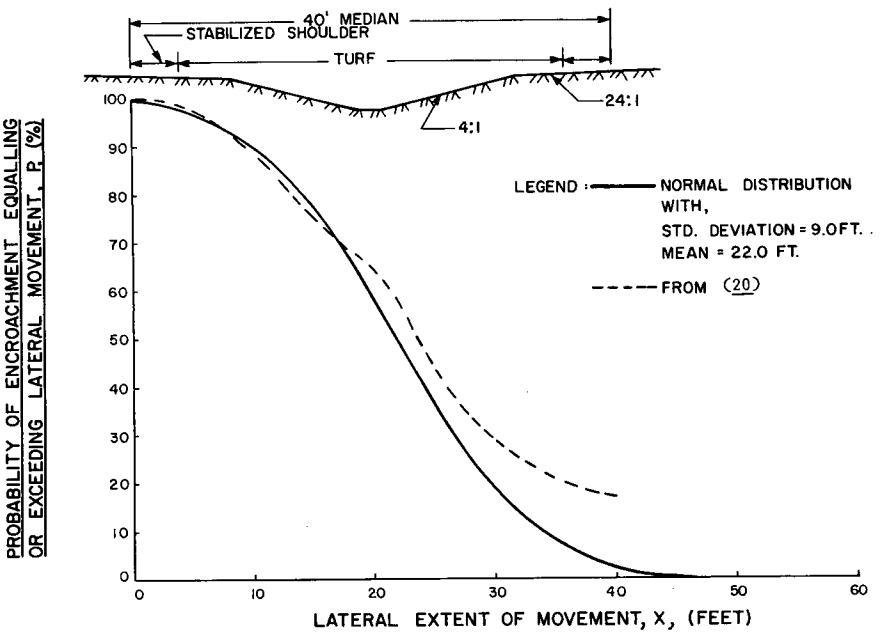

Figure C-3. Distribution of lateral movement, Case 1.

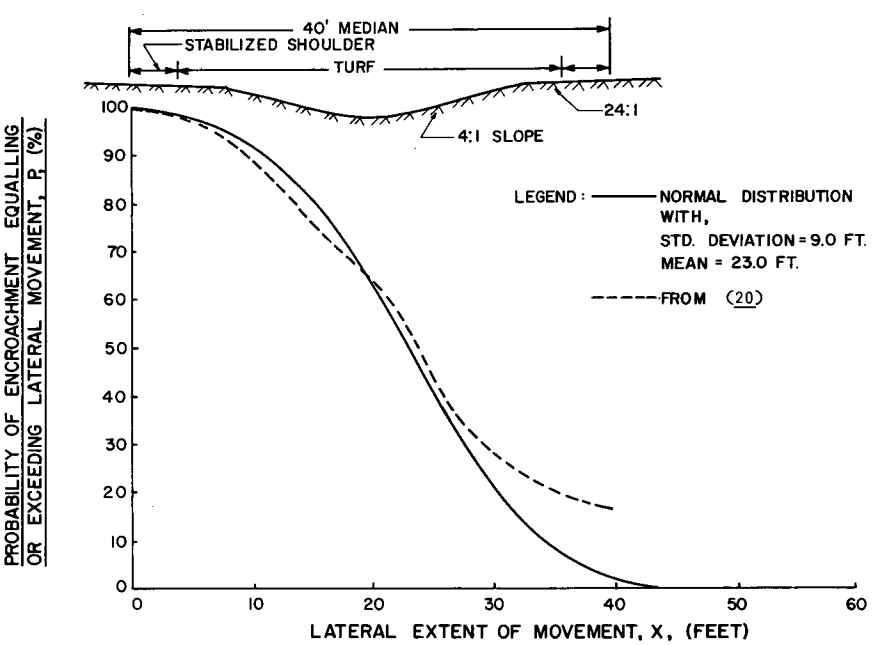

Figure C-4. Distribution of lateral movement, Case 2.

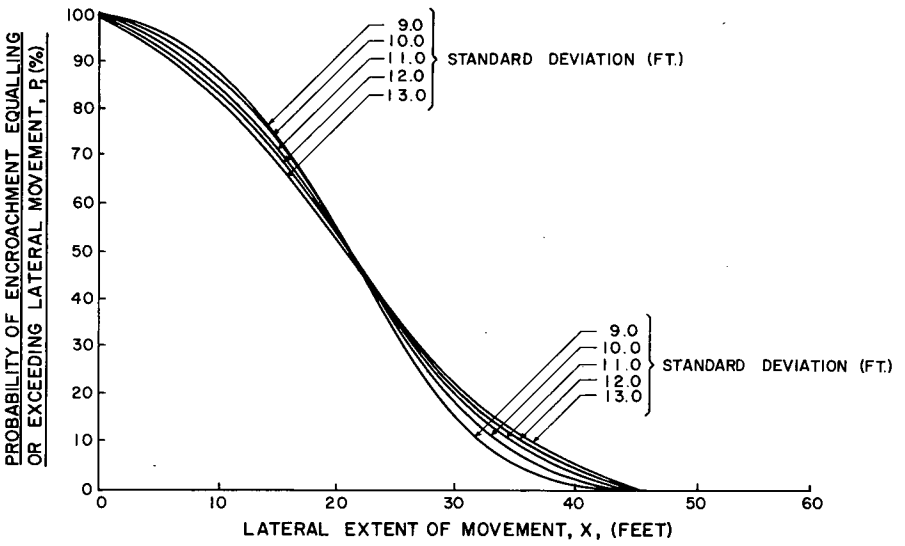

Figure C-5. Normal distribution of lateral movement, mean = 21.0 ft.

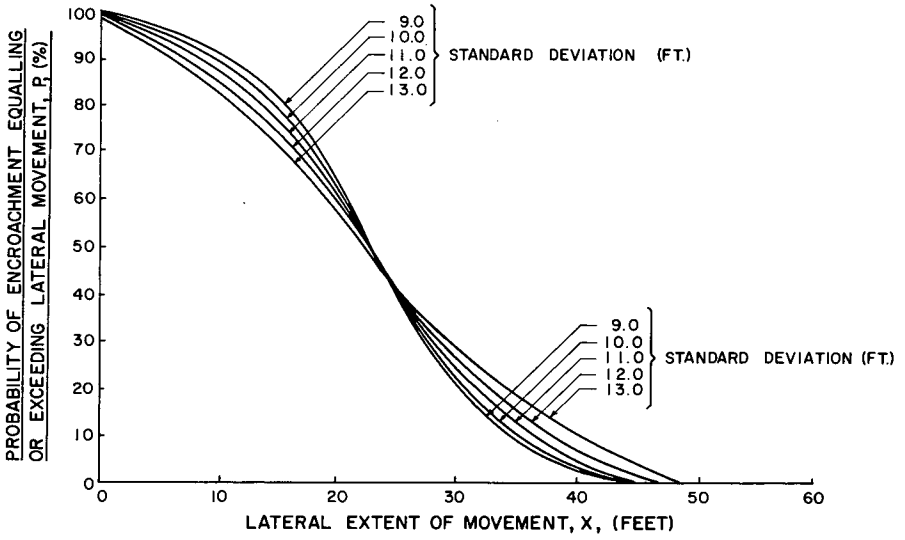

Figure C-6. Normal distribution of lateral movement, mean = 23.0 ft.

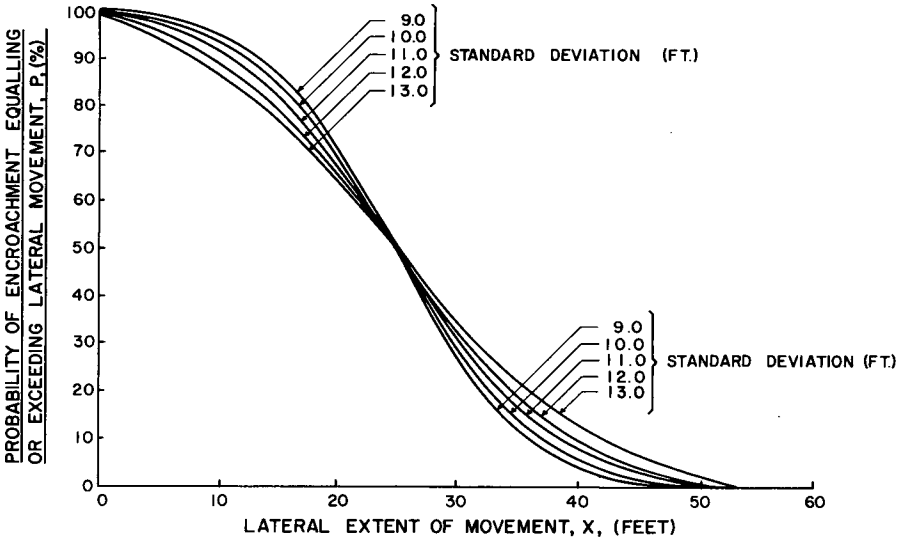

Figure C-7. Normal distribution of lateral movement, mean = 25.0 feet.

$$L_D = \frac{L_E}{\sin \theta}$$

Now consider Figures C-8 and C-9. For values of

$$x < L_L - \frac{L_E}{2 \cos (\theta)}$$

$$L_D' = 0$$

If

$$L_L - \frac{L_E}{2 \cos (\theta)} \leq x \leq L_L + \frac{L_E}{2 \cos (\theta)} \qquad \text{(C-7)}$$

$$L_D' = \frac{L_E}{2 \sin (\theta)} + \cot (\theta)\ [x - L_L] \qquad \text{(C-8)}$$

and if

$$x > L_L + \frac{L_E}{2 \cos (\theta)} \qquad \text{(C-9)}$$

$$L_D' = L_D = \frac{L_E}{\sin (\theta)} \qquad \text{(C-10)}$$

Therefore, if a vehicle has traversed a distance L_D' the chances of an impact are $2L_D'/L_S$.

The total number of impacts, H_J, occurring in year J is computed as the sum of those occurring within the limits of Eq. C-7 and those occurring in the limits of Eq. C-9.

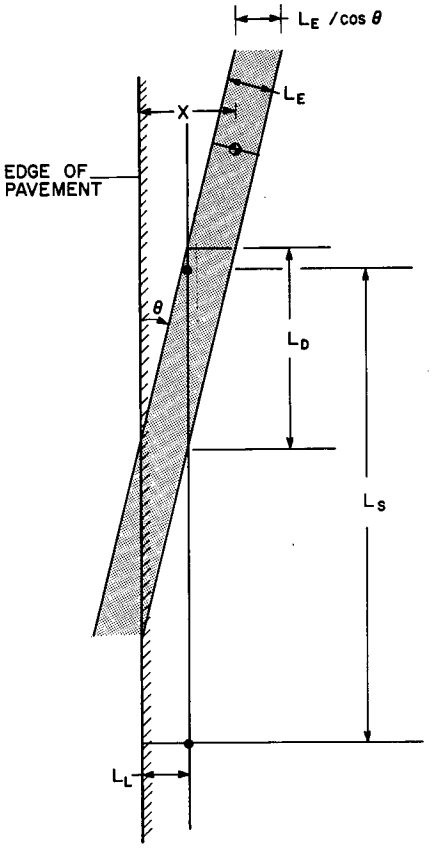

Figure C-8. Encroachment variables.

The number H_1 occurring within the limits of Eq. C-7 is computed by

$$H_1 = \int_{L_L - \frac{L_E}{2 \cos (\theta)}}^{\frac{L_E}{2 \cos (\theta)}} E_J\ (2L_D'/L_S)\ f(x)dx$$

$$= \frac{2E_J}{L_S} \int_{L_L - \frac{L_E}{2 \cos (\theta)}}^{L_L + \frac{L_E}{2 \cos (\theta)}} (L_D')f(x)dx \qquad \text{(C-11)}$$

in which

E_J = number of encroachments in year J; and
$f(x)$ = distribution function describing the lateral movement of vehicles.

Note that L_D' is a function of x in this case.

The number H_2 occurring in the limtis of Eq. C-9 is computed by

$$H_2 = \int_{L_L + \frac{L_E}{2 \cos (\theta)}}^{\infty} E_J\ (2L_D'/L_S)\ f(x)dx$$

$$= E_J \left[\frac{2L_E}{L_S \sin (\theta)} \right] \int_{L_L + \frac{L_E}{2 \cos (\theta)}}^{\infty} f(x)dx \qquad \text{(C-12)}$$

Thus,

$$H_J = H_1 + H_2 = \frac{2E_J}{L_S} \int_{L_L - \frac{L_E}{2 \cos (\theta)}}^{L_L + \frac{L_E}{2 \cos (\theta)}} (L_D')f(x)dx$$

$$+ \frac{2E_J L_E}{L_S \sin (\theta)} \int_{L_L + \frac{L_E}{2 \cos (\theta)}}^{\infty} f(x)dx \qquad \text{(C-13)}$$

As an approximation, H_J may be computed by

$$H_J = \frac{2E_J L_E}{L_S \sin (\theta)} \int_{L_L}^{\infty} f(x)dx \qquad \text{(C-14)}$$

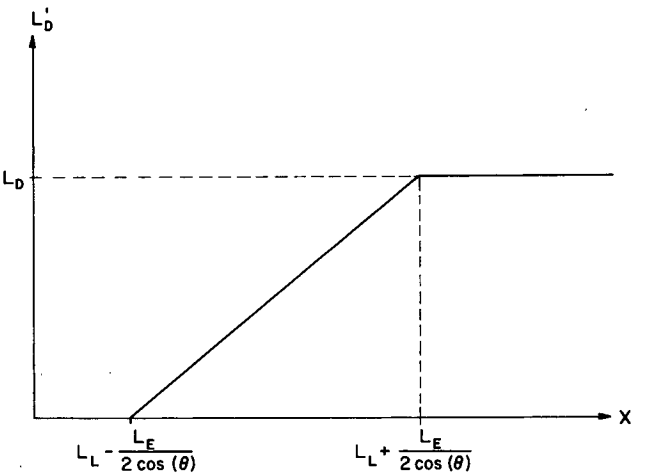

Figure C-9. Traversable distance vs distance off roadway.

Eq. C-14 can also be rewritten as

$$H_J = \frac{2E_J L_E}{L_S \sin(\theta)}\left[1 - \int_{-\infty}^{L_L} f(x)dx\right] \quad \text{(C-15)}$$

If the normal distribution is used, the value of the bracketed term in Eq. C-15 can be determined from the appropriate data in Figures C-3 through C-7.

Note that the largest possible value of H_J is

$$E_J\left[1 - \int_{-\infty}^{L_L} f(x)dx\right]$$

If the term

$$\frac{2L_E}{L_S[\sin(\theta)]} > 1.0$$

it must be set equal to 1.0.

Eq. C-5 can now be evaluated. By inserting the value of H_J from Eq. C-15 into Eq. C-5, assuming that C_{VD} remains constant,

$$C_{VDT} = \frac{(C_{VD})(2L_E)}{L_S \sin(\theta)}(P)\sum_{J=1}^{T}\frac{E_J}{(1+I)^J} \quad \text{(C-16)}$$

in which P is defined in Eq. C-6. The value of E_J is needed for each of the T years. To define E_J over that period of time, the predicted traffic volume is needed. This type of information is usually known because it is a major factor in the design of highways. If the vehicle damage costs, C_{VD}, change over the period of T years, its value must also be known for each of those T years.

When the predicted traffic volume is a linear function of time, Eq. C-16 can be modified. The present traffic volume for many highways is such that the encroachment frequency, according to Figure C-1, is in the linear range. Consider a relationship as shown in Figure C-10. Encroachment frequency is related to time, t, by the formula

$$E_J = \left(\frac{E_{JT} - E_{JO}}{T}\right)(t) + E_{JO} \quad \text{(C-17)}$$

Substituting this value of E_J into Eq. C-16, noting that the terms t and J as defined are equal, and simplifying, gives

$$C_{VDT} = \left[\frac{(C_{VD})(2L_E)}{L_S \sin(\theta)}(P)\right]\left[\left(\frac{E_{JT} - E_{JO}}{T}\right)\sum_{J=1}^{T}\frac{J}{(1+I)^J} + E_{JO}\sum_{J=1}^{T}\frac{J}{(1+I)^J}\right] \quad \text{(C-18)}$$

Now, by definition, let

$$K_E = \frac{2L_E}{L_S \sin(\theta)} \quad \text{(C-19)}$$

$$K_S = \frac{E_{JT} - E_{JO}}{T} \quad \text{(C-20)}$$

and

$$K_J = \sum_{J=1}^{T}\frac{J}{(1+I)^J} \quad \text{(C-21)}$$

With these definitions and Eq. C-3, Eq. C-18 can be rewritten as

$$C_{VDT} = (C_{VD})(K_E)(P)[(K_S)(K_J) + E_{JO}(K_T)] \quad \text{(C-22)}$$

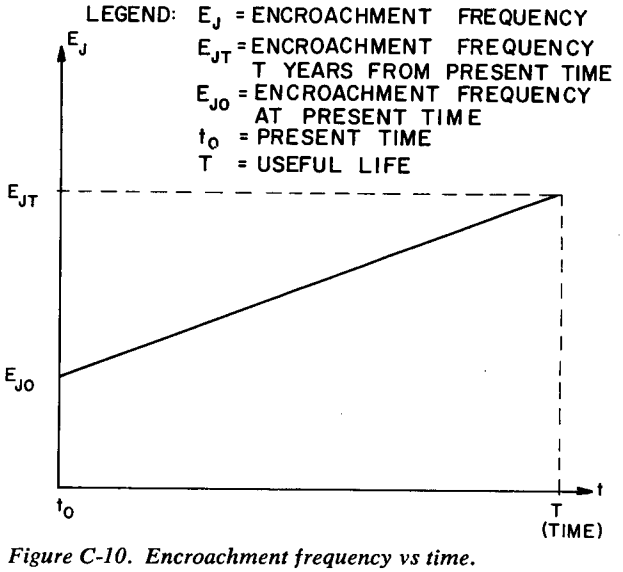

Figure C-10. Encroachment frequency vs time.

It follows that the other two accident costs can be defined in a similar manner. If C_{ODT} and C_{IDT} represent the total occupant injury costs and the total lighting installation damage per mile per year, respectively, occurring during the T years, their values in general are computed by

$$C_{ODT} = \sum_{J=1}^{T}\frac{C_{OD}H_J}{(1+I)^J} \quad \text{(C-23)}$$

and

$$C_{IDT} = \sum_{J=1}^{T}\frac{C_{ID}H_J}{(1+I)^J} \quad \text{(C-24)}$$

Applying the same assumptions and approximations as was done to get Eq. C-22 results in

$$C_{ODT} = (C_{OD})(K_E)(P)[(K_S)(K_J) + E_{JO}(K_T)] \quad \text{(C-25)}$$

and

$$C_{IDT} = (C_{ID})(K_E)(P)[(K_S)(K_J) + E_{JO}(K_T)] \quad \text{(C-26)}$$

Salvage Value

At the end of its useful life, the lighting installation may have some salvage value. The total salvage value, S_{VT}, per mile is computed by

$$S_{VT} = (N)(S_V)[1/(1+I)^T] \quad \text{(C-27)}$$

Let

$$K_V = 1/(1+I)^T$$

Eq. C-27 can then be expressed by,

$$S_{VT} = (N)(S_V)(K_V) \quad \text{(C-28)}$$

It is noted that the cost required to salvage the lighting installations may exceed its salvage value, in which case S_{VT} would be an additional cost and should be assigned a negative value in the analysis.

Total Costs

The total costs per mile, C_{TT}, occurring during the useful life of the lighting system is determined by

$$C_{TT} = C_{IT} + C_{MT} + C_{VDT} + C_{ODT} + C_{IDT} - S_{VT} \quad \text{(C-29)}$$

For the general case, the values on the right-hand side of Eq. C-29 are computed by Eqs. C-1, C-2, C-5, C-23, C-24 and C-28, respectively, and result in

$$C_{TT} = (N)(C_I) + \sum_{J=1}^{T} \frac{C_M(N)}{(1+I)^J} + \sum_{J=1}^{T} \frac{C_{VD}(H_J)}{(1+I)^J} + \sum_{J=1}^{T} \frac{C_{OD}(H_J)}{(1+I)^J} + \sum_{J=1}^{T} \frac{C_{ID}(H_J)}{(1+I)^J} - (N)(S_V)(K_V) \quad \text{(C-30)}$$

If the assumptions and approximations used in developing Eqs. C-4, C-22, C-25 and C-26 are acceptable, Eq. C-29 can be written as

$$C_{TT} = (N)(C_I) + (N)(K_T)(C_M) + (C_{VD} + C_{OD} + C_{ID})(K_E)(P)[(K_S)(K_J) + E_{JO}(K_T)] - (N)(S_V)(K_V) \quad \text{(C-31)}$$

In applying Eqs. C-30 or C-31, note that the terms C_I, C_M, C_{VD}, C_{OD}, C_{ID}, and S_V are, in general, functions of several variables. For example, consider the effects of pole spacing, L_S. As the spacing increases, the height of pole needed to provide an acceptable quality of illumination will increase, altering the values of C_I, C_M, and S_V. The larger pole will require a larger base for support, which in turn probably will increase the accident costs, C_{VD}, C_{OD}, and C_{ID}. This example is not meant to imply that increasing pole spacing increases total costs. With larger spacings, fewer poles are required, reducing the probability of accidents. The cost factors are also functions of the pole's distance from the edge of the roadway. If the pole is moved farther back from the road, accident costs probably will decrease, because, for increasing values of L_L, the speed at which the encroaching vehicle collides with the pole will, in general, decrease. If the shoulder or median slopes downward, the pole height would have to be increased to provide an acceptable quality of illumination, resulting in an increase of C_I and C_M also. As stated previously, the cost factors may also be functions of time. Vehicle damage and occupant injury costs have increased considerably within the past 10 yr, a fact documented in numerous National Safety Council reports.

The studies made by Cassel and Medville (*16*) and Thompson and Rensler (*17*), and the references given therein, are sources of information that can be used as aids in defining costs as functions of spacing and distance from the edge of roadway. Recht (*18*) has data regarding accident costs as related to time.

The number of computations necessary to reach an optimum lighting design will increase as the number of constraints on the system decrease. For example, consider the combinations possible if there were no restrictions (within practical bounds), on pole spacing, distance of the pole from the roadway, pole height, base type, etc. For all intents and purposes, a high-speed computer would be needed to reach a solution. The systems approach presented herein lends itself to computer application. On the other hand, as the number of constraints increase, the number of calculations decrease, and a solution may be feasible by other means.

Either the general expression for C_{TT} (Eq. C-30) or that of Eq. C-31 may be used to evaluate lighting costs. Examples of the use of the derived expressions follow.

Tables C-10 and C-11 are included to facilitate the use of Eq. C-31. Listed are values of K_T and K_J for values of T through 30 yr and values of I from 0% to 10%.

Examples

To demonstrate the use of the derived expressions, the following two examples are given.

In Example (1) the model is used to determine an optimum pole-base configuration for given constraints. The primary constraints are the pole locations with respect to the roadway, mounting height, and luminaire size.

Example (1)

GIVEN:

Pole spacing—$L_S = 200$ ft.
Distance of pole off roadway—$L_L = 12$ ft.
Design or useful life of lighting system—$T = 20$ yr.
Interest rate—$I = 5\%$.
Present traffic volume (one way)—$ADT = 8{,}000$.
Predicted traffic volume (one way) at end of useful life—$ADT' = 18{,}000$.
Mounting height = 40 ft.
Luminaire size = 1,000 watts.
Arm length = 10 ft.
Salvage value at end of useful life—$S_V = 5\%$ of initial costs.

REQUIRED:

Determine which of the pole-base combinations given in Table C-9 produces the optimum configuration.

SOLUTION:

Eq. C-31 is used to compute total costs per mile occurring over the useful life of the configurations given in Table C-9. All future costs are discounted to present values by use of the 5% discount rate.

$$C_{TT} = (N)(C_I) + N(K_T)(C_M) + (C_{VD} + C_{OD} + C_{ID})(K_E)(P)[(K_S)(K_J) + E_{JO}(K_T)] - (N)(S_V)(K_V) \quad \text{(C-31a)}$$

As explained in the derivation, use of this equation implies the following:

1. Maintenance and accident costs are constant during the period of time under consideration; i.e., 20 yr.
2. The traffic volume increases linearly from its present value to its predicted value, ADT'.

Table C-12 gives the initial costs, C_I, per individual installation.

TABLE C-10

VALUES OF K_T

USEFUL LIFE T (YEARS)	INTEREST RATE I (PERCENT)										
	0.0	1.0	2.0	3.0	4.0	5.0	6.0	7.0	8.0	9.0	10.0
1.0	1.000	0.990	0.980	0.971	0.962	0.952	0.943	0.935	0.926	0.917	0.909
2.0	2.000	1.970	1.941	1.913	1.886	1.859	1.833	1.808	1.783	1.759	1.736
3.0	3.000	2.941	2.884	2.829	2.775	2.723	2.673	2.624	2.577	2.531	2.487
4.0	4.000	3.902	3.808	3.717	3.630	3.546	3.465	3.387	3.312	3.240	3.170
5.0	5.000	4.853	4.713	4.580	4.452	4.329	4.212	4.100	3.993	3.890	3.791
6.0	6.000	5.795	5.601	5.417	5.242	5.076	4.917	4.767	4.623	4.486	4.355
7.0	7.000	6.728	6.472	6.230	6.002	5.786	5.582	5.389	5.206	5.033	4.868
8.0	8.000	7.651	7.325	7.020	6.733	6.463	6.210	5.971	5.747	5.535	5.335
9.0	9.000	8.565	8.162	7.786	7.435	7.108	6.802	6.515	6.247	5.995	5.759
10.0	10.000	9.471	8.982	8.530	8.111	7.722	7.360	7.024	6.710	6.418	6.145
11.0	11.000	10.367	9.787	9.253	8.760	8.306	7.887	7.499	7.139	6.805	6.495
12.0	12.000	11.254	10.575	9.954	9.385	8.863	8.384	7.943	7.536	7.161	6.814
13.0	13.000	12.133	11.348	10.635	9.986	9.393	8.853	8.358	7.904	7.487	7.103
14.0	14.000	13.003	12.106	11.296	10.563	9.899	9.295	8.745	8.244	7.786	7.367
15.0	15.000	13.864	12.849	11.938	11.118	10.380	9.712	9.108	8.559	8.061	7.606
16.0	16.000	14.717	13.577	12.561	11.652	10.838	10.106	9.447	8.851	8.313	7.824
17.0	17.000	15.561	14.292	13.166	12.166	11.274	10.477	9.763	9.122	8.544	8.022
18.0	18.000	16.397	14.992	13.753	12.659	11.689	10.828	10.059	9.372	8.756	8.201
19.0	19.000	17.225	15.678	14.324	13.134	12.085	11.158	10.336	9.604	8.950	8.365
20.0	20.000	18.044	16.351	14.877	13.590	12.462	11.470	10.594	9.818	9.129	8.514
21.0	21.000	18.856	17.011	15.415	14.029	12.821	11.764	10.836	10.017	9.292	8.649
22.0	22.000	19.659	17.658	15.937	14.451	13.163	12.042	11.061	10.201	9.442	8.772
23.0	23.000	20.454	18.292	16.443	14.857	13.488	12.303	11.272	10.371	9.580	8.883
24.0	24.000	21.242	18.914	16.935	15.247	13.799	12.550	11.469	10.529	9.707	8.985
25.0	25.000	22.022	19.523	17.413	15.622	14.094	12.783	11.654	10.675	9.823	9.077
26.0	26.000	22.794	20.121	17.877	15.983	14.375	13.003	11.826	10.810	9.929	9.161
27.0	27.000	23.558	20.706	18.327	16.330	14.643	13.210	11.987	10.935	10.027	9.237
28.0	28.000	24.315	21.281	18.764	16.663	14.898	13.406	12.137	11.051	10.116	9.307
29.0	29.000	25.064	21.844	19.188	16.984	15.141	13.591	12.278	11.158	10.198	9.370
30.0	30.000	25.806	22.396	19.600	17.292	15.372	13.765	12.409	11.258	10.274	9.427

TABLE C-11

VALUES OF K_I

USEFUL LIFE T (YEARS)	INTEREST RATE I (PERCENT)										
	0.0	1.0	2.0	3.0	4.0	5.0	6.0	7.0	8.0	9.0	10.0
1.0	1.00	0.99	0.98	0.97	0.96	0.95	0.94	0.93	0.93	0.92	0.91
2.0	3.00	2.95	2.90	2.86	2.81	2.77	2.72	2.68	2.64	2.60	2.56
3.0	6.00	5.86	5.73	5.60	5.48	5.36	5.24	5.13	5.02	4.92	4.82
4.0	10.00	9.71	9.43	9.16	8.90	8.65	8.41	8.18	7.96	7.75	7.55
5.0	15.00	14.46	13.95	13.47	13.01	12.57	12.15	11.75	11.37	11.00	10.65
6.0	21.00	20.12	19.28	18.49	17.75	17.04	16.38	15.74	15.15	14.58	14.04
7.0	28.00	26.65	25.38	24.19	23.07	22.02	21.03	20.10	19.23	18.41	17.63
8.0	36.00	34.03	32.20	30.50	28.91	27.43	26.05	24.76	23.55	22.42	21.36
9.0	45.00	42.26	39.73	37.40	35.24	33.23	31.38	29.66	28.05	26.57	25.18
10.0	55.00	51.32	47.94	44.84	41.99	39.37	36.96	34.74	32.69	30.79	29.04
11.0	66.00	61.17	56.78	52.79	49.14	45.81	42.76	39.97	37.40	35.05	32.89
12.0	78.00	71.82	66.25	61.20	56.63	52.49	48.72	45.29	42.17	39.32	36.72
13.0	91.00	83.25	76.30	70.05	64.44	59.38	54.82	50.69	46.95	43.56	40.48
14.0	105.00	95.43	86.91	79.31	72.52	66.45	61.01	56.12	51.72	47.75	44.17
15.0	120.00	108.35	98.05	88.94	80.85	73.67	67.27	61.55	56.45	51.87	47.76
16.0	136.00	121.99	109.71	98.91	89.40	81.00	73.57	66.97	61.12	55.90	51.24
17.0	153.00	136.35	121.85	109.19	98.12	88.42	79.88	72.36	65.71	59.83	54.60
18.0	171.00	151.40	134.45	119.77	107.01	95.89	86.18	77.68	70.21	63.64	57.84
19.0	190.00	167.12	147.49	130.60	116.03	103.41	92.46	82.93	74.62	67.34	60.95
20.0	210.00	183.51	160.95	141.68	125.15	110.95	98.70	88.10	78.91	70.91	63.92
21.0	231.00	200.55	174.81	152.97	134.37	118.49	104.88	93.18	83.08	74.34	66.76
22.0	253.00	218.23	189.04	164.45	143.65	126.01	110.98	98.14	87.13	77.65	69.46
23.0	276.00	236.52	203.62	176.10	152.99	133.50	117.00	102.99	91.04	80.82	72.03
24.0	300.00	255.43	218.55	187.91	162.35	140.94	122.93	107.72	94.83	83.85	74.47
25.0	325.00	274.92	233.78	199.85	171.73	148.32	128.76	112.33	98.48	86.75	76.77
26.0	351.00	294.99	249.32	211.90	181.10	155.64	134.47	116.81	101.99	89.52	78.96
27.0	378.00	315.63	265.14	224.06	190.47	162.87	140.07	121.15	105.37	92.15	81.01
28.0	406.00	336.82	281.22	236.30	199.81	170.01	145.55	125.36	108.62	94.66	82.96
29.0	435.00	358.56	297.55	248.60	209.10	177.06	150.90	129.44	111.73	97.04	84.78
30.0	465.00	380.81	314.12	260.96	218.35	184.00	156.12	133.38	114.71	99.30	86.50

TABLE C-12

INITIAL AND SALVAGE COSTS, BY INDIVIDUAL INSTALLATION

POLE AND BASE	TOTAL COST, INSTALLED ($)[a]	SALVAGE VALUE ($)[b]
(a) Steel Pole		
Steel shoe	702	35
Alum. transformer	741	37
Steel transformer	740	37
Stainless steel progressive-shear	760	38
Carbon steel progressive-shear	741	37
Steel slip	743	37
(b) Aluminum Pole		
Alum. shoe	830	42
Alum. transformer	869	43
Alum. slip	890	45

[a] Cost of pole, base, and arm from Table C-1. Lamp, luminaire and ballast costs, $174 each (*16, 17*). Installation costs, $375 each (*17*); includes cost of foundation, bolts, wiring, conduit, trenching, and all miscellaneous labor and materials.
[b] 5% of initial total cost.

The estimated annual maintenance cost, C_M, per individual installation is $50.. This value is representative of maintenance costs in Texas for the luminaire under consideration. It includes electrical power and normal maintenance, but excludes any costs due to vehicles colliding with the pole.

Accident costs used are given in Table C-9.

The other terms in Eq. C-31 are now defined:

N = number of poles per mile (one way);

$$N = \frac{5{,}280}{L_S} = \frac{5{,}280}{200};$$

$N = 26.4$ poles/mi;

$$K_T = \sum_{J=1}^{T} \frac{1}{(1+I)^J} = \sum_{J=1}^{20} \frac{1}{(1+0.05)^J}$$

$K_T = 12.46$ (from Table C-10); and

$$K_E = \frac{2L_E}{L_S \sin(\theta)}$$

in which

L_E = effective vehicle length = 12.5 ft; (assumed as ½ × length + width)

$L_S = 200$ ft;

θ = average angle of encroachment;

$\theta = 11°$ (*20*);

$$K_E = \frac{2(12.5)}{200[\sin(11°)]};$$

$K_E = 0.655$; and

P = probability of an encroaching vehicle equaling or exceeding the distance $L_L = 12$ ft.

To determine P it is assumed that the shoulder cross-section, within 12 ft of the edge of the roadway, is similar to that shown in Figure C-3. The value obtained from Figure C-3 is

$$P = 0.86 \text{ (for } x = L_L = 12 \text{ ft)}$$

$$K_S = \frac{E_{JT} - E_{JO}}{T}$$

in which

E_{JT} = encroachment rate at end of useful life, T; and

E_{JO} = present encroachment rate.

In this example, E_{JT} and E_{JO} are obtained from Figure C-1. Because the curve in Figure C-1 is for both directions of travel, one-half of the value is used for one-way traffic.

$E_{JT} = 8.1/2 = 4.05$/mi/yr (½ value at $ADT' = 18{,}000$)

$E_{JO} = 3.5/2 = 1.75$/mi/yr (½ value at $ADT = 8{,}000$)

$K_S = (4.05 - 1.75)/20$

$K_S = 0.115$

$$K_J = \sum_{J=1}^{T} \frac{J}{(1+I)^J} = \sum_{J=1}^{20} \frac{J}{(1+0.05)^J}$$

$K_J = 110.95$ (from Table C-11)

Salvage values, S_V, are given in Table C-12.

$$K_V = \frac{1}{(1+I)^J} = \frac{1}{(1+0.05)^{20}} = \frac{1}{2.653}$$

$K_V = 0.377$

Substituting these values into Eq. C-31:

$$C_{TT} = 26.4(C_I) + (26.4)(12.46)(C_M) + (C_{VD} + C_{OD} + C_{ID})(0.655)(0.86)[(0.115)(110.95) + (1.75)(12.46)] - (26.4)(0.377)(S_V)$$

or

$$C_{TT} = 26.4(C_I) + 328.9(C_M) + 19.48(C_{VD} + C_{OD} + C_{ID}) - 10.0(S_V)$$

Two different total costs are computed for each configuration considered: (1) C_{TT}', direct costs to the highway department, which excludes accident costs, (2) C_{TT}, total costs. Consider the direct costs for the steel pole—steel shoe base combination:

$C_{TT}' = 26.4(702.00) + 328.9(50.00) - 10.0(35.00)$

$C_{TT}' = \$34{,}630$

This is the total cost per mile for one direction occurring over the 20-yr period if vehicle damage and occupant injury costs are excluded. Now consider direct plus vehicle damage and occupant injury costs:

$C_{TT} = 34{,}630 + 19.48(1{,}557.00)$

$C_{TT} = \$64{,}960$

Table C-13 gives total costs for each configuration.

As shown in Table C-13, if only those costs which the highway department generally assumes (i.e., initial and maintenance costs) are considered, the rigidly mounted steel pole is the best choice. On the other hand, if accident costs are included in the total cost this configuration is the

worst choice. When accident costs are considered, the slip base used in conjunction with the steel or aluminum pole appears to be the optimum configuration. Note that for a small percentage increase in "direct" costs (highway department costs) a much larger percentage decrease in "direct plus indirect" costs (includes accident costs) is realized.

Example (2) shows the flexibility of the model as a tool in costs analysis of roadway lighting. In this case it was desired that an optimum spacing be obtained for a particular pole-base configuration. The principal constraint, in addition to the pole and base, was the distance from the edge of the roadway to the base of the light pole. The relationships between cost factors, C_I, C_M, etc., and pole spacing as used in the example were suppositions based on conjecture by the research agency. These cost factors may increase with pole spacing (within the limits considered), but it is unlikely that they will increase at a constant rate, as assumed.

Example (2)

GIVEN:

$L_L = 12$ ft.

$T = 20$ yr.

$I = 5\%$.

$ADT = 8{,}000$ (one way).

$ADT' = 18{,}000$ (one way).

Pole material—aluminum.

Base—cast aluminum.

Salvage value at end of useful life $= 5\%\ C_I$.

REQUIRED:

Determine the optimum spacing for values of L_S between 150 ft and 300 ft if the cost factors C_i are linearly related to L_s, as shown in Figure C-11.

TABLE C-13

TOTAL COSTS

POLE AND BASE	COSTS ($) DIRECT	DIRECT + INDIRECT
(a) Steel Pole		
Steel shoe	34,630	64,960
Alum. transformer	35,660	55,440
Steel transformer	35,610	62,880
Stainless steel progressive-shear	36,150	57,780
Carbon steel progressive-shear	35,640	55,410
Steel slip	35,690	51,180
(b) Aluminum Pole		
Alum. shoe (thin wall)	37,940	60,340
Alum. shoe (thick wall)	37,940	66,180
Alum. transformer	38,950	54,440
Alum. slip	39,490	53,610

The general expression for cost factor, C_i, is thus given by

$$C_i = K_{si}(L_s - L_{s1}) + C_{i1} \qquad \text{(C-32)}$$

in which

$$K_{si} = \frac{C_{i2} - C_{i1}}{L_{s2} - L_{s1}};$$

$L_{s2} = 300$ ft; and

$L_{s1} = 150$ ft.

Therefore, $K_{si} = \dfrac{C_{i2} - C_{i1}}{150}$

Table C-14 gives the values of C_{i1}, C_{i2}, and K_{si} used in this example.

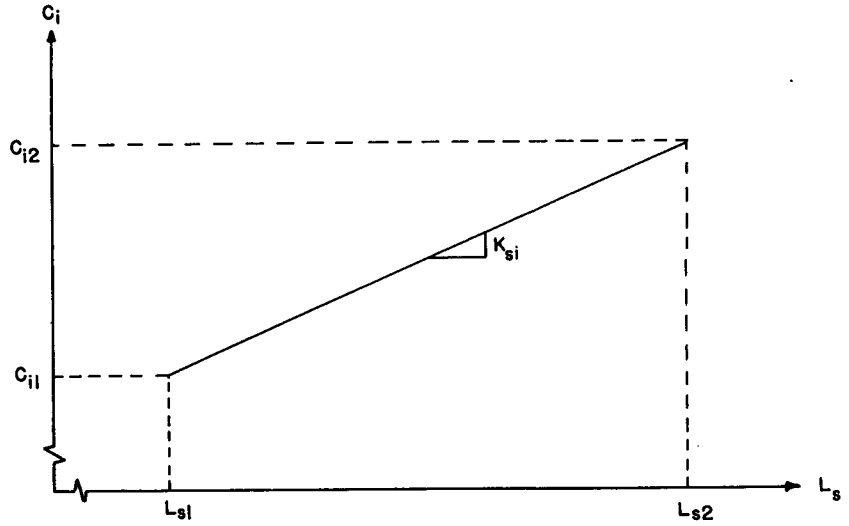

Figure C-11. Cost factors vs pole spacing.

TABLE C-14

COST AND SLOPE VALUES

i	C_{i1} ($)	C_{i2} ($)	K_{si}
I	794	1,019	1.5
M	40	70	0.2
VD	330	480	1.0
OD	155	275	0.8
ID	185	290	0.7

SOLUTION:

The equations relating the cost factors to the spacing are, therefore, as follows:

$$C_I = 1.5(L_s - 150) + 794.0;$$
$$C_M = 0.2(L_s - 150) + 40.0;$$
$$C_{VD} = 1.0(L_s - 150) + 330.0;$$
$$C_{OD} = 0.8(L_s - 150) + 155.0;$$
$$C_{ID} = 0.7(L_s - 150) + 185.0;$$
$$S_V = 0.05[1.5(L_s - 150) + 794.0].$$

Substituting the above values and the definitions of N and K_E into Eq. C-32, and simplifying, results in

$$C_{TT} = \frac{7{,}920}{L_s}(L_s + 380) + \frac{1{,}056}{L_s}(L_s + 40)(K_T) + 2.5(L_s + 118)\left[\frac{2L_E}{L_s \sin(\theta)}\right] (P)[(K_s)(K_J) + E_{JO}(K_T)] - \frac{396}{L_s}(L_s + 380)(K_V) \quad \text{(C-33)}$$

Values of all terms other than L_s in this equation are defined in Example (1) and are applicable in this example. They are as follows:

$$K_T = 12.46;$$
$$L_E = 12.5;$$
$$\theta = 11.0;$$
$$P = 0.86;$$
$$K_s = 0.115;$$
$$K_J = 110.95;$$
$$E_{JO} = 1.75; \text{ and}$$
$$K_V = 0.377.$$

It must be remembered that the value of K_E, defined by

$$K_E = \frac{2L_E}{L_s \sin(\theta)}$$

can be no greater than 1.0. In this example

$$K_E = \frac{2(12.5)}{L_s(0.191)} = \frac{131}{L_s}$$

Because the lowest value of L_s being considered is 150 ft, there need be no concern.

Substituting the above values into Eq. C-33 and simplifying,

$$C_{TT} = \frac{7{,}920}{L_s}(L_s + 380) + \frac{13{,}158}{L_s}(L_s + 50) + \frac{9{,}735}{L_s}(L_s + 118) - \frac{149}{L_s}(L_s + 380)$$

Further simplification gives

$$C_{TT} = 30{,}660 + \frac{4{,}759{,}600}{L_s} \quad \text{(C-34)}$$

Eq. C-34 is plotted in Figure C-12.

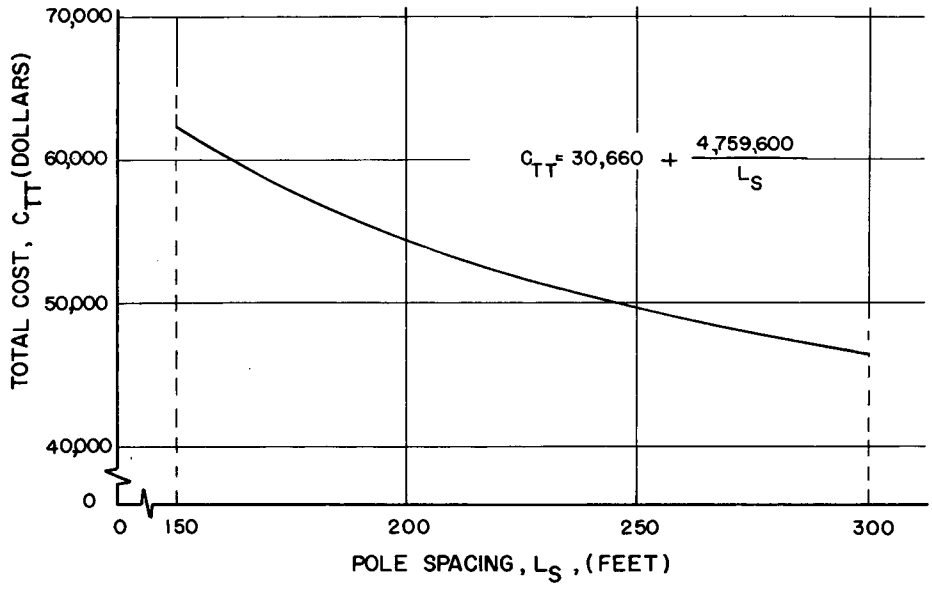

Figure C-12. Total cost vs pole spacing.

The results of Example (2) show the optimum spacing to be the extreme value considered—300 ft. It also shows that total costs continuously decrease with spacing. The applicability of these results to an actual situation obviously depends on the degree to which the actual conditions and constraints compare with those used in the example.

Note that in problems similar in nature to Example (2) the quality of illumination may not be the same for all configurations under consideration. If that is the case, its effects on the total costs must be accounted for.

Accident Case Studies

Three case studies were made to evaluate the accuracy of Eq. C-15 in predicting the rate of accidents involving light poles.

$$H_J = \frac{2E_J L_E}{L_S \sin(\theta)}\left[1 - \int_{-\infty}^{L_L} f(x)\,dx\right]$$

All three cases involved four-lane highways, two lanes each way, with side-mounted light poles. In each case the shoulder cross-section was similar to one-half of the median cross-section shown in Figure C-3. Values of L_S, L_L, and ADT were known, together with the actual number of accidents involving light poles that had occurred along a length of roadway for a period of time. Values of E_J, L_E, θ, and $f(x)$ were determined as suggested in this report because no data were available on these parameters.

Case (1)

The first area considered was a section of Interstate 35 in San Marcos, Texas. Within this area there are approximately 330 unprotected poles spaced between 180 and 190 ft apart, each pole being about 10 ft from the edge of the normally traveled roadway. Figure C-13 shows a general view of the roadway and the relative pole locations. Note the foundation of a pole in the foreground and the path taken by the vehicle which struck the standard.

A total of 2.17 yr of accident records was available for this area. During that period there were 35 vehicle accidents involving light poles. The average accident rate per year was computed to be $35/2.17 = 16.1$/yr. The total distance along the roadway over which these accidents occurred was computed by

$$\frac{N(L_S)}{K} = \frac{330(185)}{5{,}280} = 11.6 \text{ mi}$$

in which

N = number of poles;

L_S = pole spacing; and

K = conversion factor.

The actual accident rate, H_{JA}, was determined by $H_{JA} = 16.1/11.6 = 1.39$/mi/yr.

Average daily traffic for the 2.17-yr period was approximately 6,000 in each direction.

Effective vehicle length, L_E, was assumed to equal the average of the length and width of a typical automobile, $L_E = (18 + 7)/2 = 12.5$ ft.

Figure C-1 shows the median encroachment rate (considering both directions of travel) for an ADT equal to 6,000 to be 2.6. For shoulder encroachments, one-half of this value is used; i.e., $E_J = 1.3$/mi/yr.

Figure C-13. Roadway, Case (1).

The value of θ was assumed to be 11°.

The distribution function $f(x)$ for the lateral movement of encroaching vehicles was assumed to be a "normal" distribution function having a mean equal to 22.0 ft and a standard deviation equal to 9.0 ft. That particular distribution was chosen because the shoulder cross-section in the San Marcos area was very similar to that of Figure C-3; as shown in Figure C-3, this normal distribution compares favorably with observed data. The value of the bracketed term in Eq. C-15 is then obtained from Figure C-3 as 0.90 (value of P at $x = L_L = 10$ ft).

Summarizing,

$L_S = 185$ ft;

$L_L = 10$ ft;

$L_E = 12.5$ ft;

$E_J = 2.4$/mi/yr;

$\theta = 11°$; and

$$P = \left[1 - \int_{-\infty}^{L_L} f(x)\,dx\right] = 0.90.$$

Substituting these values into Eq. C-15 gives

$$H_J = \frac{2(1.3)(12.5)}{185[\sin(11°)]}(0.90) = 1.3(0.636) \qquad \text{(C-35)}$$

$$H_J = 0.83/\text{mi/yr}$$

Case (2)

The second study area was a section of the Dallas-Fort Worth Turnpike, between the Dallas Toll Station and Beckley interchange. In the section considered there are approximately 96 unprotected light poles spaced approximately 260 ft apart at a distance of 11 ft from the edge of the outer travel lane. Figure C-14 shows a general view of the roadway and the relative pole locations.

Six yr (1962 through 1967) of accident records were available. In that period there were 8 vehicle accidents

Figure C-14. Roadway, Case (2) and Case (3).

involving light poles. The average daily traffic for the 6-yr period was approximately 9,300 in each direction.

The average accident rate per year was $8/6 = 1.33/\text{yr}$.

Total distance of the section of roadway considered was

$$\frac{N(L_S)}{K} = \frac{96(260)}{5{,}280} = 4.7 \text{ mi}$$

in which N, L_S, and K are as defined in Case (1). The actual rate, H_{JA}, was determined by $H_{JA} = 1.33/4.7 = 0.283/\text{mi/yr}$.

Values of L_E, E_J, θ, and $f(x)$ were obtained as explained in Case (1). In this example, those values were as follows: $L_E = 12.5$ ft; $E_J = 2.05/\text{mi/yr}$ (for $ADT = 9{,}300$); and $P = 0.86$ (for $L_L = 11$ ft).

TABLE C-15

NUMBER OF HITS PER MILE PER YEAR

	CASE		
HITS	(1)	(2)	(3)
Actual	1.4	0.3	0.7
Predicted	0.8	0.9	1.1

As in Case (1), the shoulder cross-section in this case was similar to that shown in Figure C-3, and hence the value of P was obtained from the normal distribution function described in Case (1).

Inserting the previous values into Eq. C-15 gives

$$H_J = \frac{2(2.05)(12.5)}{260[\sin(11^\circ)]}(0.86) = 2.05(0.433) \tag{C-36}$$

$$H_J = 0.89/\text{mi/yr}$$

Case (3)

The study area was a section of the Dallas-Fort Worth Turnpike, between the Fort Worth Toll Station and Riverside interchange. There are approximately 150 unprotected poles in this section, spaced about 180 ft apart at a distance of 11 ft from the edge of the outer travel lane.

Six yr of accident data were available. During that period there were 22 vehicle accidents involving light poles. Average daily traffic for the 6-yr period was approximately 8,500, in each direction.

The average accident rate per year was $22/6 = 3.67/\text{yr}$.

Total distance of the section of roadway considered was

$$\frac{N(L_S)}{K} = \frac{150(180)}{5{,}280} = 5.1 \text{ mi}$$

in which N, L_S, and K are defined in Case (1). The actual accident rate, H_{JA}, was determined by $H_{JA} = 3.67/5.1 = 0.72/\text{mi/yr}$.

Values of L_E, E_J, θ, and $f(x)$ were obtained as explained in Case (1). In this example those values were as follows: $L_E = 12.5$ ft; $E_J = 1.85/\text{mi/yr}$ (for $ADT = 8{,}500$); and $P = 0.86$ (for $L_L = 11$ ft).

As in Case (1), the shoulder cross-section in this case was similar to that shown in Figure C-3, and hence the value of P was obtained from the normal distribution function described in Case (1).

Substituting the previous values into Eq. C-15 gives

$$H_J = \frac{2(1.85)(12.5)}{180[\sin(11^\circ)]}(0.86) = 1.85(0.625) \tag{C-37}$$

$$H_J = 1.15/\text{mi/yr}$$

The actual and predicted values of the three cases are given in Table C-15.

APPENDIX D

SELECTED FRAMES FROM FILMS OF TESTS

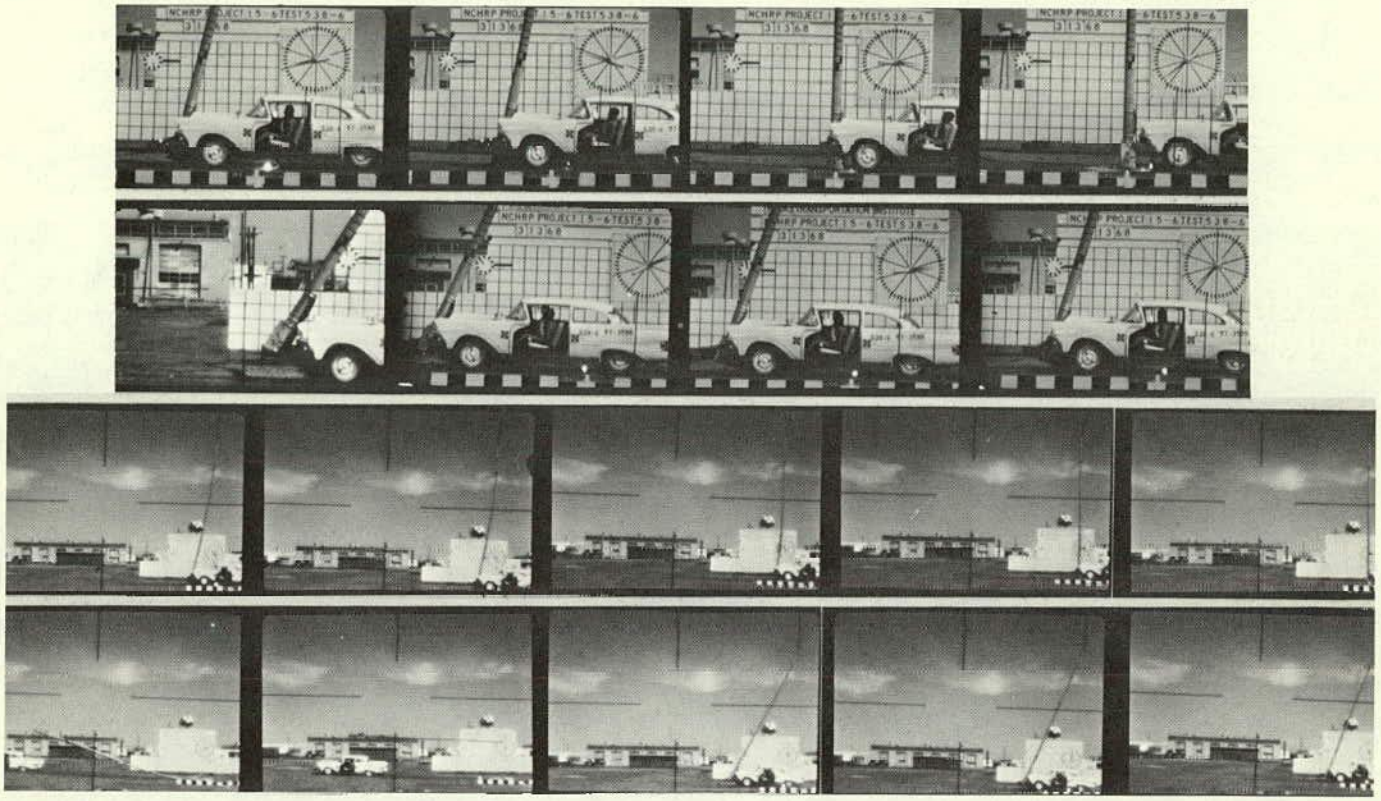

Figure D-1. Aluminum transformer base (Test 538-6).

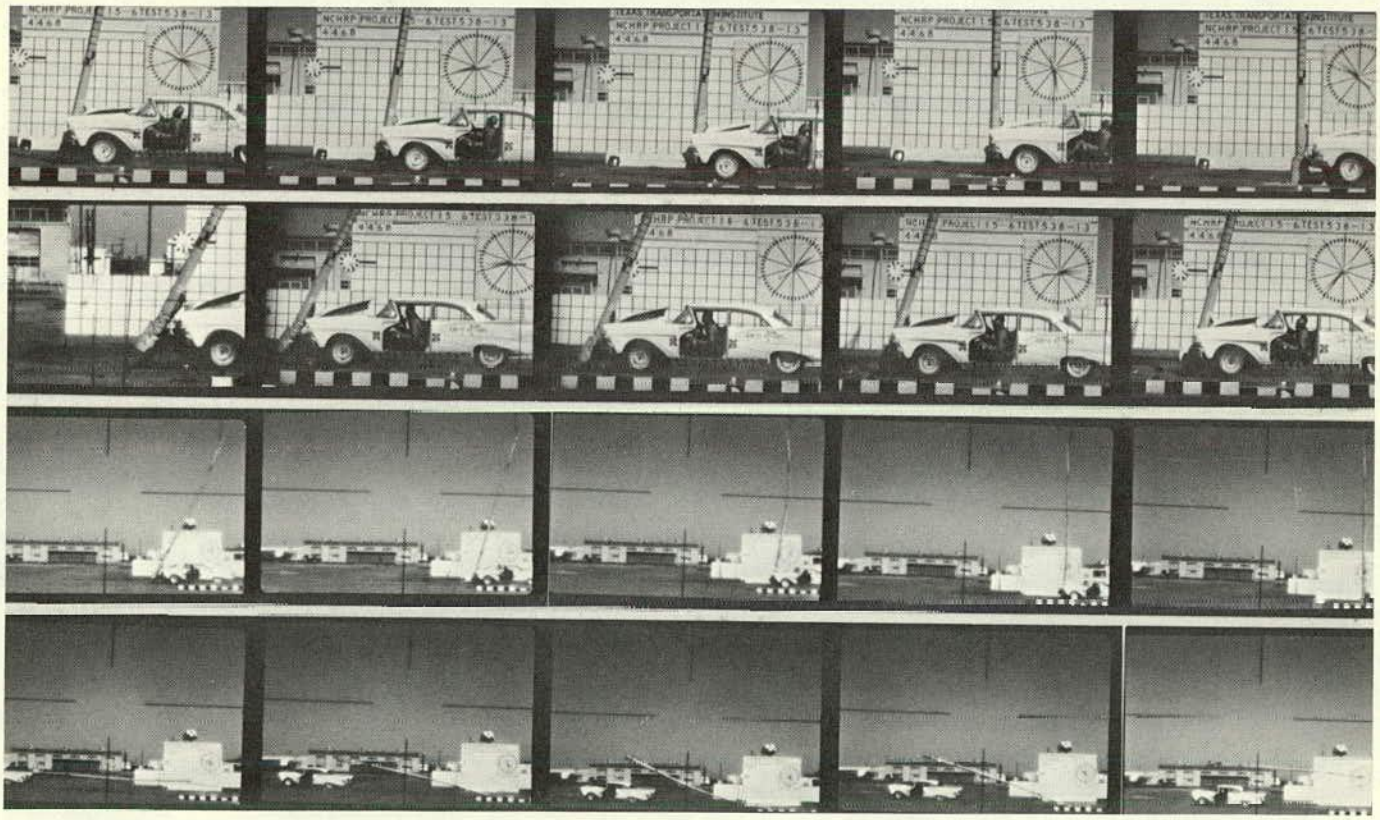

Figure D-2. Aluminum transformer base (Test 538-13).

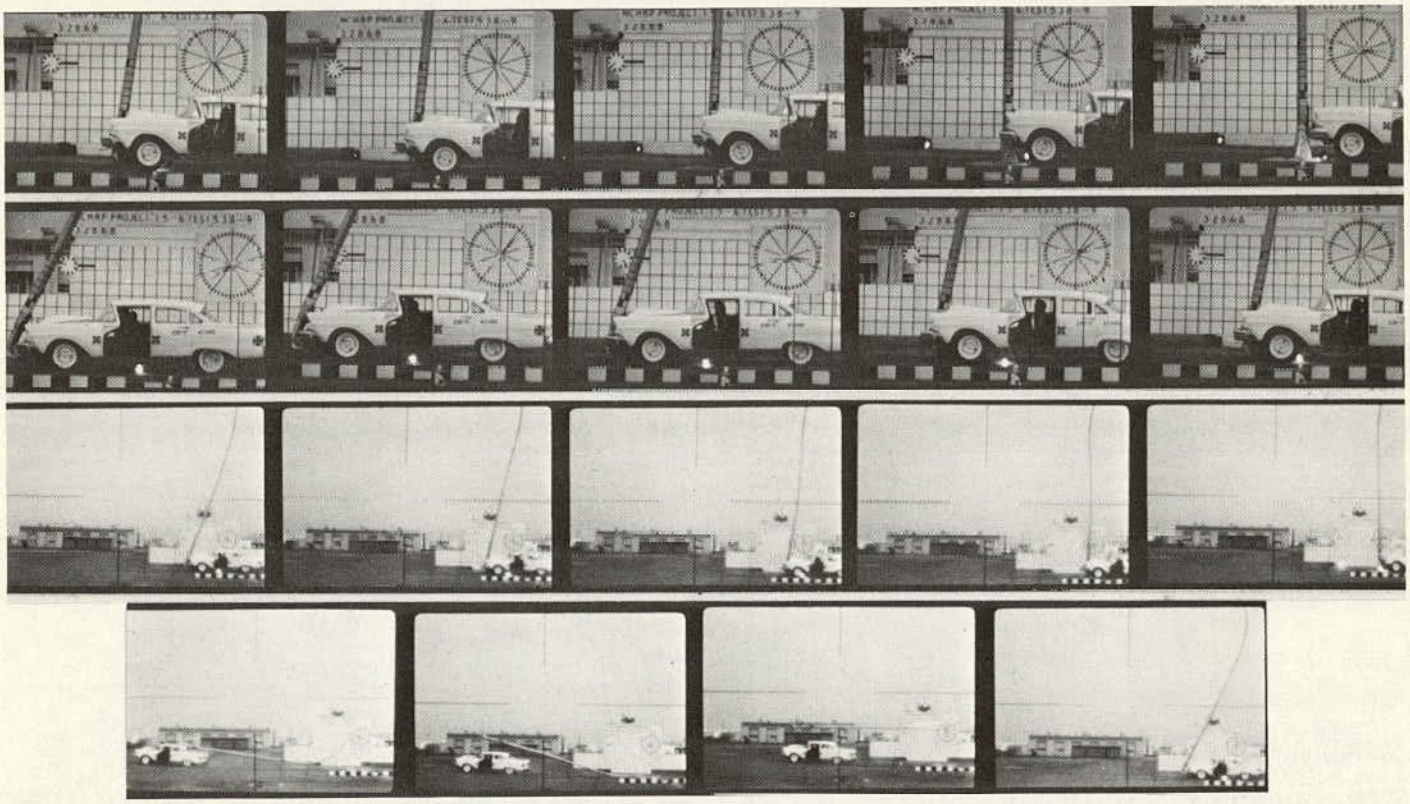

Figure D-3. Stainless steel progressive-shear base (Test 538-9).

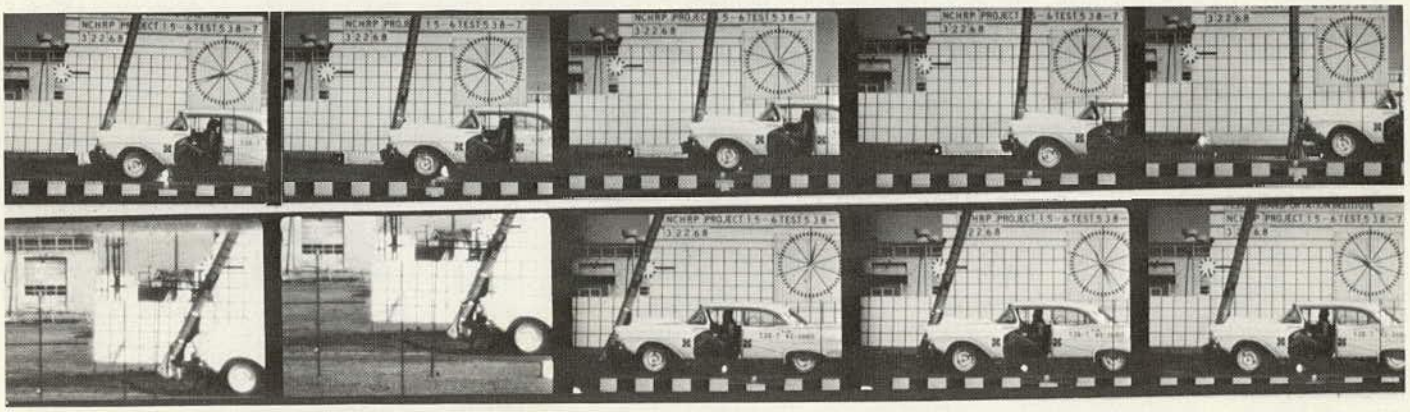

Figure D-4. Stainless steel progressive-shear base (Test 538-7).

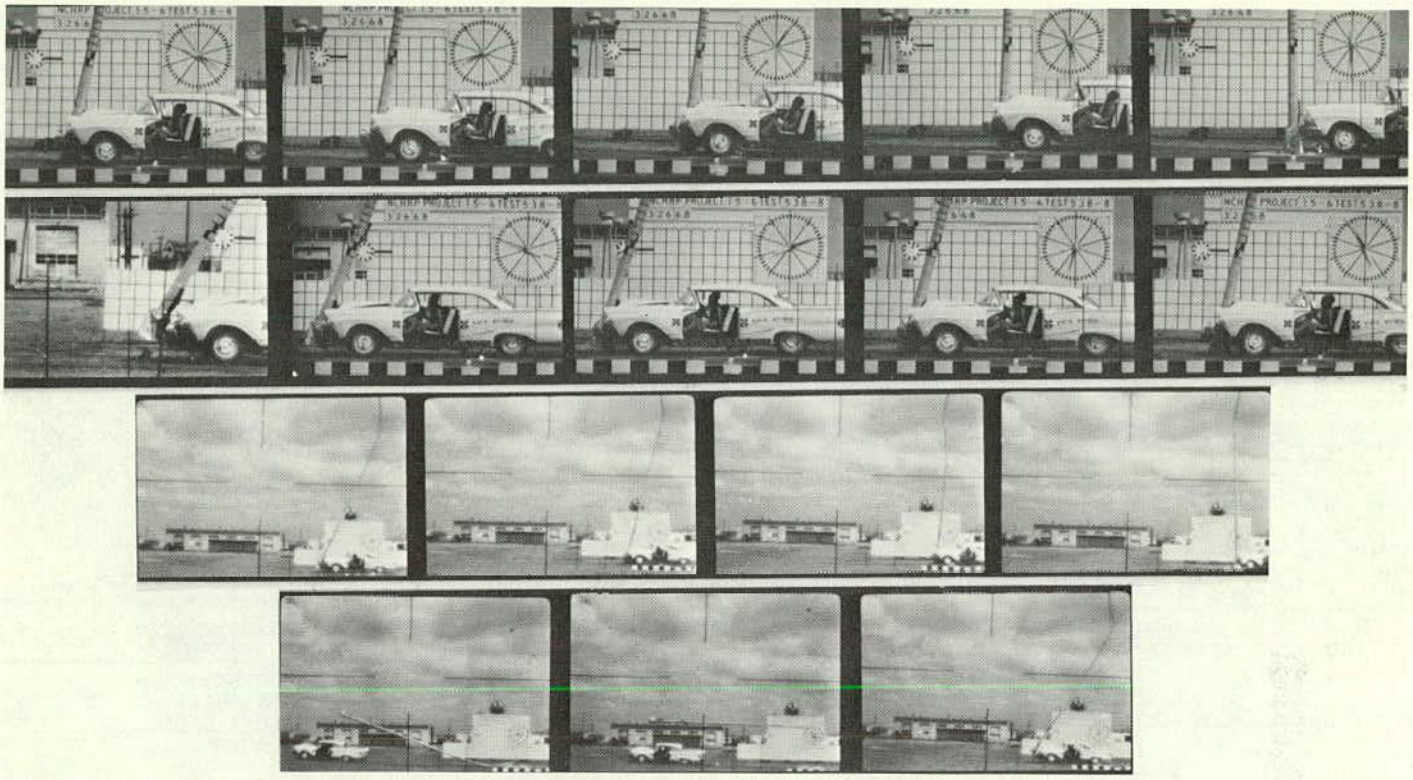

Figure D-5. Carbon steel progressive-shear T-base (Test 538-8).

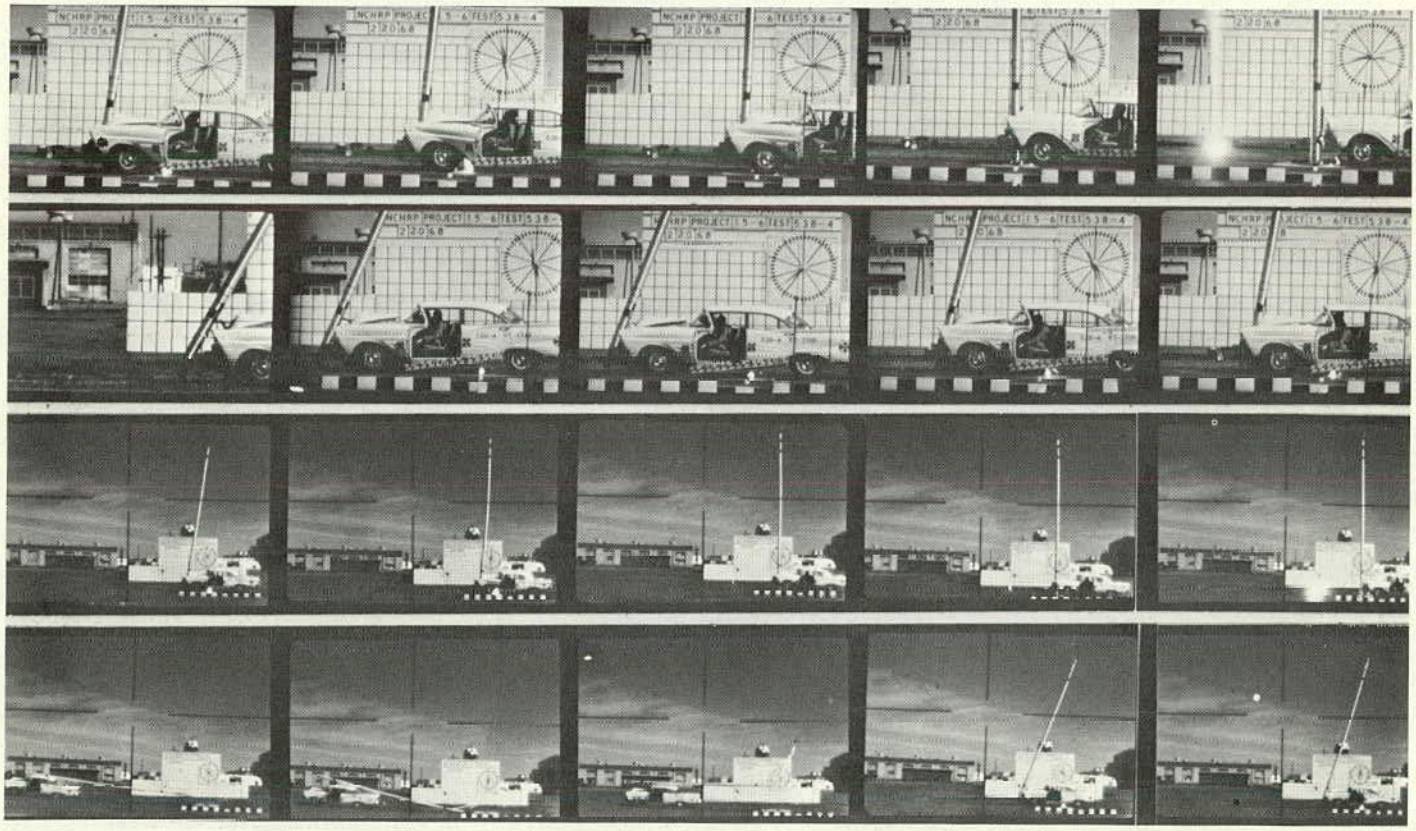

Figure D-6. Aluminum shoe base (Test 538-4).

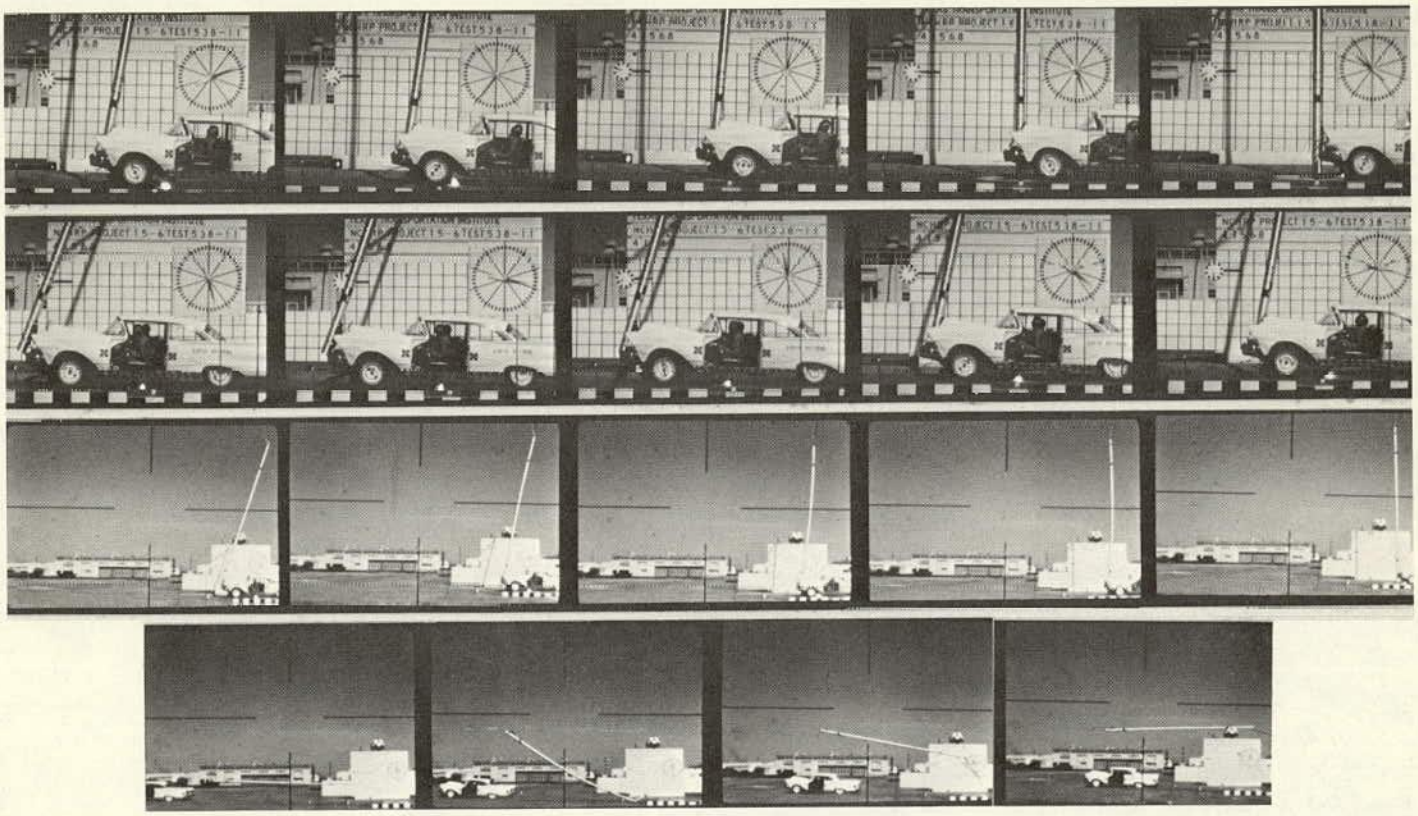

Figure D-7. Aluminum shoe base (Test 538-11).

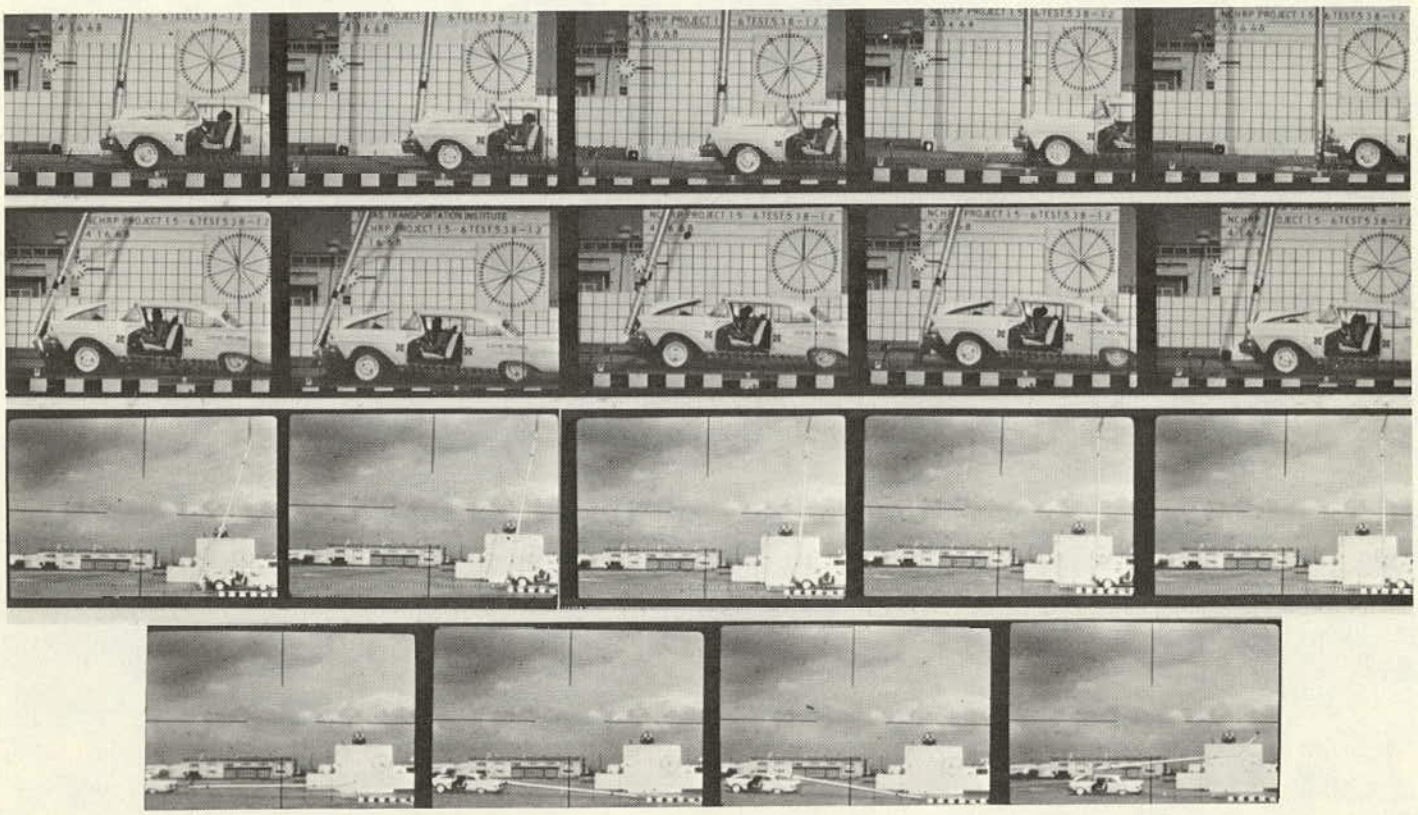

Figure D-8. Modified aluminum shoe base (Test 538-12).

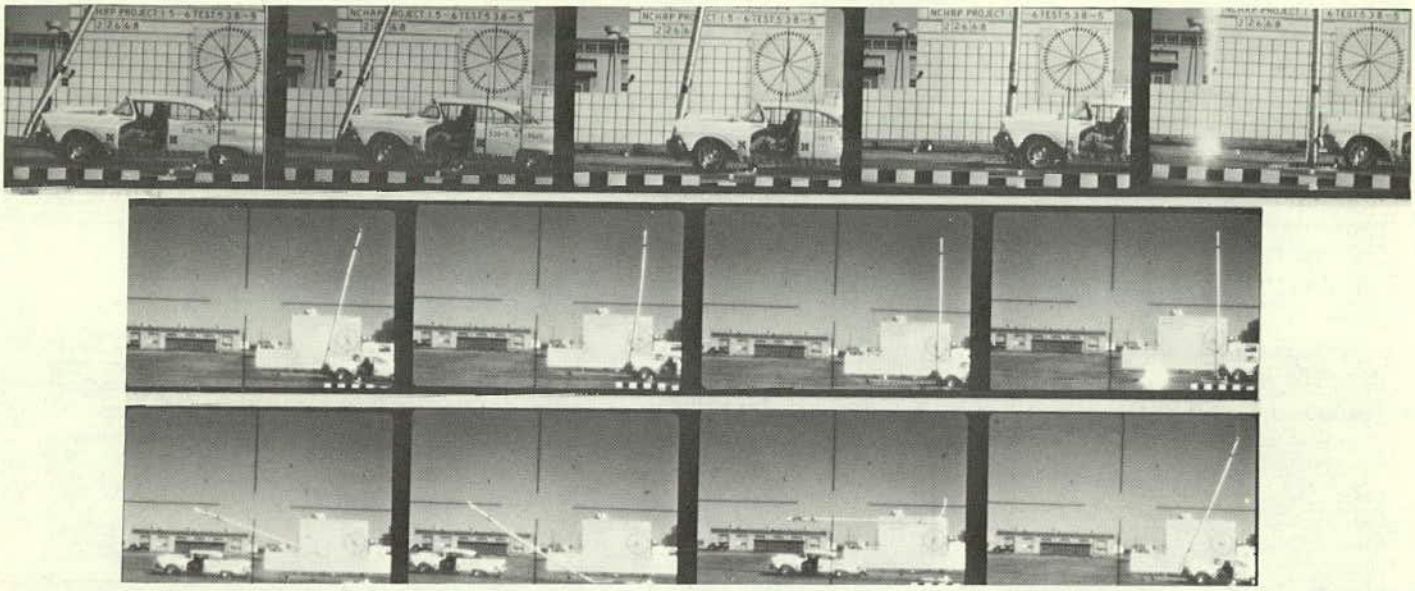

Figure D-9. Aluminum shoe base with riser (Test 538-5).

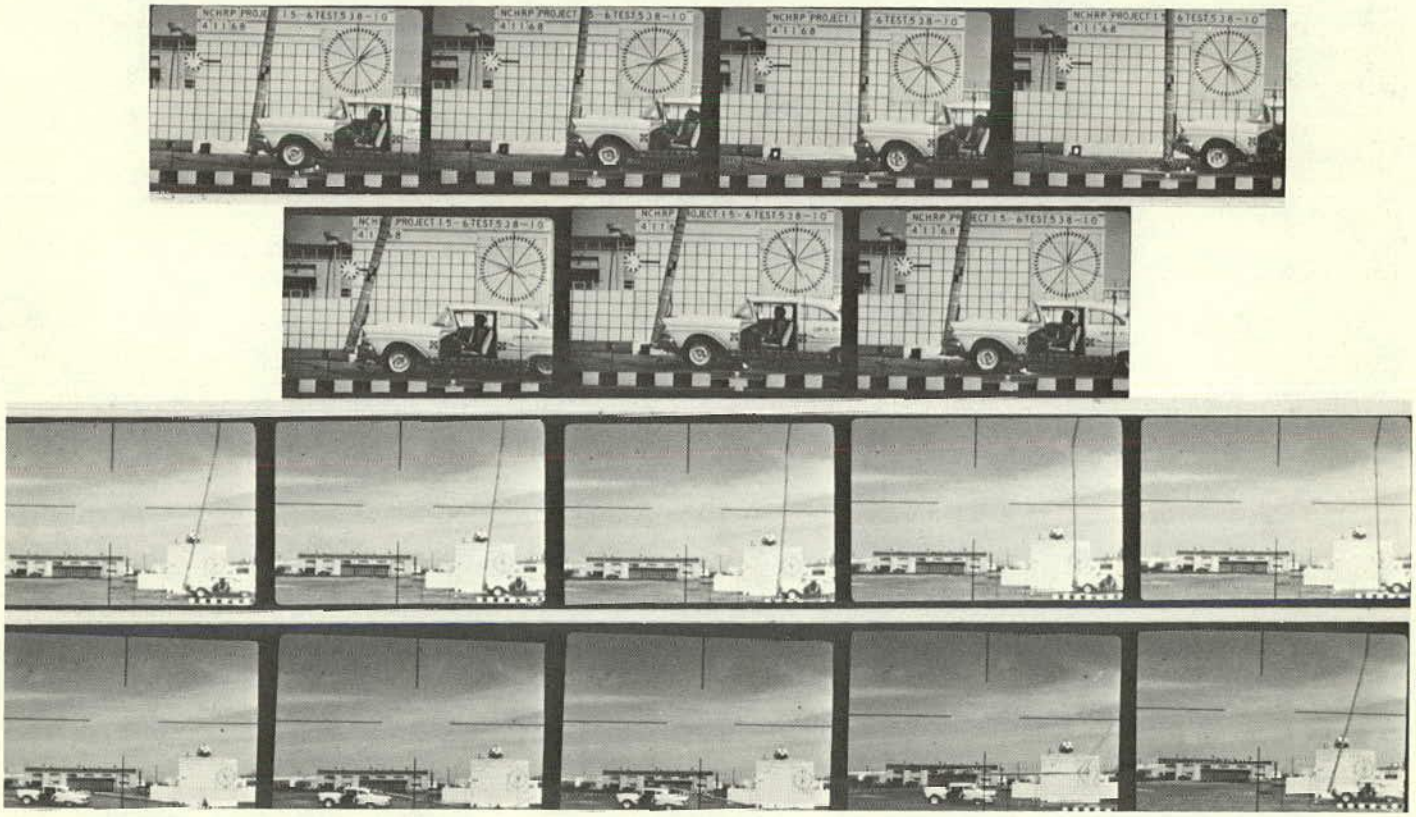

Figure D-10. Triangular slip base (Test 538-10).

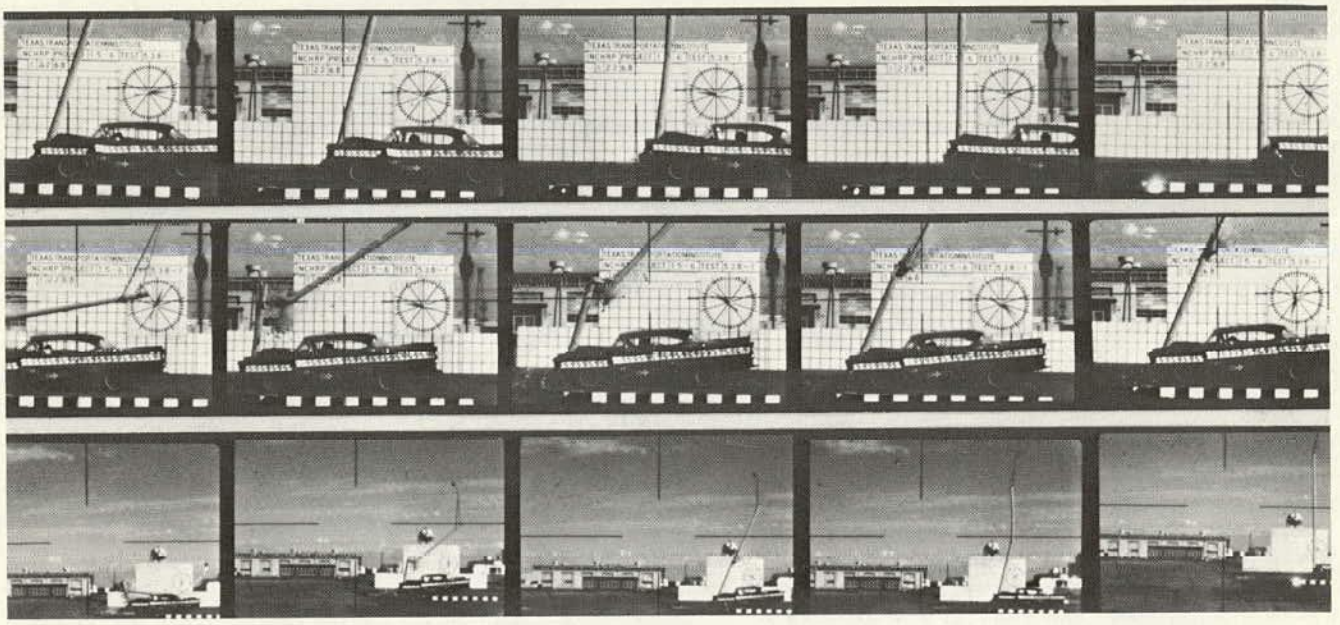

Figure D-11. Prestressed concrete support (Test 538-1).

Published reports of the

NATIONAL COOPERATIVE HIGHWAY RESEARCH PROGRAM

are available from:

Highway Research Board
National Academy of Sciences
2101 Constitution Avenue
Washington, D.C. 20418

Rep. No.	*Title*
—*	A Critical Review of Literature Treating Methods of Identifying Aggregates Subject to Destructive Volume Change When Frozen in Concrete and a Proposed Program of Research—Intermediate Report (Proj. 4-3(2)), 81 p., $1.80
1	Evaluation of Methods of Replacement of Deteriorated Concrete in Structures (Proj. 6-8), 56 p., $2.80
2	An Introduction to Guidelines for Satellite Studies of Pavement Performance (Proj. 1-1), 19 p., $1.80
2A	Guidelines for Satellite Studies of Pavement Performance, 85 p.+9 figs., 26 tables, 4 app., $3.00
3	Improved Criteria for Traffic Signals at Individual Intersections—Interim Report (Proj. 3-5), 36 p., $1.60
4	Non-Chemical Methods of Snow and Ice Control on Highway Structures (Proj. 6-2), 74 p., $3.20
5	Effects of Different Methods of Stockpiling Aggregates—Interim Report (Proj. 10-3), 48 p., $2.00
6	Means of Locating and Communicating with Disabled Vehicles—Interim Report (Proj. 3-4), 56 p. $3.20
7	Comparison of Different Methods of Measuring Pavement Condition—Interim Report (Proj. 1-2), 29 p., $1.80
8	Synthetic Aggregates for Highway Construction (Proj. 4-4), 13 p., $1.00
9	Traffic Surveillance and Means of Communicating with Drivers—Interim Report (Proj. 3-2), 28 p., $1.60
10	Theoretical Analysis of Structural Behavior of Road Test Flexible Pavements (Proj. 1-4), 31 p., $2.80
11	Effect of Control Devices on Traffic Operations—Interim Report (Proj. 3-6), 107 p., $5.80
12	Identification of Aggregates Causing Poor Concrete Performance When Frozen—Interim Report (Proj. 4-3(1)), 47 p., $3.00
13	Running Cost of Motor Vehicles as Affected by Highway Design—Interim Report (Proj. 2-5), 43 p., $2.80
14	Density and Moisture Content Measurements by Nuclear Methods—Interim Report (Proj. 10-5), 32 p., $3.00
15	Identification of Concrete Aggregates Exhibiting Frost Susceptibility—Interim Report (Proj. 4-3(2)), 66 p., $4.00
16	Protective Coatings to Prevent Deterioration of Concrete by Deicing Chemicals (Proj. 6-3), 21 p., $1.60
17	Development of Guidelines for Practical and Realistic Construction Specifications (Proj. 10-1), 109 p., $6.00
18	Community Consequences of Highway Improvement (Proj. 2-2), 37 p., $2.80
19	Economical and Effective Deicing Agents for Use on Highway Structures (Proj. 6-1), 19 p., $1.20
20	Economic Study of Roadway Lighting (Proj. 5-4), 77 p., $3.20
21	Detecting Variations in Load-Carrying Capacity of Flexible Pavements (Proj. 1-5), 30 p., $1.40
22	Factors Influencing Flexible Pavement Performance (Proj. 1-3(2)), 69 p., $2.60
23	Methods for Reducing Corrosion of Reinforcing Steel (Proj. 6-4), 22 p., $1.40
24	Urban Travel Patterns for Airports, Shopping Centers, and Industrial Plants (Proj. 7-1), 116 p., $5.20
25	Potential Uses of Sonic and Ultrasonic Devices in Highway Construction (Proj. 10-7), 48 p., $2.00
26	Development of Uniform Procedures for Establishing Construction Equipment Rental Rates (Proj. 13-1), 33 p., $1.60
27	Physical Factors Influencing Resistance of Concrete to Deicing Agents (Proj. 6-5), 41 p., $2.00
28	Surveillance Methods and Ways and Means of Communicating with Drivers (Proj. 3-2), 66 p., $2.60
29	Digital-Computer-Controlled Traffic Signal System for a Small City (Proj. 3-2), 82 p., $4.00
30	Extension of AASHO Road Test Performance Concepts (Proj. 1-4(2)), 33 p., $1.60
31	A Review of Transportation Aspects of Land-Use Control (Proj. 8-5), 41 p., $2.00
32	Improved Criteria for Traffic Signals at Individual Intersections (Proj. 3-5), 134 p., $5.00
33	Values of Time Savings of Commercial Vehicles (Proj. 2-4), 74 p., $3.60
34	Evaluation of Construction Control Procedures—Interim Report (Proj. 10-2), 117 p., $5.00
35	Prediction of Flexible Pavement Deflections from Laboratory Repeated-Load Tests (Proj. 1-3(3)), 117 p., $5.00
36	Highway Guardrails—A Review of Current Practice (Proj. 15-1), 33 p., $1.60
37	Tentative Skid-Resistance Requirements for Main Rural Highways (Proj. 1-7), 80 p., $3.60
38	Evaluation of Pavement Joint and Crack Sealing Materials and Practices (Proj. 9-3), 40 p., $2.00
39	Factors Involved in the Design of Asphaltic Pavement Surfaces (Proj. 1-8), 112 p., $5.00
40	Means of Locating Disabled or Stopped Vehicles (Proj. 3-4(1)), 40 p., $2.00
41	Effect of Control Devices on Traffic Operations (Proj. 3-6), 83 p., $3.60

* Highway Research Board Special Report 80.

Rep. No. *Title*

42 Interstate Highway Maintenance Requirements and Unit Maintenance Expenditure Index (Proj. 14-1), 144 p., $5.60

43 Density and Moisture Content Measurements by Nuclear Methods (Proj. 10-5), 38 p., $2.00

44 Traffic Attraction of Rural Outdoor Recreational Areas (Proj. 7-2), 28 p., $1.40

45 Development of Improved Pavement Marking Materials—Laboratory Phase (Proj. 5-5), 24 p., $1.40

46 Effects of Different Methods of Stockpiling and Handling Aggregates (Proj. 10-3), 102 p., $4.60

47 Accident Rates as Related to Design Elements of Rural Highways (Proj. 2-3), 173 p., $6.40

48 Factors and Trends in Trip Length (Proj. 7-4), 70 p., $3.20

49 National Survey of Transportation Attitudes and Behavior—Phase I Summary Report (Proj. 20-4), 71 p., $3.20

50 Factors Influencing Safety at Highway-Rail Grade Crossing (Proj. 3-8), 113 p., $5.20

51 Sensing and Communication Between Vehicles (Proj. 3-3), 105 p., $5.00

52 Measurement of Pavement Thickness by Rapid and Nondestructive Methods (Proj. 10-6), 82 p., $3.80

53 Multiple Use of Lands Within Highway Rights-of-Way (Proj. 7-6), 68 p., $3.20

54 Location, Selection, and Maintenance of Highway Guardrail and Median Barriers (Proj. 15-1(2)), 63 p., $2.60

55 Research Needs in Highway Transportation (Proj. 20-2), 66 p., $2.80

56 Scenic Easements—Legal, Administrative, and Valuation Problems and Procedures (Proj. 11-3), 174 p., $6.40

57 Factors Influencing Modal Trip Assignment (Proj. 8-2), 78 p., $3.20

58 Comparative Analysis of Traffic Assignment Techniques with Actual Highway Use (Proj. 7-5), 85 p., $3.60

59 Standard Measurements for Satellite Road Test Program (Proj. 1-6), 78 p., $3.20

60 Effects of Illumination on Operating Characteristics of Freeways (Proj. 5-2) 148 p., $6.00

61 Evaluation of Studded Tires—Performance Data and Pavement Wear Measurement (Proj. 1-9), 66 p., $3.00

62 Urban Travel Patterns for Hospitals, Universities, Office Buidings and Capitols (Proj. 7-1), 144 p., $5.60

63 Motorists' Needs and Services on Interstate Highways (Proj. 7-7), 88 p., $3.60

Rep. No. *Title*

64 One-Cycle Slow-Freeze Test for Evaluating Aggregate Performance in Frozen Concrete (Proj. 4-3(1)), 21 p., $1.40

65 Identification of Frost-Susceptible Particles in Concrete Aggregates (Proj. 4-3(2)), 62 p., $2.80

66 Relation of Asphalt Rheological Properties to Pavement Durability (Proj. 9-1), 45 p., $2.20

67 Relation of Asphalt Rheological Properties to Pavement Durability (Proj. 9-1), 45 p., $2.20

68 Application of Vehicle Operating Characteristics to Geometric Design and Traffic Operations (Proj 3-10), 38 p., $2.00

69 Evaluation of Construction Control Procedures—Aggregate Gradation Variations and Effects (Proj. 10-2A), 58 p., $2.80

70 Social and Economic Factors Affecting Intercity Travel (Proj. 8-1), 68 p., $3.00

71 Analytical Study of Weighing Methods for Highway Vehicles in Motion (Proj. 7-3), 63 p., $2.80

72 Theory and Practice in Inverse Condemnation for Five Representative States (Proj. 11-2), 44 p., $2.20

73 Improved Criteria for Traffic Signal Systems on Urban Arterials (Proj. 3-5/1), 55 p., $2.80

74 Protective Coatings for Highway Structural Steel (Proj. 4-6), 64 p., $2.80

75 Effect of Highway Landscape Development on Nearby Property (Proj. 2-9), 82 p., $3.60

76 Detecting Seasonal Changes in Load-Carrying Capabilities of Flexible Pavements (Proj. 1-5(2)), 38 p., $2.00

77 Development of Design Criteria for Safer Luminaire Supports (Proj. 15-6), 82 p., $3.80

Synthesis of Highway Practice

1 Traffic Control for Freeway Maintenance (Proj. 20-5, Task 1), 47 p., $2.20

2 Bridge Approach Design and Construction Practices (Proj. 20-5, Task 2), 30 p., $2.00

THE NATIONAL ACADEMY OF SCIENCES is a private, honorary organization of more than 700 scientists and engineers elected on the basis of outstanding contributions to knowledge. Established by a Congressional Act of Incorporation signed by President Abraham Lincoln on March 3, 1863, and supported by private and public funds, the Academy works to further science and its use for the general welfare by bringing together the most qualified individuals to deal with scientific and technological problems of broad significance.

Under the terms of its Congressional charter, the Academy is also called upon to act as an official—yet independent—adviser to the Federal Government in any matter of science and technology. This provision accounts for the close ties that have always existed between the Academy and the Government, although the Academy is not a governmental agency and its activities are not limited to those on behalf of the Government.

THE NATIONAL ACADEMY OF ENGINEERING was established on December 5, 1964. On that date the Council of the National Academy of Sciences, under the authority of its Act of Incorporation, adopted Articles of Organization bringing the National Academy of Engineering into being, independent and autonomous in its organization and the election of its members, and closely coordinated with the National Academy of Sciences in its advisory activities. The two Academies join in the furtherance of science and engineering and share the responsibility of advising the Federal Government, upon request, on any subject of science or technology.

THE NATIONAL RESEARCH COUNCIL was organized as an agency of the National Academy of Sciences in 1916, at the request of President Wilson, to enable the broad community of U. S. scientists and engineers to associate their efforts with the limited membership of the Academy in service to science and the nation. Its members, who receive their appointments from the President of the National Academy of Sciences, are drawn from academic, industrial and government organizations throughout the country. The National Research Council serves both Academies in the discharge of their responsibilities.

Supported by private and public contributions, grants, and contracts, and voluntary contributions of time and effort by several thousand of the nation's leading scientists and engineers, the Academies and their Research Council thus work to serve the national interest, to foster the sound development of science and engineering, and to promote their effective application for the benefit of society.

THE DIVISION OF ENGINEERING is one of the eight major Divisions into which the National Research Council is organized for the conduct of its work. Its membership includes representatives of the nation's leading technical societies as well as a number of members-at-large. Its Chairman is appointed by the Council of the Academy of Sciences upon nomination by the Council of the Academy of Engineering.

THE HIGHWAY RESEARCH BOARD, organized November 11; 1920, as an agency of the Division of Engineering, is a cooperative organization of the highway technologists of America operating under the auspices of the National Research Council and with the support of the several highway departments, the Bureau of Public Roads, and many other organizations interested in the development of transportation. The purpose of the Board is to advance knowledge concerning the nature and performance of transportation systems, through the stimulation of research and dissemination of information derived therefrom.

HIGHWAY RESEARCH BOARD
NATIONAL ACADEMY OF SCIENCES—NATIONAL RESEARCH COUNCIL
2101 Constitution Avenue Washington, D. C. 20418

ADDRESS CORRECTION REQUESTED